CALIFORNIA INSTITUTE OF TECHNOLOGY

EARTHQUAKE ENGINEERING RESEARCH LABORATORY

DYNAMIC ANALYSIS OF COUPLED SHEAR WALLS AND SANDWICH BEAMS

BY

KNUT SVERRE SKATTUM

EERL 71-06

A REPORT ON RESEARCH CONDUCTED UNDER A GRANT FROM THE NATIONAL SCIENCE FOUNDATION

PASADENA, CALIFORNIA

1971

DYNAMIC ANALYSIS OF COUPLED SHEAR WALLS AND SANDWICH BEAMS

Thesis by

Knut Sverre Skattum

In Partial Fulfillment of the Requirements

For the Degree of

Doctor of Philosophy

California Institute of Technology

Pasadena, California

1971

(Submitted May 24, 1971)

ACKNOWLEDGMENTS

The author sincerely thanks his research advisor, Professor Paul C. Jennings, for valuable guidance, suggestions and assistance in the course of research and preparation of this thesis. Additional thanks are owed to Professor Charles D. Babcock, Jr. and to the faculty of Applied Mechanics.

Financial support during the author's graduate study received from the California Institute of Technology (Earl C. Anthony Fellowship, research and teaching assistantships) and the State of California (state scholarship) is sincerely appreciated. The partial support of this investigation under a grant from the National Science Foundation is also acknowledged.

Thanks are due to Mrs. Alrae Tingley and Mrs. Alice Gear for their expert typing of the manuscript.

The author also wishes to express his deep gratitude to his wife, Helene, for her endless patience and encouragement throughout the years of graduate study.

ABSTRACT

A study is made of the free vibration of planar coupled shear walls, a common lateral load-resisting configuration in building construction where two walls are coupled together by a system of discrete spandrel beams. The differential equations and boundary conditions are obtained by the variational method, and by assuming that the spandrels can be replaced by a continuous system of laminae, or small beams.

Natural frequencies and mode shapes are determined, and the results are presented in a number of figures from which the natural frequencies of any coupled shear wall can be extracted. The importance of including vertical displacement in the analysis is discussed, and a study of the effect of neglecting the vertical inertia term is given. These cases are illustrated with graphs and with one specific example. Investigations are also made of the asymptotic behavior of the system as the spandrels become weak, as they become stiff, and as the frequencies become large.

Finally, the theory of sandwich beams is presented and compared to that for coupled shear walls. It is observed that for most cases of constant properties, the differential equations (and boundary conditions) reduce to the same mathematical form for both theories.

TABLE OF CONTENTS

Chapter I

INTRODUCTION

Shear walls have been used in building construction for a long time to resist lateral forces arising from winds and earthquakes. These walls, extending the whole height of the buildings, are usually placed on the sides of the structure, or around an interior core that houses stairs and elevators. In order to have windows, doors and service ducts, openings must be provided in the shear walls, and the resulting structure often consists of two walls, coupled together by a system of horizontal spandrel beams. This coupled shear wall will have a reduced stiffness, and the analysis will become more complicated. If the size of the openings increase, the behavior changes from that of a single-layer shear wall to two smaller independent walls.

Figure 1.1 shows an example of a building in which coupled shear walls are used for the lateral resistance. This apartment building, the McKinley building in Anchorage, Alaska, and a nearly identical one a mile away, were severely damaged during the Alaskan earthquake of 1964.

In order to analyze coupled shear walls, such as the one shown in figure 1.1, a simple planar model, figure 1.2, is introduced. This coupled shear-wall model has two walls of unequal dimensions and properties coupled together with a system of spandrel beams. The spandrels are assumed to be uniform between the two walls, but their properties and spacing along the

Fig. 1.1. McKinley building, Anchorage, Alaska

length of the structure can change. Although the differential equations of motion are derived for this general structure, most emphasis is placed on the coupled shear walls with constant properties, and in particular on the case of two equal walls.

The coupled shear wall has attracted several investigators in the last decade or so. A simple technique of analysis has been developed from the assumption that the discrete system of spandrel beams could be replaced by an equivalent continuous medium. This medium is assumed to be rigidly attached to the walls but only capable of transmitting actions of the same type as the discrete spandrels. A system of independently acting laminae, or little beams, will have this property as will be explained in Chapter II, and this device enables all the properties of the modified structure to be expressed as continuous functions of x, the longitudinal coordinate. By assuming that the spandrels have a point of contra-flexure at midspan, and that the two walls are equal and constant over the height of the structure, the equation for the static analysis of a coupled shear wall can be written as a second-order differential equation with constant coefficients.

The method was first used by L. Chitty[1] (1947) in the analysis of a cantilever composed of a series of parallel beams interconnected by cross bars. In a later paper[2], L. Chitty and W. Wan applied the technique to tall building structures under wind loads. Further extension of this method was given by Beck[3] in the case of uniform

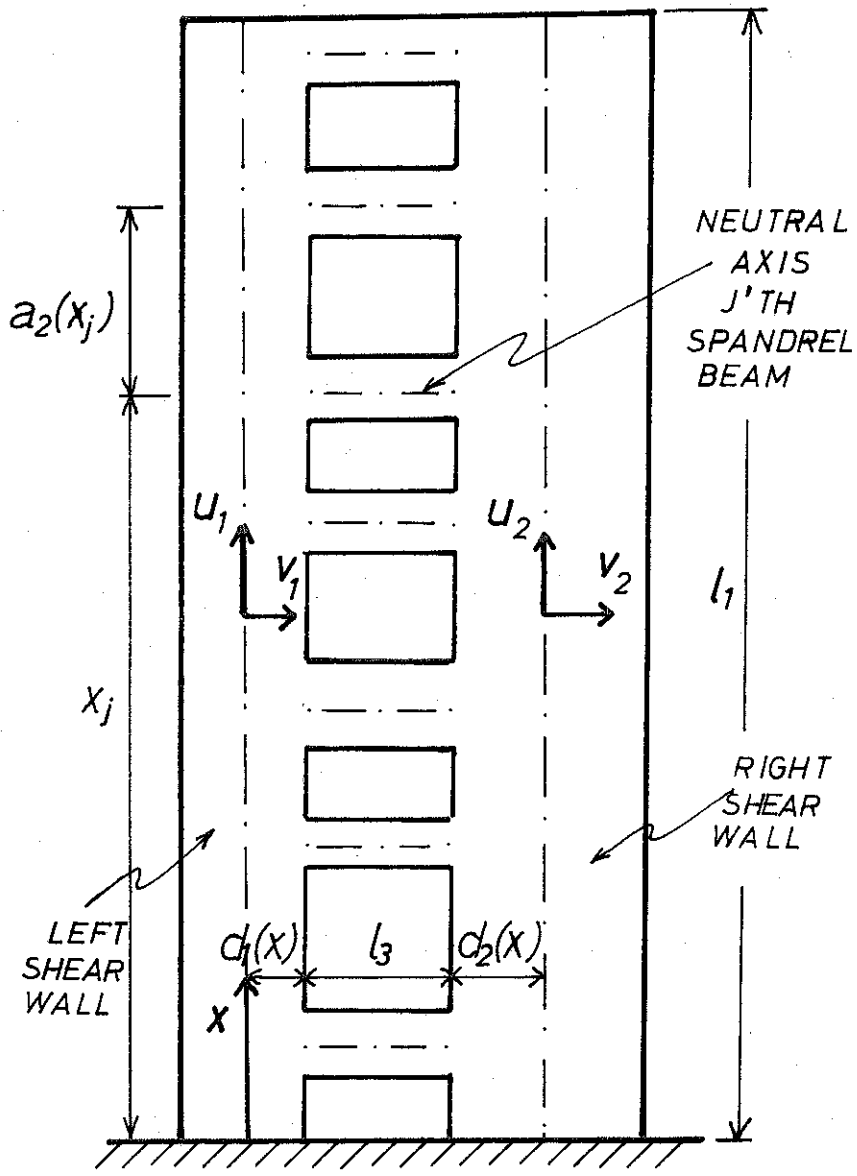

Fig. 1.2. General Coupled Shear Wall

lateral loading. Rosman[4] treated the case of a concentrated load acting on top of the structure, and Burns[5] analyzed the coupled shear wall subject to triangular loading, such as those specified in many seismic codes. Curves for determining stresses and maximum deflections were given by Coull and Choudbury[6], and in a later paper, Coull and Puri[8] extended the coupled shear-wall theory to include shearing deformations of the wall and flexibility of the joints, which, from experiments, was found to be more important than the inclusion of shearing deformations.

Walls with variable cross sections have been analyzed by Burns[5], for parabolically varying wall and beam stiffnesses, and by Traum[9], who treated the case of different, constant cross sections placed on top of each other. The extension of the analysis to walls with multiple bays, such as in figure 1.1 has been studied by Burns[5] and Coull and Puri[8].

If the two walls have different properties, or if the loading is not symmetrically applied to the two walls, then the midpoint of the spandrels will not necessarily be a point of contraflexure. Tso[12] investigated the case of unequally applied loading and concluded that for most cases, small errors were introduced by assuming symmetrical loading, and the simplified theory could hence be used with satisfactory results.

Experimental verification of the analysis of coupled shear walls has been done by Barnard and Schwaighofer[10] and Coull and Puri[8]. Jennings[17] applied the method to the building shown in figure 1.1. He found that the damage pattern exhibited by the

spandrel beams in the building was consistent with the stresses determined from the theory of coupled shear walls. Full-scale experimental studies of the behavior of spandrels in coupled shear walls have been performed by Pauley[38, 40].

In short buildings with few spandrels, the use of a continuous medium as a substitute for the spandrels becomes more questionable. For these cases, numerical methods have successfully been employed; Sensmeier[11] presented a finite difference approach based on the two-dimensional plane stress equations of elasticity and Girijavallabhan[21] applied a finite element technique.

The dynamic properties of the coupled shear wall has attracted less attention from investigators. Kanai, Tajimi, Osawa and Kobayashi[16] did a dynamic analysis in which they neglected the longitudinal deflections of the walls, and Tani, Sakurai and Iguchi[14] have done a dynamic study of a related structure; the core-wall building. Recently, Tso and Chan[13] analyzed the free vibration of a coupled shear wall with equal and unequal walls. The axial deformations of the walls were included in the analysis, and dynamic tests of two models gave good verification for the theoretical values of the fundamental modes and frequencies.

Shear-wall buildings, in which coupled shear walls are major components, have recently been analyzed by Coull and Irwin[39] (static case). Tso and Biswas[41], and Irwin and Heidebrecht[42] have studied the dynamic response of such buildings.

When the spandrels in the coupled shear wall are replaced by a fictitious continuous medium, the difference between this hypothetical structure and the sandwich beam becomes small. In essence, both structures have two beams separated by an elastic medium. The differences are due to the assumptions made on the spandrel system and the sandwich core. Because of the independence of the laminae, no longitudinal strain can be considered in the system of laminae,but for a sandwich core, longitudinal forces are sometimes included in the analysis. The major difference, however, is that the sandwich core does not admit bending strain (the analysis would in that case be considerably more complicated) while the spandrel system admits both bending and shearing deformations.

The theory of sandwich beams is somewhat older (7-8 years) than the theory of coupled shear walls, but because of the applications in airplanes, pressure bulkheads and flooring, recent emphasis has been more on sandwich panels than on sandwich beams. The literature in sandwich construction is far larger than that for coupled shear walls. A comprehensive review of work done up to 1965 is given by Habip[15]. Two recent books on sandwich construction by Plantema[36] and Allen[37] also give extensive reference listings.

Scope of Present Work

The object of this thesis is to find and study in detail the natural frequencies and mode shapes of symmetric, planar coupled shear walls. The differential equations are derived in terms of the four displacement variables shown in figure 1.2 since this formulation

is found to be more applicable to the dynamic case than the methods presented by Chitty[1], Beck[3] and others. Also, by using the variational principle, an extension of the theory to structures composed of several shear walls connected together by spandrels can easily be performed.

When the displacement variables are transformed into a new set of variables representing the symmetrical and antisymmetrical lateral and longitudinal displacements, the differential equations as well as the boundary conditions for the equal wall case uncouple into three new sets of differential equations and boundary conditions; pure longitudinal motion, antisymmetrical lateral motion,and a coupling between the symmetrical lateral and antisymmetrical longitudinal displacements. This last set of equations are the basis for the study in Chapter III where the vertical inertia term is neglected, and in Chapter IV where it is included. For both cases, natural frequencies and mode shapes are obtained. The importance of including vertical displacement is clearly indicated in the analysis as well as in the example given in Chapter IV, and although of somewhat lesser importance, the effect on the solutions of the vertical inertia is stated and explained in Chapter IV.

In order to get a better understanding of the general dynamic characteristics of coupled shear walls, to seek simplified solutions to special cases, and to obtain bounds on the natural frequencies, asymptotic studies have been included in both Chapters III and IV. Cases where the spandrels become weaker, and stiffer, as well as

where the two walls become more and more separated (usually only applicable to sandwich construction) and finally where the frequencies increase, have been studied.

In Chapter V, the theory of sandwich beams is presented, and the differential equations are derived and reduced to the case of constant, equal faces, similar to the development in Chapter II. It is found that the differential equations for this case have the same form as for the coupled shear wall, and although the two structures are different, as pointed out earlier, the differences are contained within the dimensionless parameters of the structures, so no difference in the differential equations and the boundary conditions are observed. This is also true for most cases when the faces of the sandwich beam and the walls of the coupled shear walls are constant but unequal. It is hence concluded that the analysis in Chapters III and IV do apply to the sandwich beams as well.

Chapter VI reviews some of the more important conclusions and makes recommendations for future research in the area of the thesis.

CHAPTER II

DERIVATION OF EQUATIONS OF MOTION

The objective of this chapter is to formulate the differential equations of motion for the in-plane vibrations of the coupled shear wall shown in Figure 1.2. Also shown in that figure are the displacement parameters that will be used throughout this chapter; u_1 and u_2 are the vertical (longitudinal) displacements of the neutral axis of the left and right shear walls, respectively, and similarly, v_1 and v_2 are the horizontal (lateral) displacements. Further, x is the vertical coordinate and t is time.

The differential equations will be obtained using Hamilton's variational Principle[22]

$$\delta \int_{t_0}^{t_1} (T - U)\, dt = 0 \qquad (2.1)$$

where T is the kinetic energy of the system, U is the total strain energy, and δ is the variational operator. The application of Hamilton's Principle will give the differential equations of motion as well as all the boundary conditions, which in this problem are difficult to obtain otherwise.

At the end of the chapter, the differential equations and boundary conditions will be reduced to the important practical case of two equal shear walls.

2.1. Description of the Coupled Shear Wall and the Mathematical Model

The two shear walls have the following properties:

$$
\begin{aligned}
A_i &= A_i(x) = \text{area of cross section} \\
E_i &= E_i(x) = \text{Young's Modulus} \\
I_i &= I_i(x) = \text{moment of inertia about neutral axis} \\
\rho_i &= \rho_i(x) = \text{mass per unit volume} \\
d_i &= d_i(x) = \text{distance from neutral axis to wall opening} \\
\ell_1 &= \text{length of wall}
\end{aligned}
\tag{2.2}
$$

where i equals one for the left shear wall, and i is two for the right shear wall. (See figure 1.2.)

The spandrels are assumed to be uniform between the two walls, but can vary along the length of the wall. The properties of the spandrels are therefore defined for discrete values of x, x_j, the distance to the neutral axis of the j^{th} spandrel.

$$
\begin{aligned}
A_3 &= A_3(x_j) = \text{area of cross section} \\
E_3 &= E_3(x_j) = \text{Young's Modulus} \\
I_3 &= I_3(x_j) = \text{moment of inertia about neutral axis} \\
d_3 &= d_3(x_j) = \text{total depth} \\
G_3 &= G_3(x_j) = \text{shear modulus} \\
\rho_3 &= \rho_3(x_j) = \text{mass per unit volume} \\
\ell_3 &= \text{length (constant)} \\
j &= 1, 2, \ldots, n; \quad n = \text{total number of spandrels}
\end{aligned}
\tag{2.3}
$$

It is convenient to introduce two other quantities:

$$a_1(x) = d_1(x) + d_2(x) + \ell_3$$

$$a_2(x_j) = \begin{cases} 2x_1 & ; \ j = 0 \\ x_{j+1} - x_j & ; \ j = 1,2,\ldots,n-1 \\ 2(\ell_1 - x_n) & ; \ j = n \end{cases} \tag{2.4}$$

$a_1(x)$ is the distance between the neutral axes of the shear walls at elevation x, and $a_2(x_j)$ is the distance between the neutral axes of the j^{th} and $(j+1)^{th}$ spandrel.

The shear wall system shown in Figure 1.2 and defined by equations (2.2), (2.3) and (2.4) will be analyzed by replacing the discrete spandrels by a uniform system of independent laminae, or little beams, as illustrated by Figure 2.1. The laminae are required to carry moment, shear and axial force equivalent to the original system. The laminae will be assumed to be continuously or piecewise continuously distributed along the length of the shear wall. Also, the mass of the laminae is taken equal to the mass of the spandrels they replace.

Let the properties of each lamina be defined by

$$\begin{aligned} \Delta x &= \text{depth} \\ \tilde{I}_3 = \tilde{I}_3(x) &= \text{moment of inertia} \\ \tilde{A}_3 = \tilde{A}_3(x) &= \text{area of cross section} \\ \tilde{E}_3 = \tilde{E}_3(x) &= \text{Young's Modulus} \\ \tilde{G}_3 = \tilde{G}_3(x) &= \text{shear modulus} \\ \tilde{\rho}_3 = \tilde{\rho}_3(x) &= \text{mass per unit volume} \\ \ell_3 &= \text{length} \end{aligned} \tag{2.5}$$

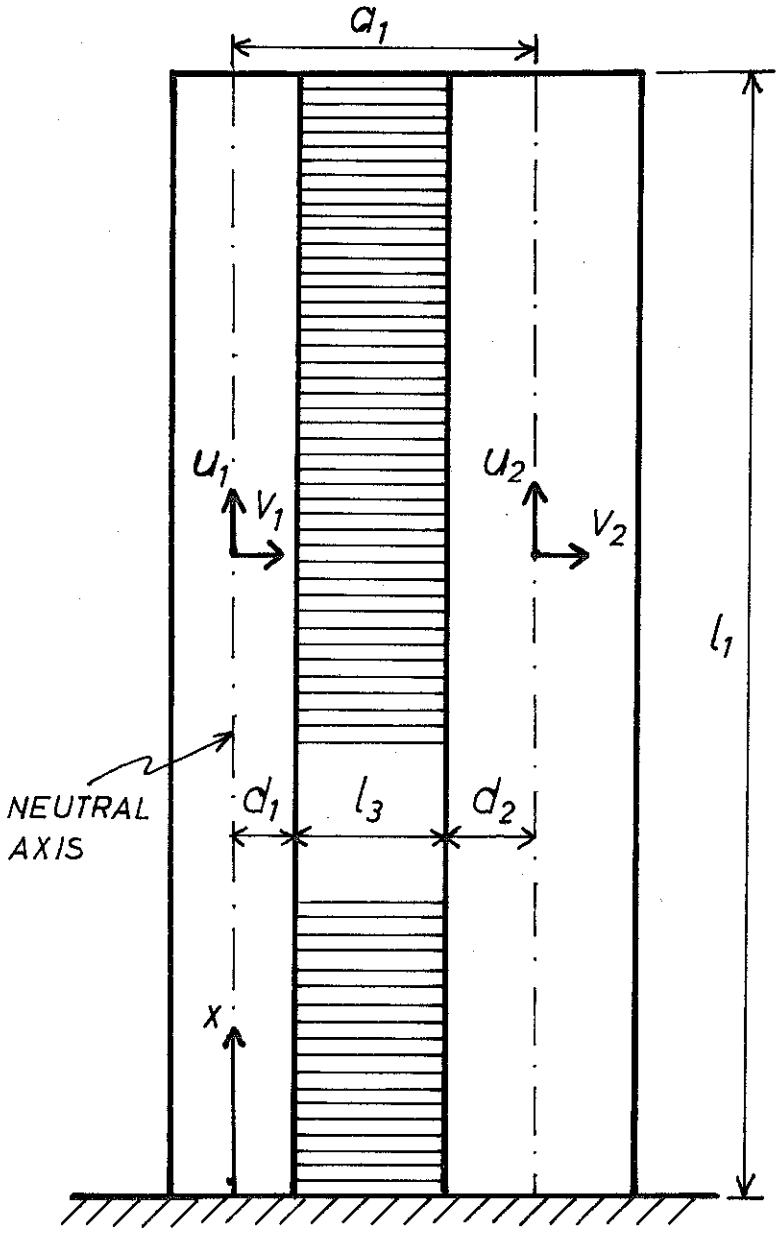

Fig. 2.1. Coupled Shear Wall with the Spandrels Replaced by a System of Continuous Laminae

The depth, Δx, is considered small and will later be allowed to approach zero, thus creating a continuous or piecewise continuous medium between the two walls. This medium is in essence a mathematical convenience in which all the laminae deform independently. Because of this, the idealized coupled shear wall is not equivalent to the usual sandwich beam, but it will be shown later (chapter V) that under certain conditions the coupled shear wall model reduces to the sandwich beam.

The medium between the two walls can now be defined by letting

$$\left.\begin{aligned} \tilde{E}_3(x) &= E_3(x_j) \\ \tilde{G}_3(x) &= G_3(x_j) \\ \tilde{\rho}_3(x) &= \rho_3(x_j) \end{aligned}\right\} \quad x \in [\, x_j - \tfrac{1}{2} a_2(x_{j-1}), x_j + \tfrac{1}{2} a_2(x_j)] \quad j = 1,2,\ldots,n \qquad (2.6)$$

$$\left.\begin{aligned} \tilde{I}_3(x) &= i_3(x)\Delta x \\ \tilde{A}_3(x) &= a_3(x)\Delta x \end{aligned}\right\} \quad \Delta x \to 0, \quad x \in [\,0,1]$$

where $i_3(x)$ and $a_3(x)$ must satisfy the relations

$$\left.\begin{aligned} \int_{x=x_j-\frac{1}{2}a_2(x_{j+1})}^{x_j+\frac{1}{2}a_2(x_j)} i_3(x)\,dx &= I_3(x_j) \\ \int_{x=x_j-\frac{1}{2}a_2(x_{j-1})}^{x_j+\frac{1}{2}a_2(x_j)} a_3(x)\,dx &= A_3(x_j) \end{aligned}\right\} \quad j = 1,2,\ldots,n \qquad (2.7)$$

When ℓ_3 is constant, equation (2.7) will ensure that the above-mentioned stiffness requirements on the system of laminae are satisfied.

In some cases, the spacing and sizes of the spandrels will be such that $i_3(x)$ and $a_3(x)$ are constants over the entire wall. This is the case in the coupled shear walls analyzed by several authors (1-6, 12-13) where the spandrels are assumed to be identical with the exception of the top spandrel, which is taken to have one-half the area, depth and moment of inertia of the other spandrels. For this case, if the opening between the spandrels are such that

$$a_2(x_i) = \begin{cases} a_2 & ; \ i = 0, 1, 2, \ldots, n-2 \\ a_2 - (\ell_1 - x_n) & ; \ i = n - 1 \end{cases} \tag{2.8}$$

then taking

$$\left.\begin{aligned} i_3(x) &= \frac{I_3}{a_2} \\ a_3(x) &= \frac{A_3}{a_2} \end{aligned}\right\} \ x \in [0, \ell_1] \tag{2.9}$$

will satisfy the conditions in equation (2.7). These relations will be used later in the chapter, but there is no need at this stage of the analysis to require conditions beyond those in equation (2.7).

Both axial and bending deformations of the shear walls will be included in the analysis, and in the spandrel beams, bending, shear and axial deformations are included. For simplicity, however, and in keeping with most applications, the shear deformations of the walls will be neglected. It can be shown(43) that this assumption implies less than 5% error if the ratio between the wavelength of the mode shape and the depth of the wall is larger than about ten. In general, this limits the practical applications of the theory to the first few modes of coupled shear walls.

The kinetic energy in equation (2.1) will include both lateral and longitudinal motion, but the rotary motions are neglected in the walls as well as in the spandrels.

Finally, all deflections will be considered small, i.e.,

$$\begin{aligned} u_i &\ll a_1 \; ; \; \frac{\partial u_i}{\partial x} \ll 1 \\ v_i &\ll \ell_1 \; ; \; \frac{\partial v_i}{\partial x} \ll 1 \end{aligned} \qquad i = 1,2 \qquad (2.10)$$

so that the linear theory of bending can be applied to the shear walls and spandrels.

2.2. Expressions for Kinetic Energy and Strain Energy

Kinetic Energy

Under the assumptions given above, the kinetic energy of the shear wall system can now be obtained. In the system of spandrels, the longitudinal and lateral displacements will be functions of both the x and y coordinate. (See figure 2.2.) From equations (A.5), (A.9), (A.11), (A.12) and (A.13) in appendix A, with the proper boundary conditions as indicated in figure 2.2, the displacement of the spandrels, neglecting rotation, can be written as

$$u^*(x,y) = u_1(x) + \frac{1}{\beta^2}\left[(\beta^2-1)\frac{y}{\ell} + 3\left(\frac{y}{\ell}\right)^2 - 2\left(\frac{y}{\ell}\right)^3\right]\left[u_2(x) - u_1(x)\right]$$

$$v^*(x,y) = v_1(x) + \frac{y}{\ell}\left[v_2(x) - v_1(x)\right] \qquad (2.11)$$

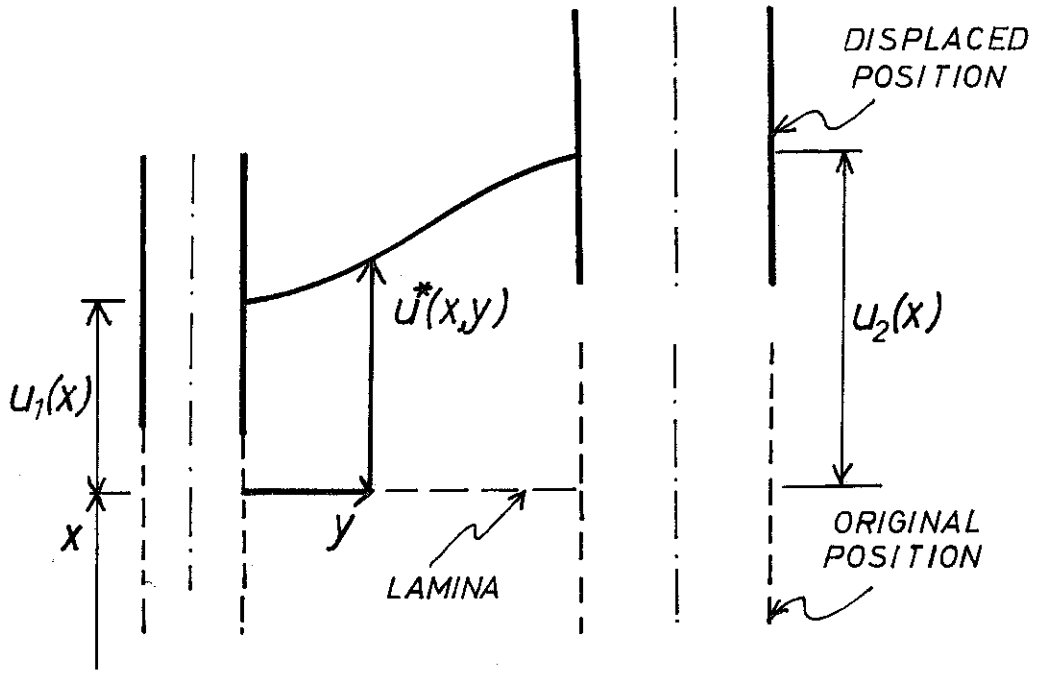

(a). LONGITUDINAL DISPLACEMENT.

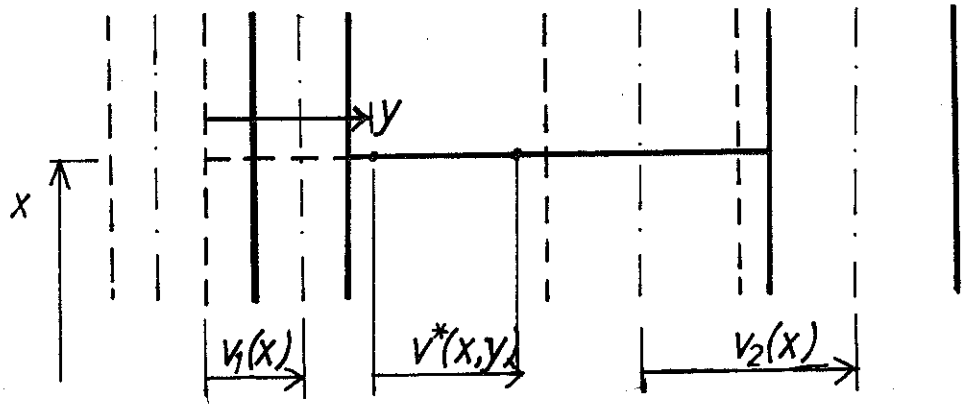

(b). LATERAL DISPLACEMENT

Fig. 2.2. Displacement of Lamina at Position x Neglecting Rotations

where the constant β^2 will be defined in equation (2.23). The kinetic energy of the system of spandrels will then be[23]

$$T_s = \frac{1}{2}\int_{x=0}^{\ell_1}\int_{y=0}^{\ell_3} \tilde{\rho}_3 a_3 \left[\left(\frac{\partial u^*}{\partial t}\right)^2 + \left(\frac{\partial v^*}{\partial t}\right)^2\right] dx\, dy \qquad (2.12)$$

By substituting equation (2.11) in (2.12), the integration over the length of the spandrel can be performed, and by adding the kinetic energy of the two shear walls, the total kinetic energy of the coupled shear wall system is given by

$$T = \frac{1}{2}\int_0^{\ell_1} \rho_1 A_1 \left[\left(\frac{\partial u_1}{\partial t}\right)^2 + \left(\frac{\partial v_1}{\partial t}\right)^2\right] + \rho_2 A_2 \left[\left(\frac{\partial u_2}{\partial t}\right)^2 + \left(\frac{\partial v_2}{\partial t}\right)^2\right]$$

$$+ \rho_3 a_3 \ell_3 \left[\frac{\partial u_1}{\partial t}\frac{\partial u_2}{\partial t} + \frac{70\beta^4+7\beta^2+1}{210\,\beta^2}\left(\frac{\partial u_2}{\partial t} - \frac{\partial u_1}{\partial t}\right)^2\right.$$

$$\left. + \frac{\partial v_1}{\partial t}\frac{\partial v_2}{\partial t} + \frac{1}{3}\left(\frac{\partial v_2}{\partial t} - \frac{\partial v_1}{\partial t}\right)^2\right] dx \qquad (2.13)$$

Strain Energy in the Shear Walls

With the shear walls restricted to axial and bending deformations, the only non-zero stress is the axial stress, and the strain energy in the shear walls is simply[23]

$$U_1 = \sum_{i=1}^{2}\left[\frac{1}{2}\int_0^{\ell_1} \frac{N_i^2\, dx}{E_i A_i} + \frac{1}{2}\int_0^{\ell_1} \frac{M_i^2\, dx}{E_i I_i}\right] \qquad (2.14)$$

where N_i is the axial force and M_i the moment in the left (i = 1)

and right (i = 2) shear wall. Expressing the axial force and bending moment in terms of the deformations

$$\left.\begin{aligned} N_i &= E_i A_i \frac{\partial u_i}{\partial x} \\ M_i &= E_i I_i \frac{\partial^2 v_i}{\partial x^2} \end{aligned}\right\} \quad i = 1,2 \tag{2.15}$$

the strain energy in the shear walls becomes

$$U_1 = \tfrac{1}{2}\int_0^{\ell_1} E_1 A_1 \left(\frac{\partial u_1}{\partial x}\right)^2 dx + \tfrac{1}{2}\int_0^{\ell_1} E_2 A_2 \left(\frac{\partial u_2}{\partial x}\right)^2 dx + \tfrac{1}{2}\int_0^{\ell_1} E_1 I_1 \left(\frac{\partial^2 v_1}{\partial x^2}\right)^2 dx$$
$$+ \tfrac{1}{2}\int_0^{\ell_1} E_2 I_2 \left(\frac{\partial^2 v_2}{\partial x^2}\right)^2 dx \tag{2.16}$$

Strain Energy in the Spandrels

The strain energy of the spandrels also has to be expressed in terms of the deformations u_i and v_i. Thus the problem reduces to obtaining the strain energy of a beam subject to rotation, elongation and lateral deflections at the ends. This analysis is included in Appendix A.

In order to obtain the correct boundary conditions for each lamina, the total deformation of the shear wall at position x must be analyzed. Figure 2.3 shows how an undeformed lamina, $\overline{BC}$, deforms to $\overline{B'C'}$. In the x_1, y_1-coordinate system centered at A, the positions of B' and C' can be obtained from the figure:

$$
\begin{aligned}
x_1(B') &= d_1(x) + v_1(x) - d_1(x)\left[1 - \cos\left(\frac{\partial v_1}{\partial x}\right)\right] \\
y_1(B') &= u_1(x) - d_1(x)\sin\left(\frac{\partial v_1}{\partial x}\right) \\
x_1(C') &= d_1(x) + \ell_3 + v_2(x) + d_2(x)\left[1 - \cos\left(\frac{\partial v_2}{\partial x}\right)\right] \\
y_1(C') &= u_2(x) + d_2(x)\sin\left(\frac{\partial v_2}{\partial x}\right)
\end{aligned}
\tag{2.17}
$$

Since only small deformations are considered, equation (2.10), the higher order terms of equation (2.17) will be dropped, giving

$$
\begin{aligned}
x_1(B') &= v_1(x) + d_1(x) \\
y_1(B') &= u_1(x) - d_1(x)\frac{\partial v_1}{\partial x} \\
x_1(C') &= d_1(x) + \ell_3 + v_2(x) \\
y_1(C') &= u_2(x) + d_2(x)\frac{\partial v_2}{\partial x}
\end{aligned}
\tag{2.18}
$$

The transformation from the x_1, y_1-system to the x_2, y_2-system is again obtained from Figure 2.3. Neglecting higher order terms, this transformation can be written in matrix notation as

$$
\begin{bmatrix} x_2 \\ y_2 \end{bmatrix} = \begin{bmatrix} 1 & -\frac{\partial v_1}{\partial x} \\ \frac{\partial v_1}{\partial x} & 1 \end{bmatrix} \begin{bmatrix} x_1 - v_1(x) - d_1(x) \\ y_1 - u_1(x) + d_1(x)\frac{\partial v_1}{\partial x} \end{bmatrix} \tag{2.19}
$$

Applying equations (2.18), (2.19) and (2.11), the coordinates of B'

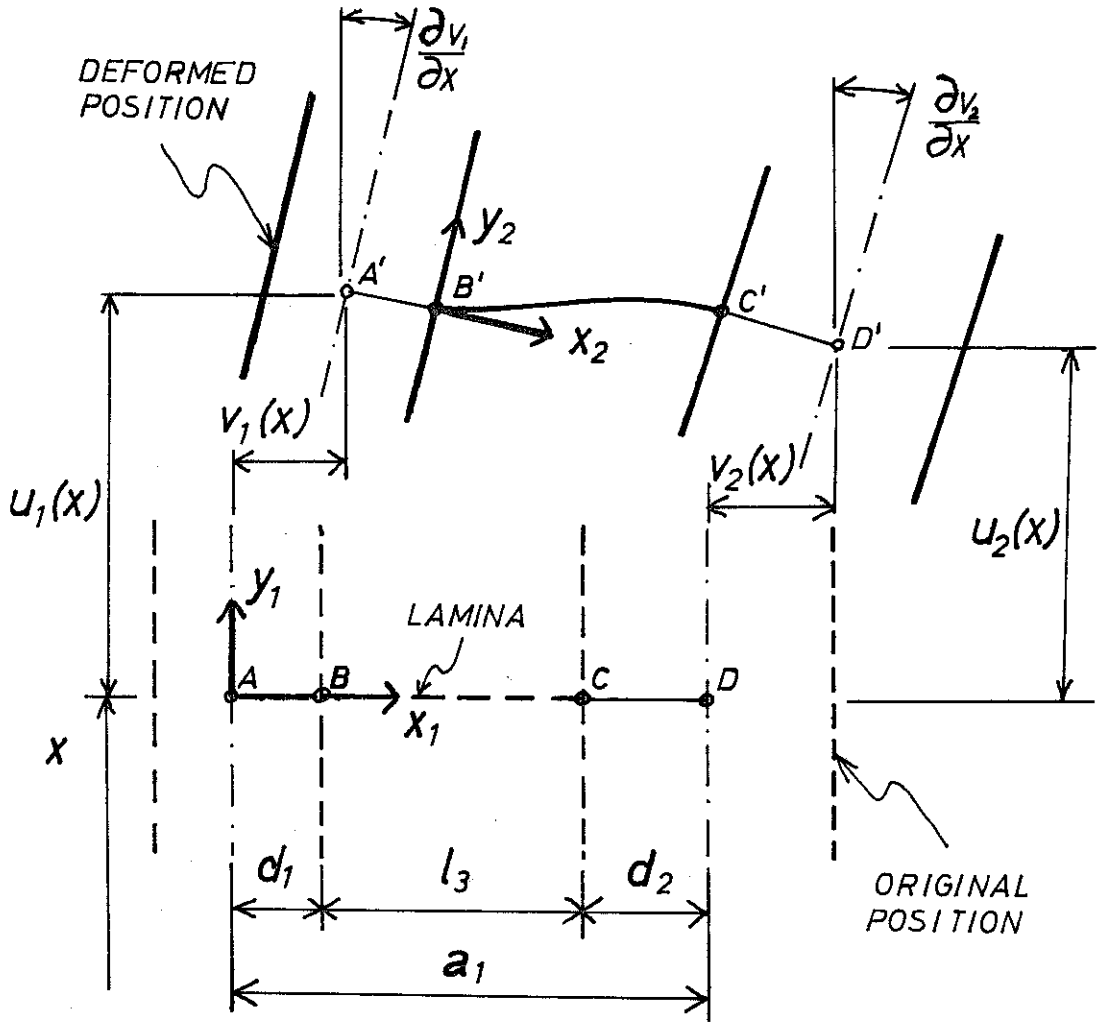

Fig. 2.3. Deformed Shape of Coupled Shear Wall at Position x

and C' in the x_2, y_2-system are found.

$$x_2(B') = y_2(B') = 0$$

$$x_2(C') = \ell_3 + v_2(x) - v_1(x) \tag{2.20}$$

$$y_2(C') = \ell_3 \frac{\partial v_1}{\partial x} + u_2(x) - u_1(x) + d_1(x) \frac{\partial v_1}{\partial x} + d_2(x) \frac{\partial v_2}{\partial x}$$

To apply the results of appendix A to the laminae, the notations θ, δ and ϵ are evaluated from Figure 2.3 and equation (2.20)

$$\theta = \frac{\partial v_1}{\partial x} - \frac{\partial v_2}{\partial x}$$

$$\epsilon = x_2(C') - \ell_3 = v_2(x) - v_1(x) \tag{2.21}$$

$$\delta = y_2(C') = u_2(x) - u_1(x) + \ell_3 \frac{\partial v_1}{\partial x} + d_1(x) \frac{\partial v_1}{\partial x} + d_2(x) \frac{\partial v_2}{\partial x}$$

For each lamina, the properties are given by equations (2.5) and (2.6). By using these properties and equation (2.21) in equation (A.17) of Appendix A, the total strain energy in one lamina is determined.

$$\Delta U_2 = \left\{ \frac{6\tilde{E}_3 i_3}{\ell_3^3 \beta^2} \left[\left(u_2 - u_1 + \ell_3 \frac{\partial v_1}{\partial x} + d_1 \frac{\partial v_1}{\partial x} + d_2 \frac{\partial v_2}{\partial x} \right) \left(u_2 - u_1 + d_1 \frac{\partial v_1}{\partial x} + d_2 \frac{\partial v_2}{\partial x} + \ell_3 \frac{\partial v_2}{\partial x} \right) + \frac{1}{12} (3 + \beta^2) \ell_3^2 \left(\frac{\partial v_1}{\partial x} - \frac{\partial v_2}{\partial x} \right)^2 \right] + \frac{\tilde{E}_3 a_3}{2\ell_3} (v_2 - v_1)^2 \right\} \Delta x \tag{2.22}$$

where

$$\beta^2 = 1 + \frac{12\tilde{E}_3 i_3 \tilde{k}}{\ell_3^2 \tilde{G}_3 a_3} \tag{2.23}$$

$$\tilde{k} = \tilde{k}(x) = k(x_j); \quad x,\ x \in [x_j - \tfrac{1}{2}a_2(x_{j-1}), x_j + \tfrac{1}{2}a_2(x_j)] \quad j = 1,2,\ldots,n \tag{2.24}$$

$k(x_j)$ is a numerical factor dependent upon the shape of the cross section of the spandrels[28]

$$k(x_j) = \frac{A_3(x_j)}{V(x_j)^2} \int_{A_3(x_j)} \tau^2 \, dA_3(x_j); \quad j = 1,2,\ldots,n \tag{2.25}$$

where τ is the shear stress and $V(x_j)$ the total shear force in the cross section of the spandrel

$$V(x_j) = \int_{A_3(x_j)} \tau \, dA_3(x_j); \quad j = 1,2,\ldots,n \tag{2.26}$$

For a rectangular cross section $k(x_j)$ is 1.2. The parameter β^2 is a measure of the relative flexural and shearing stiffnesses of the spandrel beams. Taking β^2 as unity is equivalent to neglecting the shearing resistance of the spandrels.

The strain energy in the system of laminae can finally be evaluated by letting Δx approach zero and integrating equation (2.22) over the height of the shear wall.

$$U_2 = \int_0^{\ell_3} \left\{ \frac{6\tilde{E}_3 i_3}{\ell_3^3 \beta^2} \left[\left(u_2 - u_1 + d_1 \frac{\partial v_1}{\partial x} + d_2 \frac{\partial v_2}{\partial x} + \ell_3 \frac{\partial v_1}{\partial x} \right) \left(u_2 - u_1 + d_1 \frac{\partial v_1}{\partial x} + d_2 \frac{\partial v_2}{\partial x} + \ell_3 \frac{\partial v_2}{\partial x} \right) + \frac{1}{12}(3+\beta^2)\ell_3^2 \left(\frac{\partial v_1}{\partial x} - \frac{\partial v_2}{\partial x} \right)^2 \right] + \frac{\tilde{E}_3 a_3}{2\ell_3} (v_2 - v_1)^2 \right\} dx \tag{2.27}$$

The total strain energy in the system is given by adding the contributions from the walls and spandrels, U_1 and U_2, respectively.

2.3. Derivation of Differential Equations and Boundary Conditions

Substituting from equations (2.13), (2.16) and (2.27), Hamilton's Principle, equation (2.1), becomes

$$\delta\int_{t_0}^{t_1}\int_0^{\ell_1}\Bigg\{\tfrac{1}{2}\rho_1 A_1\left[\left(\frac{\partial u_1}{\partial t}\right)^2+\left(\frac{\partial v_1}{\partial t}\right)^2\right]+\tfrac{1}{2}\rho_2 A_2\left[\left(\frac{\partial u_2}{\partial t}\right)^2+\left(\frac{\partial v_2}{\partial t}\right)^2\right]$$

$$+\tfrac{1}{2}\tilde{\rho}_3 a_3 \ell_3\left[\frac{\partial u_1}{\partial t}\frac{\partial u_2}{\partial t}+k_1\left(\frac{\partial u_2}{\partial t}-\frac{\partial u_1}{\partial t}\right)^2+\frac{\partial v_1}{\partial t}\frac{\partial v_2}{\partial t}+\frac{1}{3}\left(\frac{v_2}{\partial t}-\frac{\partial v_1}{\partial t}\right)^2\right]$$

$$-\tfrac{1}{2}E_1A_1\left(\frac{\partial u_1}{\partial x}\right)^2-\tfrac{1}{2}E_2A_2\left(\frac{\partial u_2}{\partial x}\right)^2-\tfrac{1}{2}E_1I_1\left(\frac{\partial^2 v_1}{\partial x^2}\right)^2-\tfrac{1}{2}E_2I_2\left(\frac{\partial^2 v_2}{\partial x^2}\right)^2$$

$$-\frac{6\tilde{E}_3 i_3}{\ell_3^3\beta^2}\left[\left(u_2-u_1+d_1\frac{\partial v_1}{\partial x}+d_2\frac{\partial v_2}{\partial x}+\ell_3\frac{\partial v_1}{\partial x}\right)\left(u_2-u_1+d_1\frac{\partial v_1}{\partial x}\right.\right.$$

$$\left.\left.+d_2\frac{\partial v_2}{\partial x}+\ell_3\frac{\partial v_2}{\partial x}\right)+\frac{\ell_3^2}{12}(3+\beta^2)\left(\frac{\partial v_1}{\partial x}-\frac{\partial v_2}{\partial x}\right)^2\right]$$

$$-\frac{\tilde{E}_3 a_3}{2\ell_3}(v_2-v_1)^2\Bigg\}\,dx\,dt=0 \qquad (2.28)$$

where

$$k_1=\frac{70\beta^4+7\beta^2+1}{210\beta^4} \qquad (2.29)$$

The variation in equation (2.28) is performed by varying u_i by δu_i and v_i by δv_i $(i=1,2)$, where it is understood that the variation vanishes at $t=t_0$ and $t=t_1$. Performing the variation and integrating by parts where necessary, produces the following equation:

$$\int_{t_0}^{t_1}\int_0^{\ell_1}\Big[-\rho_1 A_1 \frac{\partial^2 u_1}{\partial t^2} - \tfrac{1}{2}\tilde{\rho}_3 a_3 \ell_3 \Big\{2k_1 \frac{\partial^2 u_1}{\partial t^2} + (1-2k_1)\frac{\partial^2 u_2}{\partial t^2}\Big\} + \frac{\partial}{\partial x}\Big(E_1 A_1 \frac{\partial u_1}{\partial x}\Big)$$

$$+ \frac{6\tilde{E}_3 i_3}{\ell_3^3 \beta^2}\Big\{2u_2 - 2u_1 + (2d_1 + \ell_3)\frac{\partial v_1}{\partial x} + (2d_2 + \ell_3)\frac{\partial v_2}{\partial x}\Big\}\Big]\delta u_1 \, dx\, dt$$

$$+\int_{t_0}^{t_1}\int_0^{\ell_1}\Big[-\rho_2 A_2 \frac{\partial^2 u_2}{\partial t^2} - \tfrac{1}{2}\tilde{\rho}_3 a_3 \ell_3 \Big\{2k_1 \frac{\partial^2 u_2}{\partial t^2} + (1-2k_1)\frac{\partial^2 u_1}{\partial t^2}\Big\} + \frac{\partial}{\partial x}\Big(E_2 A_2 \frac{\partial u_2}{\partial x}\Big)$$

$$- \frac{6\tilde{E}_3 i_3}{\ell_3^3 \beta^2}\Big\{2u_2 - 2u_1 + (2d_1 + \ell_3)\frac{\partial v_1}{\partial x} + (2d_2 + \ell_3)\frac{\partial v_2}{\partial x}\Big\}\Big]\delta u_2 \, dx\, dt$$

$$+\int_{t_0}^{t_1}\int_0^{\ell_1}\Big[-\rho_1 A_1 \frac{\partial^2 v_1}{\partial t^2} - \frac{1}{6}\tilde{\rho}_3 a_3 \ell_3 \Big(2\frac{\partial^2 v_1}{\partial t^2} + \frac{\partial^2 v_2}{\partial t^2}\Big) - \frac{\partial^2}{\partial x^2}\Big(E_1 I_1 \frac{\partial^2 v_1}{\partial x^2}\Big)$$

$$+ \frac{\partial}{\partial x}\Big\{\frac{6\tilde{E}_3 i_3}{\ell_3^3 \beta^2}\Big[(\ell_3 + 2d_1)(u_2 - u_1) + 2d_1(d_1 + \ell_3)\frac{\partial v_1}{\partial x}$$

$$+ (2d_1 d_2 + \ell_3 a_1)\frac{\partial v_2}{\partial x} + \frac{\ell_3^2}{6}(3+\beta^2)\Big(\frac{\partial v_1}{\partial x} - \frac{\partial v_2}{\partial x}\Big)\Big]\Big\}$$

$$+ \frac{\tilde{E}_3 a_3}{\ell_3}(v_2 - v_1)\Big]\delta v_1 \, dx\, dt$$

$$+\int_{t_0}^{t_1}\int_0^{\ell_1}\Big[-\rho_2 A_2 \frac{\partial^2 v_2}{\partial t^2} - \frac{1}{6}\tilde{\rho}_3 a_3 \ell_3 \Big(2\frac{\partial^2 v_2}{\partial t^2} + \frac{\partial^2 v_1}{\partial t^2}\Big) - \frac{\partial^2}{\partial x^2}\Big(E_2 I_2 \frac{\partial^2 v_2}{\partial x^2}\Big)$$

$$+ \frac{\partial}{\partial x}\Big\{\frac{6\tilde{E}_3 i_3}{\ell_3^3 \beta^2}\Big[(\ell_3 + 2d_2)(u_2 - u_1) + (2d_1 d_2 + a_1 \ell_3)\frac{\partial v_1}{\partial x}$$

$$+ 2d_2(d_2 + \ell_3)\frac{\partial v_2}{\partial x} - \frac{\ell_3^2}{6}(3+\beta^2)\Big(\frac{\partial v_1}{\partial x} - \frac{\partial v_2}{\partial x}\Big)\Big]\Big\}$$

$$- \frac{\tilde{E}_3 a_3}{\ell_3}(v_2 - v_1)\Big]\delta v_2 \, dx\, dt$$

$$-\int_{t_0}^{t_1} E_1 A_1 \frac{\partial u_1}{\partial x}\,\delta u_1 \Big|_0^{\ell_1} dt - \int_{t_0}^{t_1} E_2 A_2 \frac{\partial u_2}{\partial x}\,\delta u_2 \Big|_0^{\ell_1} dt -$$

$$
- \int_{t_0}^{t_1} E_1 I_1 \frac{\partial^2 v_1}{\partial x^2} \frac{\partial \delta v_1}{\partial x} \Bigg|_0^{\ell_1} dt - \int_{t_0}^{t_1} E_2 I_2 \frac{\partial^2 v_2}{\partial x^2} \frac{\partial \delta v_2}{\partial x} \Bigg|_0^{\ell_1} dt
$$

$$
+ \int_{t_0}^{t_1} \left[\frac{\partial}{\partial x} \left(E_1 I_1 \frac{\partial^2 v_1}{\partial x^2} \right) - \frac{6 \tilde{E}_3 i_3}{\ell_3^3 \beta^2} \left\{ (2d_1 + \ell_3)(u_2 - u_1) + 2d_1 (d_1 + \ell_3) \frac{\partial v_1}{\partial x} \right. \right.
$$

$$
\left. \left. + (2d_1 d_2 + a_1 \ell_3) \frac{\partial v_2}{\partial x} + \frac{\ell_3^2}{6} (3 + \beta^2) \left(\frac{\partial v_1}{\partial x} - \frac{\partial v_2}{\partial x} \right) \right\} \right] \delta v_1 \Bigg|_0^{\ell_1} dt
$$

$$
+ \int_{t_0}^{t_1} \left[\frac{\partial}{\partial x} \left(E_2 I_2 \frac{\partial^2 v_2}{\partial x^2} \right) - \frac{6 \tilde{E}_3 i_3}{\ell_3^3 \beta^2} \left\{ (2d_2 + \ell_3)(u_2 - u_1) + (2d_1 d_2 + a_1 \ell_3) \frac{\partial v_1}{\partial x} \right. \right.
$$

$$
\left. \left. + 2d_2 (d_2 + \ell_3) \frac{\partial v_2}{\partial x} - \frac{\ell_3^2}{6} (3 + \beta^2) \left(\frac{\partial v_1}{\partial x} - \frac{\partial v_2}{\partial x} \right) \right\} \right] \delta v_2 \Bigg|_0^{\ell_1} dt
$$

$$
= 0 \qquad (2.30)
$$

If the following boundary conditions are satisfied at $x = 0$ and $x = \ell_1$,

$$
E_1 A_1 \frac{\partial u_1}{\partial x} = 0 , \quad \text{or} \quad u_1 = 0 \qquad (2.31a)
$$

$$
E_2 A_2 \frac{\partial u_2}{\partial x} = 0 , \quad \text{or} \quad u_2 = 0 \qquad (2.31b)
$$

$$
E_1 I_1 \frac{\partial^2 v_1}{\partial x^2} = 0 , \quad \text{or} \quad \frac{\partial v_1}{\partial x} = 0 \qquad (2.31c)
$$

$$
E_2 I_2 \frac{\partial^2 v_2}{\partial x^2} = 0 , \quad \text{or} \quad \frac{\partial v_2}{\partial x} = 0 \qquad (2.31d)
$$

$$\frac{\partial}{\partial x}\left(E_1 I_1 \frac{\partial^2 v_1}{\partial x^2}\right) - \frac{6\tilde{E}_3 i_3}{\ell_3^3 \beta^2}\left\{(2d_1+\ell_3)(u_2-u_1) + 2d_1(d_1+\ell_3)\frac{\partial v_1}{\partial x}\right.$$

$$\left. + (2d_1 d_2 + a_1 \ell_3)\frac{\partial v_2}{\partial x} + \frac{\ell_3^2}{6}(3+\beta^2)\left(\frac{\partial v_1}{\partial x} - \frac{\partial v_2}{\partial x}\right)\right\} = 0,$$

$$\text{or} \quad v_1 = 0 \tag{2.31e}$$

$$\frac{\partial}{\partial x}\left(E_2 I_2 \frac{\partial^2 v_2}{\partial x^2}\right) - \frac{6\tilde{E}_3 i_3}{\ell_3^3 \beta^2}\left\{(2d_2+\ell_3)(u_2-u_1) + (2d_1 d_2 + a_1 \ell_3)\frac{\partial v_1}{\partial x}\right.$$

$$\left. + 2d_2(d_2+\ell_3)\frac{\partial v_2}{\partial x} - \frac{\ell_3^2}{6}(3+\beta^2)\left(\frac{\partial v_1}{\partial x} - \frac{\partial v_2}{\partial x}\right)\right\} = 0,$$

$$\text{or} \quad v_2 = 0 \tag{2.31f}$$

then equation (2.30) implies that the differential equations of motion are

$$-\rho_1 A_1 \frac{\partial^2 u_1}{\partial t^2} - \frac{1}{2}\tilde{\rho}_3 a_3 \ell_3\left[2k_1 \frac{\partial^2 u_1}{\partial t^2} + (1-2k_1)\frac{\partial^2 u_2}{\partial t^2}\right] + \frac{\partial}{\partial x}\left(E_1 A_1 \frac{\partial u_1}{\partial x}\right)$$

$$+ \frac{6\tilde{E}_3 i_3}{\ell_3^3 \beta^2}\left[2u_2 - 2u_1 + (2d_1+\ell_3)\frac{\partial v_1}{\partial x} + (2d_2+\ell_3)\frac{\partial v_2}{\partial x}\right] = 0 \tag{2.32a}$$

$$-\rho_2 A_2 \frac{\partial^2 u_2}{\partial t^2} - \frac{1}{2}\tilde{\rho}_3 a_3 \ell_3\left[2k_1 \frac{\partial^2 u_2}{\partial t^2} + (1-2k_1)\frac{\partial^2 u_1}{\partial t^2}\right] + \frac{\partial}{\partial x}\left(E_2 A_2 \frac{\partial u_2}{\partial x}\right)$$

$$- \frac{6\tilde{E}_3 i_3}{\ell_3^3 \beta^2}\left[2u_2 - 2u_1 + (2d_1+\ell_3)\frac{\partial v_1}{\partial x} + (2d_2+\ell_3)\frac{\partial v_2}{\partial x}\right] = 0 \tag{2.32b}$$

$$-\rho_1 A_1 \frac{\partial^2 v_1}{\partial t^2} - \frac{1}{6}\tilde{\rho}_3 a_3 \ell_3 \left[2\frac{\partial^2 v_1}{\partial t^2} + \frac{\partial^2 v_2}{\partial t^2}\right] - \frac{\partial^2}{\partial x^2}\left(E_1 I_1 \frac{\partial^2 v_1}{\partial x^2}\right)$$

$$+ \frac{\partial}{\partial x}\left[\frac{6\tilde{E}_3 i_3}{\ell_3^3 \beta^2}\left\{(\ell_3 + 2d_1)(u_2 - u_1) + (2d_1 d_2 + a_1 \ell_3)\frac{\partial v_2}{\partial x}\right.\right.$$

$$\left.\left. + 2d_1(d_1 + \ell_3)\frac{\partial v_1}{\partial x} + \frac{\ell_3^2}{6}(3+\beta^2)\left(\frac{\partial v_1}{\partial x} - \frac{\partial v_2}{\partial x}\right)\right\}\right] + \frac{\tilde{E}_3 a_3}{\ell_3}(v_2 - v_1) = 0$$

(2.32c)

$$-\rho_2 A_2 \frac{\partial^2 v_2}{\partial t^2} - \frac{1}{6}\tilde{\rho}_3 a_3 \ell_3 \left[2\frac{\partial^2 v_2}{\partial t^2} + \frac{\partial^2 v_1}{\partial t^2}\right] - \frac{\partial^2}{\partial x^2}\left(E_2 I_2 \frac{\partial^2 v_2}{\partial x^2}\right)$$

$$+ \frac{\partial}{\partial x}\left[\frac{6\tilde{E}_3 i_3}{\ell_3^3 \beta^2}\left\{(\ell_3 + 2d_2)(u_2 - u_1) + (2d_1 d_2 + a_1 \ell_3)\frac{\partial v_1}{\partial x}\right.\right.$$

$$\left.\left. + 2d_2(d_2 + \ell_3)\frac{\partial v_2}{\partial x} - \frac{\ell_3^2}{6}(3+\beta^2)\left(\frac{\partial v_1}{\partial x} - \frac{\partial v_2}{\partial x}\right)\right\}\right] - \frac{\tilde{E}_3 a_3}{\ell_3}(v_2 - v_1) = 0$$

(2.32d)

Equations (2.32) are a set of partial differential equations in the space x and t, with variable coefficients. The associated boundary conditions are given in equation (2.31), including both the natural and geometric boundary conditions. That is, equations (2.31a) and (2.31b) give the appropriate conditions for no longitudinal force or no longitudinal deflection at the boundaries, equations (2.31c) and (2.31d) give the conditions for no applied moment or no slope, and finally equations (2.31e) and (2.31f) give the conditions for no applied lateral shear force or no lateral deflection at the ends of the two walls.

If no major simplifications can be made in equations (2.31) and (2.32), the solution for natural frequencies and mode shapes can only

be obtained by approximate methods, for instance the Ritz Method or the Galerkin Method.[29]

2.4. Reduction to the Case of Constant Properties

By making additional assumptions on the properties of the coupled shear walls, considerable simplifications in the differential equations and boundary conditions can be made. The first approximation will be to make all properties of the walls, equation (2.2), constant. Further, all spandrels will be assumed to be of the same material, E_3, G_3 and ρ_3, and the dimensions of the spandrels will be such that equation (2.9) is satisfied. Under these conditions, it proves convenient to introduce new deformation variables

$$\begin{aligned} \bar{u} &= u_1 + u_2 \\ \hat{u} &= u_1 - u_2 \\ \hat{v} &= v_1 + v_2 \\ \bar{v} &= v_1 - v_2 \end{aligned} \tag{2.33}$$

such that the symmetrical ($\bar{u}$ and $\hat{v}$) and antisymmetrical ($\hat{u}$ and $\bar{v}$) displacements can be distinguished. The displacements $\hat{u}$ and $\hat{v}$ are in general the most significant. The set of equations in (2.32) can now be transformed into a set of four differential equations in the variables of equation (2.33) by adding and subtracting equations (2.32a) and (2.32b), and adding and subtracting equations (2.32c) and (2.32d). For this simplified case, the following equations are obtained.

$$-\tfrac{1}{2}\left[\rho_1 A_1+\rho_2 A_2+\rho_3 A_3 \frac{\ell_3}{a_2}\right]\frac{\partial^2 \bar{u}}{\partial t^2} -\tfrac{1}{2}\left[\rho_1 A_1-\rho_2 A_2\right]\frac{\partial^2 \hat{u}}{\partial t^2}$$

$$+\tfrac{1}{2}(E_1 A_1+E_2 A_2)\frac{\partial^2 \bar{u}}{\partial x^2}+\tfrac{1}{2}(E_1 A_1-E_2 A_2)\frac{\partial^2 \hat{u}}{\partial x^2}=0 \qquad (2.34a)$$

$$-\tfrac{1}{2}\left[\rho_1 A_1+\rho_2 A_2+2k_u\rho_3 A_3 \frac{\ell_3}{a_2}\right]\frac{\partial^2 \hat{u}}{\partial t^2} -\tfrac{1}{2}\left[\rho_1 A_1-\rho_2 A_2\right]\frac{\partial^2 \bar{u}}{\partial t^2}$$

$$+\tfrac{1}{2}(E_1 A_1+E_2 A_2)\frac{\partial^2 \hat{u}}{\partial x^2}+\tfrac{1}{2}(E_1 A_1-E_2 A_2)\frac{\partial^2 \bar{u}}{\partial x^2}$$

$$+\frac{12E_3 I_3}{a_2 \ell_3^3 \beta^2}\left[-2\hat{u}+a_1\frac{\partial \hat{v}}{\partial x}+(d_1-d_2)\frac{\partial \bar{v}}{\partial x}\right]=0 \qquad (2.34b)$$

$$-\tfrac{1}{2}\left[\rho_1 A_1+\rho_2 A_2+\rho_3 A_3 \frac{\ell_3}{a_2}\right]\frac{\partial^2 \hat{v}}{\partial t^2} -\tfrac{1}{2}\left[\rho_1 A_1-\rho_2 A_2\right]\frac{\partial^2 \bar{v}}{\partial t^2}$$

$$-\tfrac{1}{2}(E_1 I_1+E_2 I_2)\frac{\partial^4 \hat{v}}{\partial x^4} -\tfrac{1}{2}(E_1 I_1-E_2 I_2)\frac{\partial^4 \bar{v}}{\partial x^4}$$

$$+\frac{6E_3 I_3 a_1}{a_2 \ell_3^3 \beta^2}\left[-2\frac{\partial \hat{u}}{\partial x}+a_1\frac{\partial^2 \hat{v}}{\partial x^2}+(d_1-d_2)\frac{\partial^2 \bar{v}}{\partial x^2}\right]=0 \qquad (2.34c)$$

$$-\tfrac{1}{2}\left[\rho_1 A_1+\rho_2 A_2+\tfrac{1}{3}\rho_3 A_3 \frac{\ell_3}{a_2}\right]\frac{\partial^2 \bar{v}}{\partial t^2} -\tfrac{1}{2}\left[\rho_1 A_1-\rho_2 A_2\right]\frac{\partial^2 \hat{v}}{\partial t^2}$$

$$-\tfrac{1}{2}(E_1 I_1+E_2 I_2)\frac{\partial^4 \bar{v}}{\partial x^4} -\tfrac{1}{2}(E_1 I_1-E_2 I_2)\frac{\partial^4 \hat{v}}{\partial x^4}$$

$$+\frac{6E_3 I_3}{a_2 \ell_3^3 \beta^2}\left[2(d_2-d_1)\frac{\partial \hat{u}}{\partial x}+a_1(d_1-d_2)\frac{\partial^2 \hat{v}}{\partial x^2}\right.$$

$$\left.+(d_1-d_2)^2\frac{\partial^2 \bar{v}}{\partial x^2}+\frac{\ell_3^2\beta^2}{3}\frac{\partial^2 \bar{v}}{\partial x^2}\right]-\frac{2E_3 A_3}{a_2 \ell_3}\bar{v}=0 \qquad (2.34d)$$

Using equation (2.29), k_u can be defined by

$$k_u = \tfrac{1}{2}[\,4k_1 - 1\,] = \frac{35\beta^4+14\beta^2+2}{210\beta^4} \tag{2.35}$$

and it can be observed that k_u is only a function of the relative shear stiffness of the spandrels. The numerical value of k_u lies between 0.167 (only shearing deformations in the spandrels) and 0.243 (only bending deformations in the spandrels).

From equation (2.23), the parameter β^2 is now given by

$$\beta^2 = 1 + \frac{12\,E_3I_3k}{G_3A_3\ell_3^2} \tag{2.36}$$

where k is defined in equation (2.25).

The boundary conditions associated with the differential equations (2.34) can similarly be obtained from equation (2.31)

$$\tfrac{1}{2}(E_1A_1+E_2A_2)\frac{\partial\bar{u}}{\partial x} + \tfrac{1}{2}(E_1A_1-E_2A_2)\frac{\partial\hat{u}}{\partial x} = 0, \quad \text{or} \quad \bar{u} = 0 \tag{2.37a}$$

$$\tfrac{1}{2}(E_1A_1+E_2A_2)\frac{\partial\hat{u}}{\partial x} + \tfrac{1}{2}(E_1A_1-E_2A_2)\frac{\partial\bar{u}}{\partial x} = 0, \quad \text{or} \quad \hat{u} = 0 \tag{2.37b}$$

$$\tfrac{1}{2}(E_1I_1+E_2I_2)\frac{\partial^2\hat{v}}{\partial x^2} + \tfrac{1}{2}(E_1I_1-E_2I_2)\frac{\partial^2\bar{v}}{\partial x^2} = 0, \text{ or } \frac{\partial\hat{v}}{\partial x} = 0 \tag{2.37c}$$

$$\tfrac{1}{2}(E_1I_1+E_2I_2)\frac{\partial^2 v}{\partial x^2} + \tfrac{1}{2}(E_1I_1-E_2I_2)\frac{\partial^2\hat{v}}{\partial x^2} = 0, \text{ or } \frac{\partial\bar{v}}{\partial x} = 0 \tag{2.37d}$$

$$\tfrac{1}{2}(E_1I_1+E_2I_2)\frac{\partial^3\hat{v}}{\partial x^3}+\tfrac{1}{2}(E_1I_1-E_2I_2)\frac{\partial^3\bar{v}}{\partial x^3}$$

$$-\frac{6E_3I_3}{a_2\ell_3^3\beta^2}\left[-2a_1\hat{u}+a_1^2\frac{\partial\hat{v}}{\partial x}+a_1(d_1-d_2)\frac{\partial\bar{v}}{\partial x}\right]=0,\quad \text{or}\quad \hat{v}=0 \tag{2.37e}$$

$$\tfrac{1}{2}(E_1I_1+E_2I_2)\frac{\partial^3\bar{v}}{\partial x^3}+\tfrac{1}{2}(E_1I_1-E_2I_2)\frac{\partial^3\hat{v}}{\partial x^3}-\frac{6E_3I_3}{a_2\ell_3^3\beta^2}\left[2(d_2-d_1)\hat{u}\right.$$

$$\left.+a_1(d_1-d_2)\frac{\partial\hat{v}}{\partial x}+\left\{(d_1-d_2)^2+\frac{\beta^2\ell_3^2}{3}\right\}\frac{\partial\bar{v}}{\partial x}\right]=0,\quad \text{or}\quad \bar{v}=0 \tag{2.37f}$$

The procedure for solving this system of linear, partial differential equations (2.34) for given boundary conditions could follow exactly the technique applied to the reduced case in chapter III, section 3.1, where a detailed analysis is given.

2.5. Application to Equal Walls with Constant Properties

In many buildings, the coupled shear wall system is symmetrical, that is, the two walls are identical. This case will be studied in detail in subsequent chapters, and it will be convenient to introduce a common notation for the properties of the two walls. Thus, in accordance with equation (2.2), A_1, E_1, I_1, ρ_1 and d_1 will subsequently denote the properties of both walls, and the properties will be taken to be constant along the height of the building.

$$-\left(\rho_1 A_1 + \frac{1}{2}\rho_3 \ell_3 \frac{A_3}{a_2}\right)\frac{\partial^2 \bar{u}}{\partial t^2} + E_1 A_1 \frac{\partial^2 \bar{u}}{\partial x^2} = 0 \tag{2.38a}$$

$$-\left(\rho_1 A_1 + k_u \rho_3 \ell_3 \frac{A_3}{a_2}\right)\frac{\partial^2 \hat{u}}{\partial t^2} + E_1 A_1 \frac{\partial^2 \hat{u}}{\partial x^2} - \frac{12 E_3 I_3}{a_2 \ell_3^3 \beta^2}\left(2\hat{u} - a_1 \frac{\partial \hat{v}}{\partial x}\right) = 0 \tag{2.38b}$$

$$-\left(\rho_1 A_1 + \frac{1}{2}\rho_3 \ell_3 \frac{A_3}{a_2}\right)\frac{\partial^2 \hat{v}}{\partial t^2} - E_1 I_1 \frac{\partial^4 \hat{v}}{\partial x^4} + \frac{6 E_3 I_3 a_1}{a_2 \ell_3^3 \beta^2}\left(a_1 \frac{\partial^2 \hat{v}}{\partial x^2} - 2\frac{\partial \hat{u}}{\partial x}\right) = 0 \tag{2.38c}$$

$$-\left(\rho_1 A_1 + \frac{1}{6}\rho_3 \ell_3 \frac{A_3}{a_2}\right)\frac{\partial^2 \bar{v}}{\partial t^2} - E_1 I_1 \frac{\partial^4 \bar{v}}{\partial x^4} + \frac{2 E_3 I_3}{a_2 \ell_3}\frac{\partial^2 \bar{v}}{\partial x^2} - \frac{2 E_3 A_3}{a_2 \ell_3}\bar{v} = 0 \tag{2.38d}$$

Similarly, the boundary conditions, equation (2.35) reduces to

$$E_1 A_1 \frac{\partial \bar{u}}{\partial x} = 0 \ , \quad \text{or} \quad \bar{u} = 0 \tag{2.39a}$$

$$E_1 A_1 \frac{\partial \hat{u}}{\partial x} = 0 \ , \quad \text{or} \quad \hat{u} = 0 \tag{2.39b}$$

$$E_1 I_1 \frac{\partial^2 \hat{v}}{\partial x^2} = 0 \ , \quad \text{or} \quad \frac{\partial \hat{v}}{\partial x} = 0 \tag{2.39c}$$

$$E_1 I_1 \frac{\partial^2 \bar{v}}{\partial x^2} = 0 \ , \quad \text{or} \quad \frac{\partial \bar{v}}{\partial x} = 0 \tag{2.39d}$$

$$E_1 I_1 \frac{\partial^3 \hat{v}}{\partial x^3} - \frac{6E_3 I_3 a_1}{a_2 \ell_3^3 \beta^2}\left(a_1 \frac{\partial \hat{v}}{\partial x} - 2\hat{u}\right) = 0 \ , \quad \text{or} \quad \hat{v} = 0 \tag{2.39e}$$

$$E_1 I_1 \frac{\partial^3 \bar{v}}{\partial x^3} - \frac{2E_3 I_3}{a_2 \ell_3} \frac{\partial \bar{v}}{\partial x} = 0 \ , \quad \text{or} \quad \bar{v} = 0 \tag{2.39f}$$

It is observed that the differential equations have been greatly simplified, uncoupling into three different problems. The symmetrical, vertical motion, $\bar{u}$, uncouples from the other deformations into the well-known differential equation for longitudinal vibration of a bar, i.e. from equation (2.38) and (2.39)

$$E_1 A_1 \frac{\partial^2 \bar{u}}{\partial x^2} - \left(\rho_1 A_1 + \frac{1}{2}\rho_3 \ell_3 \frac{A_3}{a_2}\right)\frac{\partial^2 u}{\partial t^2} = 0; \qquad x \in [0, \ell_1] \tag{2.40}$$

with

$$E_1 A_1 \frac{\partial u}{\partial x} = 0, \quad \text{or} \quad \bar{u} = 0 \quad \text{at} \quad x = 0, \ell_1 \tag{2.41}$$

The antisymmetrical horizontal motion $\bar{v}$ also uncouples from the other deformations. From equations (2.38) and (2.39)

$$E_1 I_1 \frac{\partial^4 \bar{v}}{\partial x^4} - \frac{2E_3 I_3}{a_2 \ell_3} \frac{\partial^2 \bar{v}}{\partial x^2} + \frac{2E_3 A_3}{a_2 \ell_3} \bar{v} + \left(\rho_1 A_1 + \frac{1}{6}\rho_3 \ell_3 \frac{A_3}{a_2}\right)\frac{\partial^2 \bar{v}}{\partial t^2} = 0;$$

$$x \in [0, \ell_1] \tag{2.42}$$

with

$$\left.\begin{aligned} E_1 I_1 \frac{\partial^2 \bar{v}}{\partial x^2} = 0, \quad \text{or} \quad \frac{\partial \bar{v}}{\partial x} = 0 \\ E_1 I_1 \frac{\partial^3 \bar{v}}{\partial x^3} - \frac{2E_3 I_3}{a_2 \ell_3} \frac{\partial \bar{v}}{\partial x} = 0, \quad \text{or} \quad \bar{v} = 0 \end{aligned}\right\} \text{at} \quad x = 0, \ell_1 \tag{2.43}$$

This differential equation has the same form as the equation for a beam on an elastic foundation with end loads.[30]

The two remaining variables, $\hat{u}$ and $\hat{v}$, describe the coupled, lateral and vertical motions of the shear wall system which are of the most practical importance. The two variables are coupled together in the differential equations as well as the boundary conditions. From equations (2.38) and (2.39)

$$\begin{aligned} & E_1 A_1 \frac{\partial^2 \hat{u}}{\partial x^2} + \frac{12 E_3 I_3}{a_2 \ell_3^3 \beta^2}\left(a_1 \frac{\partial \hat{v}}{\partial x} - 2\hat{u}\right) \\ & \quad - \left(\rho_1 A_1 + k_u \rho_3 \ell_3 \frac{A_3}{a_2}\right)\frac{\partial^2 \hat{u}}{\partial t^2} = 0 \\ & E_1 I_1 \frac{\partial^4 \hat{v}}{\partial x^4} - \frac{6 E_3 I_3 a_1}{a_2 \ell_3^3 \beta^2}\left(a_1 \frac{\partial^2 \hat{v}}{\partial x^2} - 2\frac{\partial \hat{u}}{\partial x}\right) \\ & \quad + \left(\rho_1 A_1 + \frac{1}{2}\rho_3 \ell_3 \frac{A_3}{a_2}\right)\frac{\partial^2 \hat{v}}{\partial t^2} = 0 \end{aligned} \qquad x \in [0, \ell_1] \quad (2.44)$$

with

$$\left.\begin{aligned} & E_1 A_1 \frac{\partial \hat{u}}{\partial x} = 0, \quad \text{or} \quad \hat{u} = 0 \\ & E_1 I_1 \frac{\partial^2 \hat{v}}{\partial x^2} = 0, \quad \text{or} \quad \frac{\partial \hat{v}}{\partial x} = 0 \\ & E_1 I_1 \frac{\partial^3 v}{\partial x^3} - \frac{6 E_3 I_3 a_1}{a_2 \ell_3^3 \beta^2}\left(a_1 \frac{\partial \hat{v}}{\partial x} - 2\hat{u}\right) = 0, \quad \text{or} \quad \hat{v} = 0 \end{aligned}\right\} \text{at } x = 0, \ell_1 \quad (2.45)$$

Equations (2.44) and (2.45) define the dynamic problem that will be studied in chapters III and IV. With regard to further reduction, it can be observed that if the spandrels become weak, $E_3 I_3 \to 0$,

then the system of equations (2.44) uncouples into a u-motion, with the same form as equation (2.40), and into an Euler-Bernoulli equation for the $\hat{v}$-motion

$$E_1 I_1 \frac{\partial^4 \hat{v}}{\partial x^4} + \left(\rho_1 A_1 + \frac{1}{2}\rho_3 \ell_3 \frac{A_3}{a_2}\right)\frac{\partial^4 \hat{v}}{\partial t^2} = 0 \qquad (2.46)$$

CHAPTER III

DYNAMIC ANALYSIS OF EQUAL-SIZED SHEAR WALLS

In this chapter the eigenvalue problem for a coupled shear wall will be solved for the case in which the two walls have the same properties. The boundary conditions will be those appropriate for a building: fixed at the base $(x = 0)$ and free at the top $(x = \ell_1)$. In order to simplify the notation and to present the results in a general way, dimensionless parameters will be introduced. In section 3.1 the eigenvalue-equation and the equation for the eigenvectors are derived. For practical application, the natural frequencies corresponding to principally horizontal motion are the most interesting cases, and it will be assumed in section 3.2 and the rest of the chapter that the term associated with the vertical inertia ($\hat{u}$-motion) can be neglected. It will be shown in chapter IV that this assumption is justified for the first few eigenvalues.

In section 3.2 the eigenvalues and mode shapes for lateral vibration are obtained; section 3.3 deals with some asymptotic behavior of these eigenvalues and mode shapes; and in section 3.4 the effects of the parameters on the solution are discussed.

3.1. Derivation of Eigenvalues and Eigenvectors

It is convenient to non-dimensionalize the length and time variables as well as the displacement variables. Thus, let

$$\xi = x/\ell_1$$

$$\tau = \omega t \qquad (3.1)$$

$$v = \hat{v}/\ell_1$$

$$u = 2\hat{u}/a_1$$

where ω is the frequency of oscillation. Further, the material and dimensional properties of the coupled shear wall can be represented by three dimensionless parameters,

$$\Pi_1 = \frac{6E_3I_3a_1^2\ell_1^2}{E_1I_1\beta^2a_2\ell_3^3}$$

$$\Pi_2 = \frac{4I_1}{a_1^2A_1} \qquad (3.2)$$

$$\Pi_3 = \frac{I_1}{\ell_1^2A_1} \cdot \frac{\rho_1A_1a_2 + k_u\rho_3\ell_3A_3}{\rho_1A_1a_2 + \frac{1}{2}\rho_3\ell_3A_3}$$

in which the properties of the spandrels are given by E_3, I_3, A_3, ℓ_3, ρ_3 (Young's Modulus, moment of inertia, cross-sectional area, length and mass density) and the properties of the two equal walls are similarly given by E_1, I_1, A_1, ℓ_1, ρ_1. a_1 is the distance between the neutral axes of the two walls; β^2 is defined in equation (2.36); and k_u are introduced in equation (2.35). The frequencies of oscillation will also be made nondimensional by introducing

$$\lambda^2 = \frac{(\rho_1A_1 + \frac{1}{2}\rho_3\ell_3\frac{A_3}{a_2})\ell_1^4\omega^2}{E_1I_1} \qquad (3.3)$$

With the use of equations (3.1), (3.2) and (3.3), the differential equations of motion, equation (2.44) can now be written as

$$\begin{aligned} v_{\xi\xi\xi\xi} - \Pi_1 v_{\xi\xi} + \Pi_1 u_{\xi} + \lambda^2 v_{\tau\tau} = 0 \\ u_{\xi\xi} + \Pi_1\Pi_2 v_{\xi} - \Pi_1\Pi_2 u - \lambda^2 \Pi_3 u_{\tau\tau} = 0 \end{aligned} \tag{3.4}$$

where the usual notation for partial derivatives has been employed.

In order to present a general method of solution for the eigenvalue problem, applicable both to the present case and also to the system of differential equations (2.34), a symbolic notation will be introduced. Equation (3.4) can thus be written as

$$\underline{L}[\underline{w}(\xi,\tau)] = \underline{0}; \qquad \xi \in \langle 0,1 \rangle; \qquad \tau > 0 \tag{3.5}$$

where

$$\underline{L}[\underline{w}] = \begin{bmatrix} L_1[\underline{w}] \\ L_2[\underline{w}] \end{bmatrix} = \begin{bmatrix} v_{\xi\xi\xi\xi} - \Pi_1 v_{\xi\xi} + \Pi_1 u_{\xi} + \lambda^2 v_{\tau\tau} \\ u_{\xi\xi} + \Pi_1\Pi_2 v_{\xi} - \Pi_1\Pi_2 u - \lambda^2 \Pi_3 u_{\tau\tau} \end{bmatrix} \tag{3.6}$$

$$\underline{w} = \begin{bmatrix} u(\xi,\tau) \\ v(\xi,\tau) \end{bmatrix} \tag{3.7}$$

L_1 and L_2 being linear, partial differential operators. Similarly, the boundary conditions given in equation (2.45) can, for a fixed-free condition, be expressed as

$$\underline{B}_1[\underline{w}(0,\tau)] = \begin{bmatrix} B_{11}[\underline{w}(0,\tau)] \\ B_{12}[\underline{w}(0,\tau)] \\ B_{13}[\underline{w}(0,\tau)] \end{bmatrix} = \begin{bmatrix} v(0,\tau) \\ v_{\xi}(0,\tau) \\ u(0,\tau) \end{bmatrix} = \underline{0}$$

$$\underline{B}_2[\underline{w}(1,\tau)] = \begin{bmatrix} B_{21}[\underline{w}(1,\tau)] \\ B_{22}[\underline{w}(1,\tau)] \\ B_{23}[\underline{w}(1,\tau)] \end{bmatrix} = \begin{bmatrix} v_{\xi\xi}(1,\tau) \\ v_{\xi\xi\xi}(1,\tau) - \Pi_1(v_{\xi}(1,\tau) - u(1,\tau)) \\ u_{\xi}(1,\tau) \end{bmatrix} = \underline{0} \tag{3.8}$$

Discussion of Parameters

Equations (3.5) and (3.8) completely describe the vibrational problem. For a given structure, the parameters Π_1, Π_2 and Π_3 are numerical constants, and it is clear that the eigenvalues and mode shapes will depend upon their numerical values. It is therefore of importance to study the physical meaning and numerical range of these parameters.

It can be observed from equation (3.2) that Π_1 includes all properties of the spandrels, in particular the bending stiffness (E_3I_3) and relative shear stiffness (β^2, equation (2.36)) which do not occur in any of the other parameters. This is an essential feature in a later comparison of theories for sandwich beams and coupled shear walls. Using equation (2.36), Π_1 can also be written as

$$\Pi_1 = \frac{6a_1^2\ell_1^2}{E_1I_1a_2\ell_3^3} \; \frac{(E_3I_3)\cdot(G_3A_3\ell_3^2)}{(G_3A_3\ell_3^2 + 12\,E_3I_3k)} \tag{3.9}$$

From this it follows that if the shearing rigidity in the spandrels is high compared to the bending rigidity, i.e. $G_3A_3\ell_3^2 >> 12\,E_3I_3k$,

$$\Pi_1 \doteq \frac{6\, E_3 I_3 a_1^2 \ell_1^2}{E_1 I_1 a_2 \ell_3^3} \tag{3.10}$$

and the spandrels deform mainly in bending. If the opposite is the case, $12\, E_3 I_3 k \gg G_3 A_3 \ell_3^2$, then

$$\Pi_1 \doteq \frac{G_3 A_3 a_1^2 \ell_1^2}{2\, E_1 I_1 a_2 \ell_3 k} \tag{3.11}$$

and the spandrels deform principally in shear. Assuming that the spandrel system deforms in shear only, k must be taken as unity since the definition of k, equation (2.25), assumed that the spandrels deformed according to bending theory. From equation (3.11), Π_1 will then become

$$\Pi_1 = \frac{G_3 A_3 a_1^2 \ell_1^2}{2\, E_1 I_1 a_2 \ell_3} \tag{3.12}$$

For this case, the system of continuous laminae could be replaced by a continuous medium which is restricted to deform in shear only. Such a medium would deform in straight lines and, in effect, adjacent, horizontal elements of the medium would deform independently of the next, exactly like the system of laminae, provided the laminae deform only as shear beams.

From the above expressions for Π_1, it can also be observed that, with constant wall properties, Π_1 gives a general measure of the stiffness of the spandrels. Large values of Π_1 indicate stiff spandrels whereas Π_1 becomes smaller with decreasing spandrel strength. Setting Π_1 equal to zero eliminates the spandrel system,

and the differential equations reduce to that of a simple Euler-Bernoulli beam, equation (2.46). There are no theoretical restrictions on the range of Π_1, except that it be positive, but for most applications to building structures, Π_1 appears to lie between 1 and 10,000. In the models studied by W. K. Tso[13], Π_1 varied from about 2 to about 1,000.

The parameter Π_2 always appears together with Π_1 as a product, but for later work it proves convenient to define it as done in equation (3.2). Essentially, Π_2 is a measure of the relative axial and bending stiffnesses of the shear wall system. When a_1, or A_1, increases, Π_2 decreases and the vertical motion, u, will become smaller in magnitude. In order to neglect this displacement altogether, Π_2 can be taken as zero, but this leads to erroneous results for most cases as will be shown in section 3.3. If the two shear walls have rectangular cross sections, then an upper limit for Π_2 can be found. In this case

$$I_1 = \frac{1}{12} A_1 (2d_1)^2 \tag{3.13}$$

and Π_2 can be written as

$$\Pi_2 = \frac{4}{3}\left(\frac{d_1}{a_1}\right)^2 = \frac{4}{3}\left(\frac{d_1}{2d_1 + \ell_3}\right)^2 \tag{3.14}$$

which implies that

$$\Pi_2 < \frac{1}{3} \tag{3.15}$$

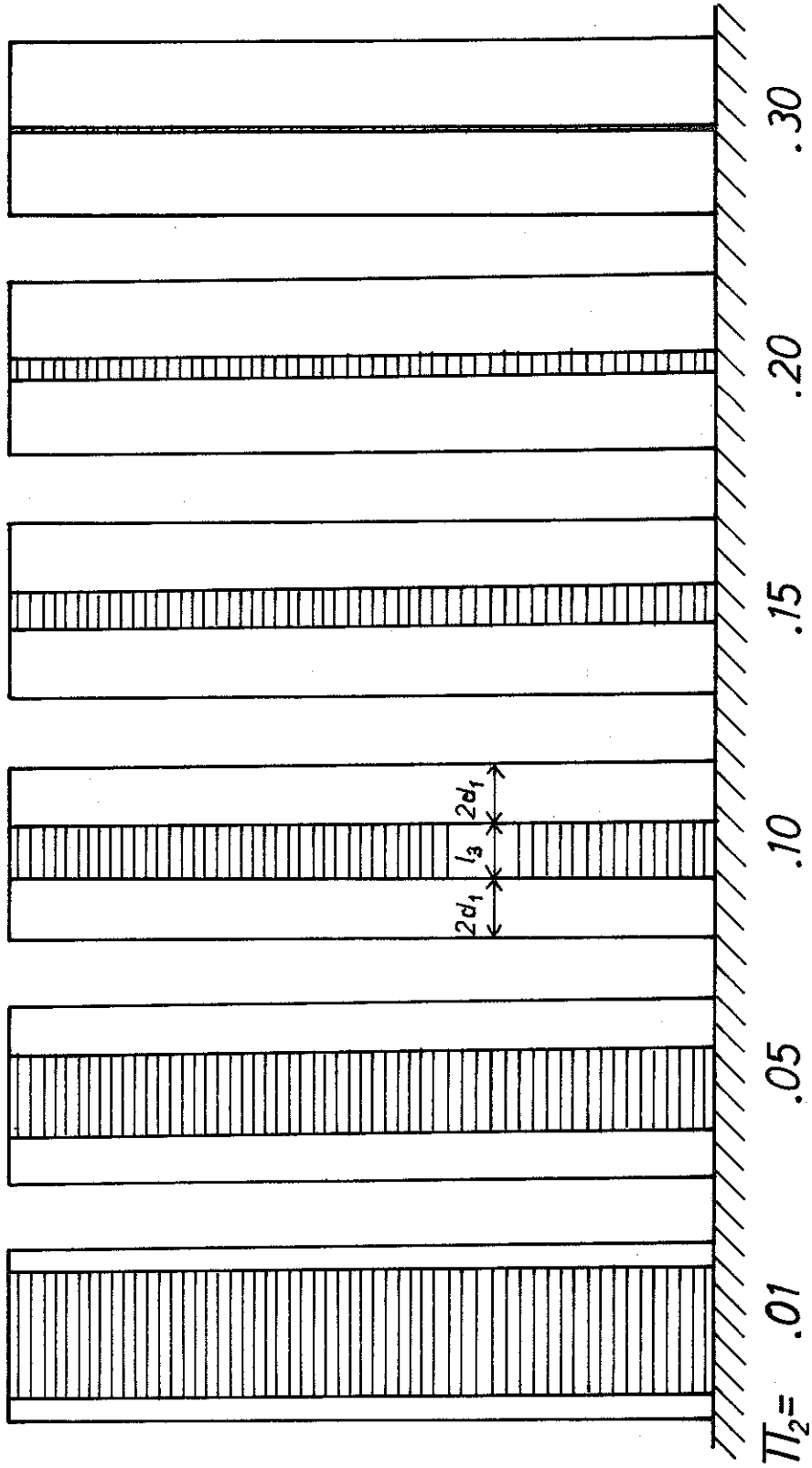

Fig. 3.1. Identical Shear Walls with Different Values of Π_2

Figure 3.1 illustrates the influence the opening (ℓ_3) and the depth of the two walls ($2d_1$) have upon the parameter Π_2.

The parameter Π_3 appears only in the vertical inertia beam (equation (3.4)) and can therefore be said to be a measure of the relative influence of this term. Later in this chapter, the vertical inertia will be neglected, which can be done by setting Π_3 equal to zero.

From equation (2.35) it can be observed that k_u is always less than $\frac{1}{2}$. Further, if the two shear walls have rectangular cross sections, such that equation (3.12) holds, then

$$\Pi_3 < \frac{1}{3}\left(\frac{d_1}{\ell_1}\right)^2 \tag{3.16}$$

For the shear wall dimensions considered in the analysis, the length to depth ratio of each wall should be larger than five, or

$$\frac{d_1}{\ell_1} < 10 \tag{3.17}$$

which gives an approximate upper bound on realistic values of Π_3

$$\Pi_3 < \frac{1}{300} \tag{3.18}$$

Solution of the Equations

The differential equation (3.5) can be reduced to a single differential equation in the lateral displacement v. By differentiating L_2 with respect to ξ and replacing u_ξ by the expression for v obtained from L_1, the resulting equation is

$$v_{\xi\xi\xi\xi\xi\xi} - \Pi_1(1 + \Pi_2)v_{\xi\xi\xi\xi} - \Pi_3\lambda^2 v_{\xi\xi\xi\xi\tau\tau} + \lambda^2(1 + \Pi_1\Pi_3)v_{\xi\xi\tau\tau}$$

$$- \lambda^2\Pi_1\Pi_2 v_{\tau\tau} - \lambda^4\Pi_3 v_{\tau\tau\tau\tau} = 0 \qquad (3.19)$$

Equation (3.19) could be used in deriving the eigenvalue equation, but the following procedure has the advantage of being more readily applied to possible study of the case of unequal walls, equation (2.34).

The procedure begins by assuming an oscillatory solution to the free vibration described by equations (3.5) and (3.8)

$$\underline{w}(\xi,\tau) = \underline{W}(\xi)e^{i\tau} \qquad (3.20)$$

where

$$\underline{W}(\xi) = \begin{bmatrix} U(\xi) \\ V(\xi) \end{bmatrix} \qquad (3.21)$$

By substituting this equation into equation (3.5), two ordinary differential equations are obtained

$$\underline{L}^*[\underline{W}(\xi)] = \underline{0} \qquad \xi \in \langle 0,1 \rangle \qquad (3.22)$$

or

$$\begin{aligned} V'''' - \Pi_1 V'' + \Pi_1 U' - \lambda^2 V = 0 \\ U'' + \Pi_1\Pi_2 V' - (\Pi_1\Pi_2 - \lambda^2\Pi_3)U = 0 \end{aligned} \qquad (3.23)$$

in which

$$(\,)' \equiv \frac{d}{d\xi}$$

Similarly, the boundary conditions, equations (3.8), become

$$\underline{B}_1^*[\underline{W}(0)] = \begin{bmatrix} V(0) \\ V'(0) \\ U(0) \end{bmatrix} = \underline{0}$$

$$\underline{B}_2^*[\underline{W}(1)] = \begin{bmatrix} V''(1) \\ V'''(1) - \Pi_1(V'(1) - U(1)) \\ U'(1) \end{bmatrix} = \underline{0} \tag{3.24}$$

Since all coefficients in (3.23) are constants, the solution will be of the form

$$\underline{W}(\xi) = \begin{bmatrix} \eta_1 \\ \eta_2 \end{bmatrix} e^{r\xi} \tag{3.25}$$

and when this equation is substituted into equation (3.23), two homogeneous equations in η_1 and η_2 are obtained

$$\begin{bmatrix} (\Pi_1 r) & (r^4 - \Pi_1 r^2 - \lambda^2) \\ (r^2 - (\Pi_1\Pi_2 - \lambda^2\Pi_3)) & (\Pi_1\Pi_2 r) \end{bmatrix} \begin{bmatrix} \eta_1 \\ \eta_2 \end{bmatrix} = \begin{bmatrix} 0 \\ 0 \end{bmatrix} \tag{3.26}$$

In order to avoid trivial solutions, the determinant must equal zero, i.e.

$$r^6 - (\Pi_1 + \Pi_1\Pi_2 - \lambda^2\Pi_3)r^4 - \lambda^2(1 + \Pi_1\Pi_3)r^2 + \lambda^2(\Pi_1\Pi_2 - \lambda^2\Pi_3) = 0 \tag{3.27}$$

which has six roots in r, r_i, $i = 1,2,\ldots,6$. For all six roots, equation (3.26) implies that

$$\begin{bmatrix} \eta_1 \\ \eta_2 \end{bmatrix} = \begin{bmatrix} r_i^4 - \Pi_1 r_i^2 - \lambda^2 \\ -\Pi_1 r_i \end{bmatrix} C \; ; \quad i = 1,2,\ldots,6 \qquad (3.28)$$

where C is an arbitrary constant.

Defining

$$q = r^2 \qquad (3.29)$$

the sixth order equation (3.27) is reduced to a third order equation

$$q^3 - (\Pi_1 + \Pi_1\Pi_2 - \lambda^2\Pi_3)q^2 - \lambda^2(1 + \Pi_1\Pi_3)q + \lambda^2(\Pi_1\Pi_2 - \lambda^2\Pi_3) = 0 \qquad (3.30)$$

in which the roots will be denoted by q_1, q_2 and q_3. It will be shown in chapter IV that the roots of (3.30) are always real. Thus the roots r_i; $i = 1,2,\ldots,6$ will either be real or pure imaginary,

$$\begin{aligned} r_{2i-1} &= \sqrt{q_i} \\ r_{2i} &= -\sqrt{q_i} \end{aligned} \quad ; \quad i = 1,2,3 \qquad (3.31)$$

Assuming that all r_i's are distinct, i.e.

$$r_i \neq r_j \qquad i \neq j; \quad \begin{matrix} i = 1,2,\ldots,6 \\ j = 1,2,\ldots,6 \end{matrix} \qquad (3.32)$$

then the complete solution can be written using equations (3.25) and (3.28)

$$\underline{W}(\xi) = \begin{bmatrix} U(\xi) \\ V(\xi) \end{bmatrix} = \sum_{i=1}^{6} C_i \begin{bmatrix} r_i^4 - \Pi_1 r_i^2 - \lambda^2 \\ -\Pi_1 r_i \end{bmatrix} e^{r_i \xi} \qquad (3.33)$$

Substituting this into the boundary conditions, equation (3.24), six homogeneous equations in the six unknown quantities C_i are obtained:

$$\underline{B}_1^*[\underline{W}(0)] = \sum_{i=1}^{6} C_i \begin{bmatrix} -\Pi_1 r_i \\ -\Pi_1 r_i^2 \\ r_i^4 - \Pi_1 r_i^2 - \lambda^2 \end{bmatrix} = \begin{bmatrix} 0 \\ 0 \\ 0 \end{bmatrix}$$

$$\underline{B}_2^*[W(1)] = \sum_{i=1}^{6} C_i \begin{bmatrix} -\Pi_i r_i^3 \\ -\Pi_1 \lambda^2 \\ r_i(r_i^4 - \Pi_1 r_i^2 - \lambda^2) \end{bmatrix} e^{r_i} = \begin{bmatrix} 0 \\ 0 \\ 0 \end{bmatrix} \qquad (3.34)$$

Defining

$$D_i = q_i^2 - \Pi_1 q_i - \lambda^2 ; \quad i = 1,2,3 \qquad (3.35)$$

the system of equations in (3.31) can be simplified into one matrix equation

$$\begin{bmatrix} \sqrt{q_1} & -\sqrt{q_1} & \sqrt{q_2} & -\sqrt{q_2} & \sqrt{q_3} & -\sqrt{q_3} \\ q_1 & q_1 & q_2 & q_2 & q_3 & q_3 \\ D_1 & D_1 & D_2 & D_2 & D_3 & D_3 \\ q_1^{\frac{3}{2}} e^{\sqrt{q_1}} & -q_1^{\frac{3}{2}} e^{-\sqrt{q_1}} & q_2^{\frac{3}{2}} e^{\sqrt{q_2}} & -q_2^{\frac{3}{2}} e^{-\sqrt{q_2}} & q_3^{\frac{3}{2}} e^{\sqrt{q_3}} & -q_3^{\frac{3}{2}} e^{-\sqrt{q_3}} \\ e^{\sqrt{q_1}} & e^{-\sqrt{q_1}} & e^{\sqrt{q_2}} & e^{-\sqrt{q_2}} & e^{\sqrt{q_3}} & e^{-\sqrt{q_3}} \\ \sqrt{q_1}D_1 e^{\sqrt{q_1}} & -\sqrt{q_1}D_1 e^{-\sqrt{q_1}} & \sqrt{q_2}D_2 e^{\sqrt{q_2}} & -\sqrt{q_2}D_2 e^{-\sqrt{q_2}} & \sqrt{q_3}D_3 e^{\sqrt{q_3}} & -\sqrt{q_3}D_3 e^{-\sqrt{q_3}} \end{bmatrix} \begin{bmatrix} C_1 \\ C_2 \\ C_3 \\ C_4 \\ C_5 \\ C_6 \end{bmatrix} = \begin{bmatrix} 0 \\ 0 \\ 0 \\ 0 \\ 0 \\ 0 \end{bmatrix} \quad (3.36)$$

and in order to have non-trivial solutions, the determinant of the matrix, denoted by F, must vanish. Since $q_i = q_i(\lambda^2)$ and $D_i = D_i(\lambda^2)$, F will be a function of λ^2, and the zeros of F will determine the eigenvalues of the system

$$F(\lambda_n^2) = 0 \tag{3.37}$$

where n denotes the n^{th} eigenvalue ordered such that

$$\lambda_1^2 \leq \lambda_2^2 \leq \ldots \leq \lambda_n^2 \leq \ldots \tag{3.38}$$

By some simple manipulations of the determinant in equation (3.36), F can be written as

$$F(\lambda^2) = 8\sqrt{q_1 q_2 q_3} \begin{vmatrix} 1 & 0 & 1 & 0 & 1 & 0 \\ 0 & q_1 & 0 & q_2 & 0 & q_3 \\ 0 & D_1 & 0 & D_2 & 0 & D_3 \\ q_1 c_1 & q_1^2 s_1 & q_2 c_2 & q_2^2 s_2 & q_3 c_3 & q_3^2 s_3 \\ s_1 & c_1 & s_2 & c_2 & s_3 & c_3 \\ D_1 c_1 & q_1 D_1 s_1 & D_2 c_2 & q_2 D_2 s_2 & D_3 c_3 & q_3 D_3 s_3 \end{vmatrix} \tag{3.39}$$

in which

$$\begin{aligned} s_i(\xi) &= \frac{1}{2\sqrt{q_i}} \left(e^{\sqrt{q_i}\xi} - e^{-\sqrt{q_i}\xi}\right) \\ c_i(\xi) &= \frac{1}{2} \left(e^{\sqrt{q_i}\xi} + e^{-\sqrt{q_i}\xi}\right) \qquad i = 1,2,3 \\ s_i &= s_i(1), \qquad c_i = c_i(1) \end{aligned} \tag{3.40}$$

Further reduction of (3.39) gives

$$F(\lambda^2) = 8\sqrt{q_1 q_2 q_3}$$

$$\times \begin{vmatrix} (q_1^2 Q_1 s_1 + q_2^2 Q_2 s_2 + q_3^2 Q_3 s_3) & (q_2 c_2 - q_1 c_1) & (q_3 c_3 - q_1 c_1) \\ (Q_1 c_1 + Q_2 c_2 + Q_3 c_3) & (s_2 - s_1) & (s_3 - s_1) \\ (q_1 D_1 Q_1 s_1 + q_2 D_2 Q_2 s_2 + q_3 D_3 Q_3 s_3) & (D_2 c_2 - D_1 c_1) & (D_3 c_3 - D_1 c_1) \end{vmatrix} \tag{3.41}$$

and, by observing from equation (3.40) that

$$c_i^2 - q_i s_i^2 = 1 \; ; \quad i = 1,2,3 \tag{3.42}$$

F can be written in its simplest form

$$F(\lambda^2) = 8\sqrt{q_1 q_2 q_3}[\, Q_2 Q_3 (2 + (q_2 + q_3) s_2 s_3) c_1 + Q_3 Q_1 (2 + (q_3 + q_1) s_3 s_1) c_2$$

$$+ Q_1 Q_2 (2 + (q_1 + q_2) s_1 s_3) c_3 + (Q_1^2 + Q_2^2 + Q_3^2) c_1 c_2 c_3] \tag{3.43}$$

where

$$\begin{aligned} Q_1 &= q_3 D_2 - q_2 D_3 = (q_2 - q_3)(q_2 q_3 + \lambda^2) \\ Q_2 &= q_1 D_3 - q_3 D_1 = (q_3 - q_1)(q_3 q_1 + \lambda^2) \\ Q_3 &= q_2 D_1 - q_1 D_2 = (q_1 - q_2)(q_1 q_2 + \lambda^2) \end{aligned} \tag{3.44}$$

Since it was assumed that the r_i's are distinct, it follows from equation (3.31) that

$$q_i \neq 0 \qquad i \; ; \quad i = 1,2,3 \tag{3.45}$$

and therefore the bracket in equation (3.43) must be equal to zero.

$$f(\lambda_n) = Q_2Q_3[\,2+(q_2+q_3)s_2s_3]\,c_1 + Q_3Q_1[\,2+(q_3+q_1)s_3s_1]\,c_2$$

$$+ Q_1Q_2[\,2+(q_1+q_2)s_1s_2]\,c_3 + [\,Q_1^2+Q_2^2+Q_3^2]\,c_1c_2c_3 = 0 \quad (3.46)$$

This is the eigenvalue equation, and solutions for λ_n can be obtained by numerical methods.

The eigenvectors can now be obtained by solving equation (3.36) for the constants C_i. In order to simplify the matrix problem somewhat, the constants C_i will be transformed into a set of new constants $\overline{C}_i$ by the transformation

$$2C_{2i-1} = \overline{C}_{2i-1} + \frac{1}{\sqrt{q_i}}\,\overline{C}_{2i}$$

$$i = 1,2,3 \qquad (3.47)$$

$$2C_{2i} = \overline{C}_{2i-1} - \frac{1}{\sqrt{q_i}}\,\overline{C}_{2i}$$

This reduces equation (3.36) to

$$\begin{bmatrix} 0 & 1 & 0 & 1 & 0 & 1 \\ q_1 & 0 & q_2 & 0 & q_3 & 0 \\ D_1 & 0 & D_2 & 0 & D_3 & 0 \\ q_1^2s_1 & q_1c_1 & q_2^2s_2 & q_2c_2 & q_3^2s_3 & q_3c_3 \\ c_1 & s_1 & c_2 & s_2 & c_3 & s_3 \\ q_1D_1s_1 & D_1c_1 & q_2D_2s_2 & D_2c_2 & q_3D_3s_3 & D_3c_3 \end{bmatrix} \begin{bmatrix} \overline{C}_1 \\ \overline{C}_2 \\ \overline{C}_3 \\ \overline{C}_4 \\ \overline{C}_5 \\ \overline{C}_6 \end{bmatrix} = \begin{bmatrix} 0 \\ 0 \\ 0 \\ 0 \\ 0 \\ 0 \end{bmatrix} \qquad (3.47)$$

Since the determinant of this matrix is zero by condition (3.46), the constants $\overline{C}_1$ through $\overline{C}_5$ can be expressed as a function of $\overline{C}_6$. Dropping the fifth equation in (3.47), the matrix equation reduces to

$$\begin{bmatrix} 0 & 1 & 0 & 1 & 0 \\ q_1 & 0 & q_2 & 0 & q_3 \\ D_1 & 0 & D_2 & 0 & D_3 \\ q_1^2 s_1 & q_1 c_1 & q_2^2 s_2 & q_2 c_2 & q_3^2 s_3 \\ q_1 D_1 s_1 & D_1 c_1 & q_2 D_2 s_2 & D_2 c_2 & q_3 D_3 s_3 \end{bmatrix} \begin{bmatrix} \overline{C}_1 \\ \overline{C}_2 \\ \overline{C}_3 \\ \overline{C}_4 \\ \overline{C}_5 \end{bmatrix} = -\overline{C}_6 \begin{bmatrix} 1 \\ 0 \\ 0 \\ q_3 c_3 \\ D_3 c_3 \end{bmatrix} \tag{3.48}$$

which can be solved for the constants $\overline{C}_i$

$$\begin{bmatrix} \overline{C}_1 \\ \overline{C}_2 \\ \overline{C}_3 \\ \overline{C}_4 \\ \overline{C}_5 \end{bmatrix} = \frac{\overline{C}_6}{Q_2 Q_3 (q_2 s_2 - q_3 s_3) c_1 - Q_3 Q_1 (q_3 s_3 - q_1 s_1) c_2} \times \begin{bmatrix} Q_1 (Q_1 c_2 c_3 + Q_2 c_3 c_1 + Q_3 c_1 c_2) \\ Q_3 Q_1 (q_3 s_3 - q_1 s_1) c_2 - Q_1 Q_2 (q_1 s_1 - q_2 s_2) c_3 \\ Q_2 (Q_1 c_2 c_3 + Q_2 c_3 c_1 + Q_3 c_1 c_2) \\ Q_1 Q_2 (q_1 s_1 - q_2 s_2) c_3 - Q_2 Q_3 (q_2 s_2 - q_3 s_3) c_1 \\ Q_3 (Q_1 c_2 c_3 + Q_2 c_3 c_1 + Q_3 c_1 c_2) \end{bmatrix} \tag{3.49}$$

and finally

$$\begin{bmatrix} \overline{C}_1 \\ \overline{C}_2 \\ \overline{C}_3 \\ \overline{C}_4 \\ \overline{C}_5 \\ \overline{C}_6 \end{bmatrix} = C \begin{bmatrix} Q_1\gamma_4 \\ \gamma_2 - \gamma_3 \\ Q_2\gamma_4 \\ \gamma_3 - \gamma_1 \\ Q_3\gamma_4 \\ \gamma_1 - \gamma_2 \end{bmatrix} \tag{3.50}$$

where C is a constant and

$$\begin{aligned} \gamma_1 &= Q_2Q_3(q_2s_2 - q_3s_3)c_1 \\ \gamma_2 &= Q_3Q_1(q_3s_3 - q_1s_1)c_2 \\ \gamma_3 &= Q_1Q_2(q_1s_1 - q_2s_2)c_3 \\ \gamma_4 &= Q_1c_2c_3 + Q_2c_3c_1 + Q_3c_1c_2 \end{aligned} \tag{3.51}$$

The u and v displacements corresponding to the eigenvector in equation (3.50) can now be obtained. From equation (3.33), making use of equations (3.35), (3.40) and (3.47)

$$\begin{aligned} U(\xi) &= \overline{C}_1D_1c_1(\xi) + \overline{C}_2D_1s_1(\xi) + \overline{C}_3D_2c_2(\xi) + \overline{C}_4D_2c_2(\xi) \\ &\quad + \overline{C}_5D_3c_3(\xi) + \overline{C}_6D_3s_3(\xi) \\ V(\xi) &= -\Pi_1[\overline{C}_1q_1s(\xi) + \overline{C}_2c_1(\xi) + \overline{C}_3q_2s_2(\xi) + \overline{C}_4c_2(\xi) \\ &\quad + \overline{C}_5q_3s_3(\xi) + \overline{C}_6c_3(\xi)] \end{aligned} \tag{3.52}$$

and substituting the values for $\overline{C}_i$ given in equation (3.50)

$$U(\xi) = C[\gamma_4(Q_1 D_1 c_1(\xi) + Q_2 D_2 c_2(\xi) + Q_3 D_3 c_3(\xi)) + D_1(\gamma_2 - \gamma_3)s_1(\xi) + D_2(\gamma_3 - \gamma_1)s_2(\xi) + D_3(\gamma_1 - \gamma_2)s_3(\xi)] \tag{3.53}$$

$$V(\xi) = -\Pi_1 C[\gamma_4(Q_1 q_1 s_1(\xi) + Q_2 q_2 s_2(\xi) + Q_3 q_3 s_3(\xi)) + (\gamma_2 - \gamma_3)c_1(\xi) + (\gamma_3 - \gamma_1)c_2(\xi) + (\gamma_1 - \gamma_2)c_3(\xi)]$$

It should be noted that, so far, no assumptions have been made about the coefficients in the characteristic equation (3.30). Thus, the eigenvalue equation (3.46) and the equations for the displacements (3.53) are applicable for all possible solutions to equation (3.30) as long as q_1, q_2 and q_3 are distinct, real and unequal to zero.

3.2. Natural Frequencies and Mode Shapes for Lateral Vibration

For an engineer interested in the dynamic response of a coupled shear wall building, the lateral vibration is the most important feature. Because of the usual nature the excitation, lateral wind loads or earthquakes, the longitudinal, antisymmetrical motion (u-displacements) is seldom excited. Thus it is of greater practical interest to obtain the frequencies for primarily lateral motion (v-displacements), and it will be assumed for the rest of this chapter that the vertical inertia term can be neglected. The next chapter will show that this assumption is acceptable for the first few natural frequencies. For practical applications, the higher frequencies are

usually not of prime interest, so a detailed study in which the vertical inertia term is neglected seems justified.

By setting

$$\Pi_3 = 0 \tag{3.54}$$

the differential equations (3.4) reduce to

$$\begin{aligned} v_{\xi\xi\xi\xi} - \Pi_1 v_{\xi\xi} + \Pi_1 u_\xi + \lambda^2 v_{\tau\tau} = 0 \\ u_{\xi\xi} + \Pi_1\Pi_2 v_\xi - \Pi_1\Pi_2 u = 0 \end{aligned} \tag{3.55}$$

where it is apparent that the vertical inertia is neglected. The characteristic equation (3.30) now becomes

$$q^3 - \Pi_1(1+\Pi_2)q^2 - \lambda^2 q + \lambda^2\Pi_1\Pi_2 = 0 \tag{3.56}$$

and this equation will have three real and unequal roots in q[19] if

$$\frac{b^2}{4} + \frac{a^2}{27} < 0 \tag{3.57}$$

in which

$$\begin{aligned} a &= -\frac{1}{3}[3\lambda^2 + \Pi_1^2(1+\Pi_2)^2] \\ b &= -\frac{1}{27}[2\Pi_1^3(1+\Pi_2)^3 + 9\lambda^2\Pi_1(1-2\Pi_2)] \end{aligned} \tag{3.58}$$

Employing equation (3.58), it is found after some algebra that

$$\frac{b^2}{4} + \frac{a^3}{27} = -\frac{\lambda^2}{27}\left[\lambda^4 + \frac{\Pi_1^2}{4}(1+20\Pi_2-8\Pi_2^2)\lambda^2 + \Pi_1^4\Pi_2(1+\Pi_2)^3\right] \tag{3.59}$$

Defining

$$R(\lambda^2) = \lambda^4 + \frac{\Pi_1^2}{4}(1 + 20\Pi_2 - 8\Pi_2^2)\lambda^2 + \Pi_1^4\Pi_2(1+\Pi_2)^3 \qquad (3.60)$$

and noting from equation (3.2) that $\Pi_2 > 0$, the sign of the discriminant can be evaluated. First, it is seen that when λ^2 is zero, R is positive. Thus, if there are no values of Π_2 such that $R(\lambda^2)$ is zero for $\lambda^2 > 0$ then R will always be positive and equation (3.59) will, in turn, always be negative. The roots of $R(\lambda^2)$ are found to be

$$\lambda^2 = -\frac{\Pi_1^2}{8}\left[20\,\Pi_2 - 8\Pi_2^2 + 1 \pm (8\Pi_2 - 1)\sqrt{2(\tfrac{1}{8} - \Pi_2)}\right] \qquad (3.61)$$

When $\Pi_2 > \frac{1}{8}$, the roots of this equation are imaginary. It is also easy to show that the roots are real, but negative, when $0 < \Pi_2 \leq \frac{1}{8}$. Therefore, $R(\lambda^2)$ is everywhere positive, and by virtue of inequality equation (3.57), equation (3.56) will have three real and unequal roots.

By application of Descartes Rule[34] it is found that equation (3.56) possesses either zero or two real, positive roots and at most one negative root, implying that two of the roots are positive and one is negative. The three roots of equation (3.56) can now be written as[19]

$$q_i = \frac{2}{3}\sqrt{3\lambda^2 + \Pi_1^2(1+\Pi_2)^2}\,\cos\left(\frac{\phi}{3} + \frac{2\pi i}{3}\right) + \frac{\Pi_1(1+\Pi_2)}{3}\,;\ i = 1,2,3 \qquad (3.62)$$

in which

$$\phi = \cos^{-1}\left[\frac{\Pi_1^3(1+\Pi_2)^3 + \frac{9}{2}\lambda^2\Pi_1(1-2\Pi_2)}{(3\lambda^2 + \Pi_1^2(1+\Pi_2)^2)^{3/2}}\right] \qquad (3.63)$$

The roots, q_i, are written such that $q_1 < 0$ while q_2 and q_3 are positive. Defining

$$p_i = \sqrt{|q_i|} \; ; \; i = 1,2,3 \tag{3.64}$$

the expressions for s_i and c_i, equation (3.40) can now be replaced by

$$\begin{aligned} s_1(\xi) &= \frac{1}{p_1} \sin p_i \xi \\ s_i(\xi) &= \frac{1}{p_i} \sinh p_i \xi \; ; \; i = 2,3 \\ c_1(\xi) &= \cos p_1 \xi \\ c_i(\xi) &= \cosh p_i \xi \; ; \; i = 2,3 \end{aligned} \tag{3.65}$$

and the frequency equation (3.46) becomes

$$\begin{aligned} f(\lambda_n) = {} & Q_2 Q_3 \left(2 + \frac{q_2+q_3}{p_2 p_3} \sinh p_2 \sinh p_3\right) \cos p_1 \\ & + Q_3 Q_1 \left(2 + \frac{q_3+q_1}{p_3 p_1} \sinh p_3 \sin p_1\right) \cosh p_2 \\ & + Q_1 Q_2 \left(2 + \frac{q_1+q_2}{p_1 p_2} \sin p_1 \sinh p_2\right) \cosh p_3 \\ & + (Q_1^2 + Q_2^2 + Q_3^2) \cos p_1 \cosh p_2 \cosh p_3 = 0 \end{aligned} \tag{3.66}$$

in which

$$\begin{aligned} Q_1 &= (q_2 - q_3)(q_2 q_3 + \lambda^2) \\ Q_2 &= (q_3 - q_1)(q_3 q_1 + \lambda^2) \\ Q_3 &= (q_1 - q_2)(q_1 q_2 + \lambda^2) \end{aligned} \tag{3.44}$$

Because of the complexity of this equation, a closed-form solution for λ_n does not seem possible. One numerical scheme, which is applied later, consists of first solving equation (3.66) for incremental values of λ, starting with $\lambda = 0$. Where $f(\lambda)$ changes sign an eigenvalue lies between adjacent increments, and a modified Newton's Method (Method of False Position[27]) can be used to converge rapidly to the eigenvalue. When the eigenvalues have been determined, the natural frequencies are obtained using equation (3.3)

$$\omega_n = \frac{\lambda_n}{\ell_1^2}\sqrt{\frac{E_1 I_1 a_2}{(\rho_1 A_1 a_2 + \frac{1}{2}\rho_3 \ell_3 A_3)}} \tag{3.67}$$

The mode shapes associated with these natural frequencies are given by equation (3.53). Employing equation (3.65) they can now be written as

$$V(\xi) = C^*[\,\gamma_4(-Q_1 p_1 \sin p_1\xi + Q_2 p_2 \sinh p_2\xi + Q_3 p_3 \sinh p_3\xi + (\gamma_2 - \gamma_3)\cos p_1\xi + (\gamma_3 - \gamma_1)\cosh p_2\xi + (\gamma_1 - \gamma_2)\cosh p_3\xi] \tag{3.68}$$

where C^* is an arbitrary constant, and, from equation (3.51)

$$\begin{aligned}
\gamma_1 &= Q_2 Q_3 (p_2 \sinh p_2 - p_3 \sinh p_3)\cos p_1 \\
\gamma_2 &= Q_3 Q_1 (p_3 \sinh p_3 + p_1 \sin p_1)\cosh p_2 \\
\gamma_3 &= Q_1 Q_2 (-p_1 \sin p_1 - p_2 \sinh p_2)\cosh p_3 \\
\gamma_4 &= Q_1 \cosh p_2 \cosh p_3 + Q_2 \cosh p_3 \cos p_1 + Q_3 \cos p_1 \cosh p_2
\end{aligned} \tag{3.69}$$

The longitudinal motion at the natural frequencies is obtained from equation (3.53)

$$U(\xi) = -\frac{C^*}{\Pi_1}\left[\gamma_4(Q_1D_1\cos p_1\xi + Q_2D_2\cosh p_2\xi + Q_3D_3\cosh p_3\xi)\right.$$
$$\left. + (\gamma_2-\gamma_3)\frac{D_1}{p_1}\sin p_1\xi + (\gamma_3-\gamma_1)\frac{D_2}{p_2}\sinh p_2\xi + (\gamma_1-\gamma_2)\frac{D_3}{p_3}\sinh p_2\xi\right] \tag{3.70}$$

in which D_i is given by equation (3.35).

In order to compare the relative values of lateral and longitudinal components of the mode shape, the dimensionless displacements U and V must be converted back to the physical displacements. From equation (3.1), this can be done by letting

$$\hat{V}(\xi) = \ell_1 V(\xi)$$
$$\hat{U}(\xi) = \frac{a_1}{2} U(\xi) \tag{3.71}$$

3.3. Asymptotic Behavior

Although no closed form solution seems possible for the general case, the values of Π_1 and Π_2 may sometimes be such that the eigenvalues and eigenvectors may be approximated by an asymptotic value plus a first correction term. The object of this section is to look at four different asymptotic behaviors, namely (a) $\lambda_n \to \infty$ (the higher natural frequencies), (b) $\Pi_1 \to 0$ (the spandrels become weak), (c) $\Pi_1 \to \infty$ (the spandrels become nearly rigid) and (d) $\Pi_2 \to 0$, which from fig. 3.1 can be seen to be the case

when the walls get thinner and thinner. This last asymptotic case is not too important for a coupled shear wall, where Π_2 usually lies between 0.1 and 0.2, but for the sandwich beam in chapter VI the values of Π_2 can become very small.

For the first three cases, the asymptotic values will be determined by studying the eigenvalue equation (3.66) which can be written in the following form

$$f(\lambda_n, \Pi_1, \Pi_2) = 0 \tag{3.72}$$

By letting ϵ denote the small parameter (e.g. $\epsilon = 1/\lambda_n$, Π_1 or $1/\Pi_1$) this eigenvalue equation can be written as

$$f(\lambda_n) = g_1(\epsilon) \cdot (f_0 + f_1\epsilon + f_2\epsilon^2 + f_3\epsilon^3 + \ldots) = 0 \tag{3.73}$$

where $g_1(\epsilon) \neq 0 \quad \forall\, \epsilon > 0$, $\Pi_1 > 0$, $\Pi_2 > 0$, $\lambda_n^2 > 0$ such that the eigenvalue equation reduces to

$$f_0 + f_1\epsilon + f_2\epsilon^2 + f_3\epsilon^3 + \ldots = 0 \tag{3.74}$$

in which f_i is a function of all parameters excluding ϵ. The series (3.74) is thus a regular power series in ϵ with constant coefficients since all parameters except ϵ are assumed to be kept constant.

It will be impossible to obtain the general n^{th} term of the series, and the convergence must therefore be studied in each particular case.

It should be observed that equation (3.74) implies that

$$f_0 = O(\epsilon)$$

$$f_0 + \epsilon f_1 = O(\epsilon^2) \tag{3.75}$$

$$f_0 + \epsilon f_1 + \epsilon^2 f_2 = O(\epsilon^3)$$

which again imply that

$$f_0 + \epsilon(f_1 + \alpha_1 f_0) = O(\epsilon^2)$$

$$f_0 + \epsilon(f_1 + \alpha_1 f_0) + \epsilon^2(f_2 + \alpha_1 f_1 + \alpha_2 f_0) = O(\epsilon^3) \tag{3.76}$$

where α_1 and α_2 are any constants of O(1). Thus it is seen that equation (3.74) is equivalent to the equation

$$f_0 + \epsilon(f_1 + \alpha_1 f_0) + \epsilon^2(f_2 + \alpha_1 f_1 + \alpha_2 f_0)$$

$$+ \epsilon^3(f_3 + \alpha_1 f_2 + \alpha_2 f_1 + \alpha_3 f_0) + \ldots = 0 \tag{3.77}$$

where α_1, α_2 and α_3 can be chosen such that this equation is more convenient than the original equation (3.74). The eigenvalues can now be determined by terminating equation (3.77) after a finite number of terms

$$f_0 + \epsilon f_1^* + \epsilon^2 f_2^* + \ldots + f_n^* \epsilon^n = O(\epsilon^{n+1}) \tag{3.78}$$

where

$$f_1^* = f_1 + \alpha_1 f_0$$

$$f_2^* = f_2 + \alpha_1 f_1 + \alpha_2 f_0, \quad \text{etc.}$$

as given in equation (3.77). The resulting expressions for the eigen-

values can be written as

$$\lambda_n = \lambda_{n0} + \epsilon\lambda_{n1} + \epsilon^2\lambda_{n2} + O(\epsilon^2) \tag{3.79}$$

and this solution is unique.

Similarly the asymptotic approximation to the mode shapes can be obtained from equation (3.68), and the form can generally be written as

$$V_n(\epsilon,\xi) = C^* g_2(\epsilon)[\, h_0(\xi) + \epsilon h_1(\xi) + \epsilon^2 h_2(\xi) + O(\epsilon^3)] \tag{3.80}$$

where $g_2(\epsilon) \neq 0 \quad \forall\, \epsilon > 0$, $\Pi_1 > 0$, $\Pi_2 > 0$, $\lambda_n > 0$, ϵ being the small parameter, and ξ being x/ℓ_1. Since C^* is any arbitrary constant it may now be chosen for each ϵ as

$$C^* = \frac{1}{g_2(\epsilon)} \tag{3.81}$$

such that equation (3.80) becomes

$$V_n(\epsilon,\xi) = h_0(\xi) + \epsilon h_1(\xi) + \epsilon^2 h_2(\xi) + O(\epsilon^3) \tag{3.82}$$

But again, as in the case of the eigenvalues, an equivalent mode shape equation would be

$$V_n^*(\epsilon,\xi) = h_0(\xi) + \epsilon(h_1(\xi) + \beta_1 h_0(\xi)) + \epsilon^2(h_2(\xi) + \beta_1 h_1(\xi) + \beta_2 h_0(\xi)) + O(\epsilon^3) \tag{3.83}$$

where β_1 and β_2 are two arbitrary constants of $O(1)$, chosen so equation (3.83) will have a more convenient form than equation (3.82).

Equation (3.83) could also have been obtained directly from the original mode shape equation (3.80) by defining

$$C^* = \frac{1}{g_2(\epsilon)}(1 + \beta_1\epsilon + \beta_2\epsilon^2) \tag{3.84}$$

It might seem that the mode shapes given by $V_n(\epsilon,\xi)$ and $V_n^*(\epsilon,\xi)$ differ because the $O(\epsilon)$-terms and $O(\epsilon^2)$-terms are different. This is not the case though since it can be shown that if $V_n(\epsilon,\xi)$ and $V_n^*(\epsilon,\xi)$ are normalized, they are indeed identical. For example, let both the functions be normalized such that their values at $\xi = 1$ are unity, i.e.,

$$\begin{aligned} \overline{V}_n(\epsilon,\xi) &= \frac{V_n(\epsilon,\xi)}{V_n(\epsilon,1)} \\ \overline{V}_n^*(\epsilon,\xi) &= \frac{V_n^*(\epsilon,\xi)}{V_n^*(\epsilon,1)} \end{aligned} \tag{3.85}$$

then subtracting these two functions and using equations (3.82) and (3.83) will show that

$$\overline{V}_n(\epsilon,\xi) - \overline{V}_n^*(\epsilon,\xi) = O(\epsilon^3) \tag{3.86}$$

The difference of $V_n(\epsilon,\xi)$ and $V_n^*(\epsilon,\xi)$ is thus only a matter of normalization.

The asymptotic behavior of the eigenvalues when $\Pi_2 \to 0$ cannot be obtained by the above procedure, and a regular perturbation method[24] will be applied to the original system of differential equations (3.55).

In the following sections it will be useful to have three relations between the roots q_i which are directly obtained from equation (3.56).

$$q_1 + q_2 + q_3 = \Pi_1(1 + \Pi_2)$$

$$q_1q_2 + q_2q_3 + q_3q_1 = -\lambda^2 \tag{3.87}$$

$$q_1q_2q_3 = -\lambda^2\Pi_1\Pi_2$$

(a) Asymptotic behavior for $\lambda_n \to \infty$

In order to evaluate the eigenvalue equation it will be necessary to obtain the expressions for q_i. From equation (3.63)

$$\cos^2\phi = \frac{\Pi_1^6(1+\Pi_2)^6+9\lambda^2\Pi_1^4(1+\Pi_2)^3(1-2\Pi_2)+\frac{81}{4}\lambda^4\Pi_1^2(1-2\Pi_2)^2}{27\lambda^6+27\lambda^4\Pi_1^2(1+\Pi_2)^2+9\lambda^2\Pi_1^4(1+\Pi_2)^4+\Pi_1^6(1+\Pi_2)^6} \tag{3.88}$$

which can be written in an asymptotic expansion in $1/\lambda$.

$$\cos^2\phi = \frac{3}{4}\Pi_1^2(1-2\Pi_2)^2\frac{1}{\lambda^2} + 3\frac{\Pi_1^2(1+\Pi_2)^2(22\Pi_2-5)}{1-2\Pi_2}\frac{1}{\lambda^4} + O(\lambda^{-6}) \tag{3.89}$$

For rectangular shear walls, $\Pi_2 < 1/3$ (equation (3.15)) such that $1 - 2\Pi_2 > 0$ which implies that the second term is of $O(\lambda^{-4})$. From expression (3.63) it is observed that $\cos\phi > 0$, therefore equation (3.89) gives

$$\cos\phi = \frac{\sqrt{3}}{2}\Pi_1(1-2\Pi_2)\frac{1}{\lambda} + O(\lambda^{-2})$$

$$\sin\phi = 1 - \frac{3}{8}\Pi_1^2(1-2\Pi_2)^2\frac{1}{\lambda^2} + O(\lambda^{-4}) \tag{3.90}$$

With the help of these expressions,

$$\phi = \frac{\pi}{2} - \frac{\sqrt{3}}{6}\Pi_1(1-2\Pi_1)\frac{1}{\lambda} + O(\lambda^{-2}) \tag{3.91}$$

and

$$\cos\frac{\phi}{3} = \frac{1}{2}\sqrt{3} + \frac{\sqrt{3}}{12}\Pi_1(1-2\Pi_2)\frac{1}{\lambda} + O(\lambda^{-2})$$

$$\cos\left(\frac{\phi}{3}+\frac{2\pi}{3}\right) = -\frac{1}{2}\sqrt{3} + \frac{\sqrt{3}}{12}\Pi_1(1-2\Pi_2)\frac{1}{\lambda} + O(\lambda^{-2}) \tag{3.92}$$

$$\cos\left(\frac{\phi}{3}+\frac{4\pi}{3}\right) = -\frac{\sqrt{3}}{6}\Pi_1(1-2\Pi_2)\frac{1}{\lambda} + O(\lambda^{-2})$$

Expressions for q_i can now be evaluated using equation (3.62)

$$\begin{bmatrix} q_1 \\ q_2 \\ q_3 \end{bmatrix} = \begin{bmatrix} -\lambda + \frac{1}{2}\Pi_1 + O(\lambda^{-1}) \\ \Pi_1\Pi_2 + O(\lambda^{-1}) \\ +\lambda + \frac{1}{2}\Pi_1 + O(\lambda^{-1}) \end{bmatrix} \tag{3.93}$$

Higher order terms in the expressions for q_i can be found by setting

$$\begin{bmatrix} q_1 \\ q_2 \\ q_3 \end{bmatrix} = \begin{bmatrix} -\lambda + \frac{\Pi_1}{2} + a_1\lambda^{-1} + a_2\lambda^{-2} + a_3\lambda^{-3} + O(\lambda^{-4}) \\ \Pi_1\Pi_2 + b_1\lambda^{-1} + b_2\lambda^{-2} + b_3\lambda^{-3} + O(\lambda^{-4}) \\ \lambda + \frac{\Pi_1}{2} + c_1\lambda^{-1} + c_2\lambda^{-2} + c_3\lambda^{-3} + O(\lambda^{-4}) \end{bmatrix} \tag{3.94}$$

Using equation (3.87) the following relations for the unknowns a_i, b_i and c_i are obtained

$$
\begin{aligned}
a_1 + b_1 + c_1 &= 0 \\
a_2 + b_2 + c_2 &= 0 \\
a_3 + b_3 + c_3 &= 0 \\
a_1 - c_1 + \frac{\Pi_1^2}{4} + \Pi_1^2\Pi_2 &= 0 \\
(a_1 + c_1)(\Pi_1\Pi_2 + \frac{\Pi_1}{2}) + b_1\Pi_1 + a_2 - c_2 &= 0 \qquad (3.95) \\
(a_1+c_1)b_1 + a_1c_1 + \frac{\Pi_1}{2}(a_2+c_2) + \Pi_1 b_2 + (a_2+c_2)\Pi_1\Pi_2 + a_3 - c_3 &= 0 \\
b_1 &= 0 \\
(\frac{\Pi_1^2}{4} + a_1 - c_1)\Pi_1\Pi_2 - b_2 &= 0 \\
(a_1 - c_1)b_1 + b_1\frac{\Pi_1^2}{4} + \frac{\Pi_1^2\Pi_2}{2}(a_1+c_1) + (a_2 - c_2)\Pi_1\Pi_2 - b_3 &= 0
\end{aligned}
$$

which can be solved for the unknown quantities. Finally, q_i is given by

$$
\begin{bmatrix} q_1 \\ q_2 \\ q_3 \end{bmatrix} = \begin{bmatrix} -\lambda + \frac{\Pi_1}{2} - \frac{\Pi_1^2}{8}(1+4\Pi_2)\lambda^{-1} + \frac{\Pi_1^3\Pi_2^2}{2}\lambda^{-2} + a_3\lambda^{-3} + O(\lambda^{-4}) \\ \Pi_1\Pi_2 - \Pi_1^3\Pi_2^2\lambda^{-2} + O(\lambda^{-4}) \\ \lambda + \frac{\Pi_1}{2} + \frac{\Pi_1^2}{8}(1+4\Pi_2)\lambda^{-1} + \frac{\Pi_1^3\Pi_2^2}{2}\lambda^{-2} - a_3\lambda^{-3} + O(\lambda^{-4}) \end{bmatrix} \qquad (3.96)
$$

where

$$a_3 = \frac{\Pi_1^4}{128}(1 + 8\Pi_2 + 48\Pi_2^2 - 64\Pi_2^3) \tag{3.97}$$

The expressions for Q_i are obtained by using equation (3.96) in equation (3.44)

$$\begin{aligned} Q_1 &= -\lambda^3 - \frac{\Pi_1}{2}\lambda^2 - \frac{\Pi_1^2}{8}(1 + 12\Pi_2 - 8\Pi_2^2)\lambda + O(1) \\ Q_2 &= -\Pi_1^2\Pi_2\lambda + O(\lambda^{-1}) \\ Q_3 &= -\lambda^3 + \frac{\Pi_1}{2}\lambda^2 - \frac{\Pi_1^2}{8}(1 + 12\Pi_2 - 8\Pi_2^2)\lambda + O(1) \end{aligned} \tag{3.98}$$

or, expressed in ratios

$$\begin{aligned} \frac{Q_2}{Q_1} &= \Pi_1^2\Pi_2\lambda^{-2} + O(\lambda^{-3}) \\ \frac{Q_3}{Q_1} &= 1 - \Pi_1\lambda^{-1} + \frac{\Pi_1^2}{2}\lambda^{-2} + O(\lambda^{-3}) \end{aligned} \tag{3.99}$$

Equation (3.66) can now be written as

$$\begin{aligned} Q_1^2\Bigg[& \left(\Pi_1^2\Pi_2\lambda^{-2} + O(\lambda^{-3})\right) \\ & \times \left(2 + \frac{\lambda + \frac{\Pi_1}{2}(1 + 2\Pi_2) + O(\lambda^{-1})}{\sqrt{\lambda\Pi_1\Pi_2 + (\Pi_1^2\Pi_2/2) + O(\lambda^{-1})}} \sinh p_2 \sinh p_3\right) \cos p_1 \\ & + \left(1 - \Pi_1\lambda^{-1} + \frac{\Pi_1^2}{2}\lambda^{-2} + O(\lambda^{-3})\right) \\ & \times \left(2 + \frac{\Pi_1 + O(\lambda^{-2})}{\sqrt{\lambda^2 + \Pi_1^2\Pi_2 + O(\lambda^{-2})}} \sinh p_3 \sin p_1\right) \cosh p_2 \quad + \end{aligned}$$

$$+\left(\Pi_1^2\Pi_2\lambda^{-2}+O(\lambda^{-3})\right)$$

$$\times\left(2+\frac{-\lambda+\frac{\Pi_1}{2}(1+2\Pi_2)+O(\lambda^{-1})}{\sqrt{\lambda\Pi_1\Pi_2-(\Pi_1^2\Pi_2/2)+O(\lambda^{-2})}}\sin p_1\sinh p_2\right)\cosh p_3$$

$$+\left(1+\Pi_1^4\Pi_2^2\lambda^{-4}+1-2\Pi_1\lambda^{-1}+2\Pi_1^2\lambda^{-2}+O(\lambda^{-3})\right)\cos p_1\cosh p_2\cosh p_3\Big]=0 \tag{3.100}$$

From equations (3.96) and (3.64) it is observed that

$$p_3=\sqrt{\lambda+\frac{\Pi_1}{2}+O(\lambda^{-1})}=\lambda^{1/2}+\frac{\Pi_1}{4}\lambda^{-1/2}+O(\lambda^{-3/2}) \tag{3.101}$$

and therefore, for large λ,

$$e^{-p_3}\ll 1 \tag{3.102}$$

Specifically, it can be shown that

$$\begin{aligned} e^{\sqrt{\lambda}} &> \lambda \qquad \forall\, \lambda > 0 \\ e^{\sqrt{\lambda}} &> \lambda^2 \qquad \forall\, \lambda > 81 \\ e^{\sqrt{\lambda}} &> \lambda^3 \qquad \forall\, \lambda > 289 \end{aligned} \tag{3.103}$$

such that one can replace e^{-p_3} by

$$e^{-p_3}\leq O(\lambda^{-2}) \tag{3.104}$$

for those values of λ that are larger than 81. (It will be shown later

that the first three eigenvalues usually are below this limit.) The approximation is thus usually valid only for the fourth and higher eigenvalues. With the use of equation (3.104) $\sinh p_3$ and $\cosh p_3$ can now be replaced by

$$\cosh p_3 = \frac{1}{2} e^{p_3} + O(\lambda^{-2})$$
$$\sinh p_3 = \frac{1}{2} e^{p_3} + O(\lambda^{-2}) \qquad (3.105)$$

and equation (3.100) can finally be written in the form of equation (3.73)

$$f(\lambda_n) = e^{p_3} Q_1^2 \left[\cos p_1 \cosh p_2 - \Pi_1 \lambda_n^{-1} (\cos p_1 - \frac{1}{2} \sin p_1) \cosh p_2 \right.$$
$$\left. + \frac{\Pi_1^2 \Pi_2}{2\sqrt{\Pi_1 \Pi_2}} \lambda_n^{-1.5} (\cos p_1 \sinh p_2 - \sin p_1 \sinh p_2) + O(\lambda_n^{-2}) \right] = 0 \qquad (3.106)$$

It is observed from equation (3.98) that

$$e^{p_3} Q_1^2 \neq 0 \qquad \lambda_n > 0 \qquad (3.107)$$

and by virtue of the discussion in the beginning of this section, the term $\cos p_1 \cosh p_2$ of the $O(\lambda_n^{-1})$-terms can be subtracted out yielding an eigenvalue equation similar to equation (3.78)

$$\cosh p_2 [\cos p_1 + \frac{1}{2} \Pi_1 \lambda_n^{-1} \sin p_1] = O(\lambda_n^{-1.5}) \qquad (3.108)$$

Or, since $\cosh p_2$ is a constant different from zero

$$\cos p_1 + \frac{1}{2} \Pi_1 \lambda_n^{-1} \sin p_1 = O(\lambda_n^{-1.5}) \qquad (3.109)$$

To solve equation (3.109) for p_1, a solution of the form

$$p_1 = \alpha_1 + \alpha_2 \lambda_n^{-1} + O(\lambda_n^{-1.5}) \tag{3.110}$$

is assumed. Substituting into equation (3.109)

$$\cos \alpha_1 + \alpha_2 \lambda_n^{-1} \sin \alpha_1 - \frac{1}{2} \Pi_1 \lambda_n^{-1} \sin \alpha_1 = O(\lambda_n^{-1.5}) \tag{3.111}$$

which implies that the $O(\lambda_n^0)$- and $O(\lambda_n^{-1})$-terms both must equal zero identically,

$$\begin{aligned} \cos \alpha_1 &= 0 \\ (\alpha_2 - \tfrac{1}{2}\Pi_1) \sin \alpha_1 &= 0 \end{aligned} \tag{3.112}$$

resulting in

$$\begin{aligned} \alpha_1 &= \frac{2n-1}{2} \pi \\ \alpha_2 &= \Pi_1/2 \end{aligned} \tag{3.113}$$

and

$$p_1 = \frac{2n-1}{2} \pi + \frac{\Pi_1}{2} \lambda_n^{-1} + O(\lambda_n^{-1.5}) \tag{3.114}$$

Employing equations (3.64) and (3.96)

$$\lambda_n - \left[\frac{\Pi_1}{2} + \left(\frac{2n-1}{2} \pi \right)^2 \right] - \left[\frac{2n-1}{2} \pi \Pi_1 - \frac{\Pi_1^2}{8} (1 + 4\Pi_2) \right] \lambda_n^{-1} + O(\lambda_n^{-1}) = 0 \tag{3.115}$$

which gives the final result for the eigenvalue as n becomes large

$$\lambda_n = \left(\frac{2n-1}{2}\pi\right)^2 + \frac{\Pi_1}{2} + O(\lambda_n^{-1/2}) \; ; \qquad n, \; n \text{ large} \tag{3.116}$$

where, for later use it is observed that $\left(\frac{2n-1}{2}\pi\right)^2 = O(\lambda_n)$ while $\Pi_1/2 = O(1)$.

In appendix B it is shown that the asymptotic values for an Euler-Bernoulli Beam are $\left(\frac{2n-1}{2}\pi\right)^2$. The eigenvalues in equation (3.116) approaches that value plus a constant, $\Pi_1/2$, which is a function of the spandrel stiffness. This reflects the fact that for increasing spandrel stiffness, the strain energy in the system becomes larger while the kinetic energy is constant, resulting in higher nautral frequencies and eigenvalues.

It should also be noted, from equations (3.109) and (3.116) that the asymptotic values of the eigenvalues are good approximations only when $\Pi_1 \lambda_n^{-1}$ is small.

From equation (3.114)

$$\cos p_1 = (-1)^n \frac{\Pi_1}{2} \lambda_n^{-1} + O(\lambda_n^{-1.5}) \tag{3.117}$$

The mode shape is obtained from equation (3.68). Making use of equations (3.117), (3.99), (3.105) and keeping the terms of $O(\lambda_n^{-1})$ and higher order, one obtains

$$V_n(\xi) = -C^* p_1 Q_1^2 \frac{e^{p_3}}{2} \cosh p_2 \left[\left(\sin p_1\xi - \cos p_1\xi + e^{-p_3\xi} + (-1)^{n+1} e^{p_3(\xi-1)}\right)\right.$$
$$\left. - \frac{\Pi_1}{2}\lambda_n^{-1}\left(e^{-p_3\xi} + (-1)^{n+1} e^{p_3(\xi-1)} - \cos p_1\xi\right) + O(\lambda_n^{-2})\right] \tag{3.118}$$

which is of the form of equation (3.80). According to the discussion preceeding equation (3.80) the mode shape can also be written in the form

$$V_n(\xi) = \sin p_1\xi - \cos p_1\xi + e^{-p_3\xi} + (-1)^{n+1} e^{p_3(\xi-1)} + \frac{\Pi_1}{2}\lambda_n^{-1}\sin p_1\xi + O(\lambda_n^{-2}) \tag{3.119}$$

which was obtained by adding the zeroeth order term of equation (3.118) multiplied by $\frac{\Pi_1}{2}\lambda_n^{-1}$ to the first order term and letting

$$C^* = -\frac{2e^{-p_3}}{p_1 Q_1^2 \cosh p_2} \tag{3.120}$$

Equation (3.119) is still not too useful since p_1 and p_3 are complicated functions involving λ_n and Π_1. Expansions at p_1 and p_3 in λ_n can be obtained from equations (3.114), (3.96) and (3.64)

$$p_1 = \frac{2n-1}{2}\pi + \frac{\Pi_1}{2}\lambda_n^{-1} + O(\lambda_n^{-1.5})$$

$$p_3 = \frac{2n-1}{2}\pi + \frac{\Pi_1}{2}\lambda_n^{-1/2} + \frac{\Pi_1}{2}\lambda_n^{-1} + O(\lambda_n^{-1.5}) \tag{3.121}$$

With the use of these equations, the terms in equation (3.119) can be written as series in λ_n of the following form,

$$\sin p_1\xi = \sin\frac{2n-1}{2}\pi\xi + \frac{1}{2}\Pi_1\lambda_n^{-1}\xi\cos\frac{2n-1}{2}\pi\xi + O(\lambda_n^{-2})$$

$$\cos p_1\xi = \cos\frac{2n-1}{2}\pi\xi - \frac{1}{2}\Pi_1\lambda_n^{-1}\xi\sin\frac{2n-1}{2}\pi\xi + O(\lambda_n^{-2})$$

$$e^{-p_3\xi} = e^{-\frac{2n-1}{2}\pi\xi}\left(1-\frac{\Pi_1}{2}\lambda_n^{-1/2}\xi-\frac{\Pi_1}{2}\lambda_n^{-1}\xi\left(1-\frac{\Pi_1}{4}\xi\right)+O(\lambda_n^{-1.5})\right) \tag{3.122}$$

$$e^{-p_3(1-\xi)} = e^{-\frac{2n-1}{2}\pi(1-\xi)}\left(1-\frac{\Pi_1}{2}\lambda_n^{-1/2}(1-\xi)-\frac{\Pi_1}{2}\lambda_n^{-1}(1-\xi)\left(1-\frac{\Pi_1}{4}(1-\xi)\right)+O(\lambda_n^{-1.5})\right)$$

These expressions are then substituted into equation (3.119), giving

$$\begin{aligned}V_n(\xi) = {} & \left(\sin\frac{2n-1}{2}\pi\xi-\cos\frac{2n-1}{2}\pi\xi+e^{-\frac{2n-1}{2}\pi\xi}+(-1)^{n+1}e^{-\frac{2n-1}{2}\pi(1-\xi)}\right)\\ & -\frac{\Pi_1}{2}\lambda_n^{-1/2}\left(\xi e^{-\frac{2n-1}{2}\pi\xi}+(1-\xi)(-1)^{n+1}e^{-\frac{2n-1}{2}\pi(1-\xi)}\right)\\ & +\frac{\Pi_1}{2}\lambda_n^{-1}\left[(1+\xi)\sin\frac{2n-1}{2}\pi\xi+\xi\cos\frac{2n-1}{2}\pi\xi-\xi\left(1-\frac{\Pi_1}{4}\xi\right)e^{-\frac{2n-1}{2}\pi\xi}\right.\\ & \left.-(-1)^{n+1}(1-\xi)\left(1-\frac{\Pi_1}{4}(1-\xi)\right)e^{-\frac{2n-1}{2}\pi(1-\xi)}\right]+O(\lambda_n^{-1.5})\end{aligned} \tag{3.123}$$

or, by observing from equation (3.116) that

$$\lambda_n^{-1/2} = \frac{2}{(2n-1)\pi} + O(\lambda_n^{-1.5})$$

$$\lambda_n^{-1} = \frac{4}{(2n-1)^2\pi^2 + 2\Pi_1} + O(\lambda_n^{-2}) \tag{3.124}$$

$$V_n(\xi) = \sin\frac{2n-1}{2}\pi\xi - \cos\frac{2n-1}{2}\pi\xi + e^{-\frac{2n-1}{2}\pi\xi} + (-1)^{n+1}e^{-\frac{2n-1}{2}\pi(1-\xi)}$$

$$+ \frac{\Pi_1}{(2n-1)\pi}\left[\xi e^{-\frac{2n-1}{2}\pi\xi} + (1-\xi)(-1)^{n+1}e^{-\frac{2n-1}{2}\pi(1-\xi)}\right]$$

$$+ \frac{2\Pi_1}{2\Pi_1 + (2n-1)^2\pi^2}\left[(1+\xi)\sin\frac{2n-1}{2}\pi\xi + \xi\cos\frac{2n-1}{2}\pi\xi\right.$$

$$\left. - \xi(1 - \frac{\Pi_1}{4}\xi)e^{-\frac{2n-1}{2}\pi\xi} - (-1)^{n+1}(1-\xi)(1-\frac{\Pi_1}{4}(1-\xi))e^{-\frac{2n-1}{2}\pi(1-\xi)}\right]$$

$$+ O(\lambda_n^{-1.5}) \qquad (3.125)$$

By reference to appendix B it can be observed that the mode shape equation (3.125) approaches equation (B.15), the corresponding equation for an Euler-Bernoulli beam, and thus the coupled shear wall and the cantilever beam have the same asymptotical mode shapes while the asymptotes for the eigenvalues differ by a constant.

(b) Asymptotic behavior when $\Pi_1 \to 0$

The solution for $\Pi_1 \to 0$ can be obtained the same way as in the previous case. In fact, from equation (3.63) it can be observed that

$$\phi = \phi(\epsilon, \Pi_2) \qquad (3.126)$$

where

$$\epsilon = \frac{\Pi_1}{\lambda} \qquad (3.127)$$

which can be utilized in equation (3.62) to yield

$$q_i = \lambda\left[\frac{2}{3}\sqrt{3+(1+\Pi_2)^2\epsilon^2}\cos\left(\frac{\phi}{3}+\frac{2\pi i}{3}\right)+\frac{1+\Pi_2}{3}\epsilon\right] \; ; \; i = 1,2,3 \qquad (3.128)$$

Hence, the asymptotic expansion of q_i as $\epsilon \to 0$ will be the same as when $\lambda \to \infty$, and the equations for q_i can be obtained immediately from equation (3.96)

$$\begin{bmatrix} q_1 \\ q_2 \\ q_3 \end{bmatrix} = \begin{bmatrix} -\lambda + \frac{1}{2}\Pi_1 - \frac{1}{8\lambda}(1+4\Pi_2)\Pi_1^2 + \frac{\Pi_2^2}{2\lambda^2}\Pi_1^3 + O(\Pi_1^4) \\ \Pi_2\Pi_1 - \frac{\Pi_2^2}{\lambda^2}\Pi_1^3 + O(\Pi_1^4) \\ \lambda + \frac{1}{2}\Pi_1 + \frac{1}{8\lambda}(1+4\Pi_2)\Pi_1^2 + \frac{\Pi_2^2}{2\lambda^2}\Pi_1^3 + O(\Pi_1^4) \end{bmatrix} \qquad (3.129)$$

Furthermore, the expression for $f(\lambda)$ can be obtained directly from equation (3.100), and collecting terms of the same order, this equation can be written as

$$\begin{aligned} f(\lambda) = Q_1^2\Big[&\cosh p_2\Big\{(2+2\cos p_1\cosh p_3) \\ &- \frac{\Pi_1}{\lambda}(2-\sin p_1\sinh p_3+2\cos p_1\cosh p_3)\Big\} \\ &+ \frac{\sqrt{\Pi_2}}{\lambda\sqrt{\lambda}}\Pi_1\sqrt{\Pi_1}\,(\sinh p_2\sinh p_3\cos p_1-\sin p_1\sinh p_2\cosh p_3) \\ &+ O(\Pi_1^2)\Big] \end{aligned} \qquad (3.130)$$

The first order term of this equation can be reduced according to equation (3.78), and the eigenvalues are then obtained from the zeros of equation (3.130)

$$2+2\cos p_1\cosh p_3+\frac{\Pi_1}{\lambda_n}\sin p_1\sinh p_3 = O(\Pi_1^{1.5}) \qquad (3.131)$$

From equations (3.129) and (3.64)

$$p_1 = \lambda^{1/2} - \frac{1}{4}\lambda^{-1/2}\Pi_1 + \frac{1}{32}(1 + 8\Pi_2)\lambda^{-3/2}\Pi_1^2 + O(\Pi_1^3)$$

$$p_2 = \lambda^{1/2} + \frac{1}{4}\lambda^{-1/2}\Pi_1 + \frac{1}{32}(1 + 8\Pi_2)\lambda^{-3/2}\Pi_1^2 + O(\Pi_1^3) \tag{3.132}$$

and substituting these into equation (3.131)

$$2 + 2\cos\sqrt{\lambda_n}\cosh\sqrt{\lambda_n} + \left\{\frac{1}{2}\lambda_n^{-1/2}(\cosh\sqrt{\lambda_n}\sin\sqrt{\lambda_n} + \cos\sqrt{\lambda_n}\sinh\sqrt{\lambda_n} + \lambda_n^{-1}\sin\sqrt{\lambda_n}\sinh\sqrt{\lambda_n}\right\}\Pi_1 + O(\Pi_1^{1.5}) = 0 \tag{3.133}$$

Let the solution to equation (3.133) be

$$\lambda_n = \lambda_n^* + \Pi_1\lambda_{1n} + O(\Pi_1^{1.5}) \tag{3.134}$$

where λ_n^* is the solution to the equation

$$1 + \cos\sqrt{\lambda_n^*}\cosh\sqrt{\lambda_n^*} = 0 \tag{3.135}$$

The numerical values of λ_n^* are given in appendix B, equation (B.7). The substitution of equation (3.134) in equation (3.133) leads to

$$(1 + \cos\sqrt{\lambda_n^*}\cosh\sqrt{\lambda_n^*}) + \Pi_1\left[\frac{\lambda_{n1}}{2\sqrt{\lambda_n^*}}(\cos\sqrt{\lambda_n^*}\sinh\sqrt{\lambda_n^*} - \sin\sqrt{\lambda_n^*}\cosh\sqrt{\lambda_n^*}) + \frac{1}{4\sqrt{\lambda_n^*}}(\cosh\sqrt{\lambda_n^*}\sin\sqrt{\lambda_n^*} + \cos\sqrt{\lambda_n^*}\sinh\sqrt{\lambda_n^*}) + \frac{1}{2\lambda_n^*}\sin\sqrt{\lambda_n^*}\sinh\sqrt{\lambda_n^*}\right] + O(\Pi_1^{1.5}) = 0 \tag{3.136}$$

The zeroeth order term in this equation is zero by equation (3.135). Setting the first order terms equal to zero leads to an equation for the unknown quantity λ_{1n}.

$$\lambda_{1n} = \frac{\cosh\sqrt{\lambda_n^*}\sin\sqrt{\lambda_n^*} + \cos\sqrt{\lambda_n^*}\sinh\sqrt{\lambda_n^*} + \frac{2}{\sqrt{\lambda_n^*}}\sin\sqrt{\lambda_n^*}\sinh\sqrt{\lambda_n^*}}{2(\sin\sqrt{\lambda_n^*}\cosh\sqrt{\lambda_n^*} - \cos\sqrt{\lambda_n^*}\sinh\sqrt{\lambda_n^*})} \tag{3.137}$$

This expression can be simplified by observing from equation (3.135) that

$$\cosh\sqrt{\lambda_n^*} = -\frac{1}{\cos\sqrt{\lambda_n^*}}$$
$$\sinh\sqrt{\lambda_n^*} = (-1)^n \frac{\sin\sqrt{\lambda_n^*}}{\cos\sqrt{\lambda_n^*}} \tag{3.138}$$

and equation (3.137) thereby becomes

$$\lambda_{1n} = \frac{(-1)^n - \cos\sqrt{\lambda_n^*} - \frac{2}{\sqrt{\lambda_n^*}}\sin\sqrt{\lambda_n^*}}{2(-1)^n + 2\cos\sqrt{\lambda_n^*}} \tag{3.139}$$

The eigenvalues, equation (3.135) can finally be written as

$$\lambda_n = \lambda_n^* + \frac{(-1)^n - \cos\sqrt{\lambda_n^*} - \frac{2}{\sqrt{\lambda_n^*}}\sin\sqrt{\lambda_n^*}}{2(-1)^n + 2\cos\sqrt{\lambda_n^*}}\Pi_1 + O(\Pi_1^{1.5}); n=1,2,\ldots \tag{3.140}$$

Equation (3.140) shows that these eigenvalues are independent of Π_2 to the first approximation. Hence, when Π_1 is small, Π_2 can be set equal to zero, simplifying the problem considerably. This case,

which implies that $u = 0$, is treated in appendix C.

The horizontal components of the mode shape corresponding to the eigenvalues in equation (3.140) can again be obtained by utilizing equations (3.68) and (3.83)

$$\begin{aligned} V_n(\xi) = {} & (\cos p_1 + \cosh p_3)(\sin p_1\xi - \sinh p_3\xi) \\ & - (\sin p_1 + \sinh p_3)(\cos p_1\xi - \cosh p_3\xi) \\ & + \frac{\Pi_1}{2\lambda_n}\Big[2\cosh p_3 \sin p_1\xi + (\cos p_1 - \cosh p_3)\sinh p_3\xi \\ & - \sinh p_3(\cos p_1\xi - \cosh p_3\xi)\Big] + O(\Pi_1^{1.5}) \end{aligned} \tag{3.141}$$

This equation is identical to equation (C.15) in appendix C, implying that the mode shapes are also independent of Π_2 to the first approximation. If the values for p_1 and p_2, equation (3.118), are substituted into this equation, one obtains

$$\begin{aligned} V_n(\xi) = {} & (\cos\sqrt{\lambda_n} + \cosh\sqrt{\lambda_n})(\sin\sqrt{\lambda_n}\xi - \sinh\sqrt{\lambda_n}\xi) \\ & - (\sin\sqrt{\lambda_n} + \sinh\sqrt{\lambda_n})(\cos\sqrt{\lambda_n}\xi - \cosh\sqrt{\lambda_n}\xi) \\ & - \frac{\Pi_1}{4\sqrt{\lambda_n}}\Big\{(1-\xi)(\sin\sqrt{\lambda_n} + \sinh\sqrt{\lambda_n})(\sinh\sqrt{\lambda_n}\xi - \sin\sqrt{\lambda_n}\xi) \\ & + \xi(\cos\sqrt{\lambda_n} + \cosh\sqrt{\lambda_n})(\cosh\sqrt{\lambda_n}\xi + \cos\sqrt{\lambda_n}\xi) \\ & + (\cosh\sqrt{\lambda_n} - \cos\sqrt{\lambda_n})(\cos\sqrt{\lambda_n}\xi - \cosh\sqrt{\lambda_n}\xi)\Big\} \\ & + \frac{\Pi_1}{2\lambda_n}\Big\{2\cosh\sqrt{\lambda_n}\sin\sqrt{\lambda_n}\xi + (\cos\sqrt{\lambda_n} - \cosh\sqrt{\lambda_n})\sinh\sqrt{\lambda_n}\xi \\ & - \sinh\sqrt{\lambda_n}(\cos\sqrt{\lambda_n}\xi - \cosh\sqrt{\lambda_n}\xi)\Big\} + O(\Pi_1^{1.5}) \end{aligned} \tag{3.142}$$

λ_n can finally be substituted from equation (3.140), with the result that the zeroeth order term becomes the same as the mode shapes for an ordinary cantilever beam, equation (B.8) in appendix B, i.e.

$$\lim_{\Pi_1 \to 0} V_n(\xi) = \text{const.} \left[\cosh\sqrt{\lambda_n^*}\xi - \cos\sqrt{\lambda_n^*}\xi - \frac{\sin\sqrt{\lambda_n^*}}{(-1)^{n+1} - \cos\sqrt{\lambda_n^*}} (\sinh\sqrt{\lambda_n^*}\xi - \sin\sqrt{\lambda_n^*}\xi) \right] \quad n,\ n = 1,2,\ldots \tag{3.143}$$

(c) Asymptotic Behavior when $\Pi_1 \to \infty$

A procedure similar to that in part (a) will in the case of $\Pi_1 \to \infty$ lead to the following expressions

$$\begin{aligned} q_1 &= -\alpha - \beta\Pi_1^{-1} + O(\Pi_1^{-2}) \\ q_2 &= \alpha - \beta\Pi_1^{-1} + O(\Pi_1^{-2}) \\ q_3 &= (1 + \Pi_2)\Pi_1 + 2\beta\Pi_1^{-1} + O(\Pi_1^{-2}) \end{aligned} \tag{3.144}$$

in which

$$\begin{aligned} \alpha &= \lambda\sqrt{\frac{\Pi_2}{1+\Pi_2}} \\ \beta &= \frac{\lambda^2}{2(1+\Pi_2)^2} \end{aligned} \tag{3.145}$$

Since β is a function of λ^2 it should be clear that the expansion converges much faster for the smaller eigenvalues than for the larger. In other words, λ/Π_1 should be small in order to assure convergence, contrary to what was observed in part (a) and (b) where

Π_1/λ was required to be small. In this analysis, Π_2 will be assumed to be nonzero such that $\alpha > 0$. (The case when $\Pi_2 = 0$ is treated in appendix C.) With these restrictions, the values of p_i are obtained from equations (3.64) and (3.145)

$$\begin{aligned} p_1 &= \sqrt{\alpha} + \frac{\beta}{2\sqrt{\alpha}} \Pi_1^{-1} + O(\Pi_1^{-2}) \\ p_2 &= \sqrt{\alpha} - \frac{\beta}{2\sqrt{\alpha}} \Pi_1^{-1} + O(\Pi_1^{-2}) \\ p_3 &= \sqrt{1 + \Pi_2}\, \Pi_1^{1/2} + O(\Pi_1^{-3/2}) \end{aligned} \tag{3.146}$$

If $\Pi_1 > 81$, equation (3.103) implies that

$$e^{-\sqrt{\Pi_1}} \leq O(\Pi_1^{-2}) \tag{3.147}$$

such that $\sinh p_3$ and $\cosh p_3$ can be written as

$$\sinh p_3 = \cosh p_3 + O(\Pi_1^{-2}) = \frac{1}{2} e^{p_3} + O(\Pi_1^{-2}) \tag{3.148}$$

Using equations (3.144), (3.148) and (3.44) the eigenvalue equation (3.66) can now be written as

$$\begin{aligned} f(\lambda) = \frac{1}{2} Q_1^2 e^{p_s} \Big[& (2 + 2 \cos p_1 \cosh p_2) \\ & - \frac{2\beta}{\alpha} \Pi_1^{-1} (2 + 2 \cos p_1 \cosh p_2 + \sin p_1 \sinh p_2) \\ & - \frac{4\beta}{\sqrt{\alpha(1+\Pi_2)}} \Pi_1^{-1.5} (\cos p_1 \sinh p_2 + \sin p_1 \cosh p_2) + O(\Pi_1^{-2}) \Big] = 0 \end{aligned} \tag{3.149}$$

Dividing out the constant term and reducing the first order term

according to equation (3.78), the above equation reduces to

$$1 + \cos p_1 \cosh p_2 - \frac{\beta}{\alpha} \Pi_1^{-1} \sin p_1 \sinh p_2 = O(\Pi_1^{-1.5}) \qquad (3.150)$$

which has the same form as equation (3.131). Solving this equation in a similar manner leads to a solution of the form

$$\alpha_n = \lambda_n^* - \lambda_{1n} \Pi_1^{-1} + O(\Pi_1^{-1.5}) \qquad (3.151)$$

where, again, λ_n^* is the solution to equation (3.135), and

$$\alpha_n = \lambda_n \sqrt{\frac{\Pi_2}{1 + \Pi_2}}$$

$$\lambda_{1n} = \beta \frac{\sin\sqrt{\lambda_n^*}\cosh\sqrt{\lambda_n^*} + \cos\sqrt{\lambda_n^*}\sinh\sqrt{\lambda_n^*} + \frac{2}{\sqrt{\lambda_n^*}}\sin\sqrt{\lambda_n^*}\sinh\sqrt{\lambda_n^*}}{\sin\sqrt{\lambda_n^*}\cosh\sqrt{\lambda_n^*} - \cos\sqrt{\lambda_n^*}\sinh\sqrt{\lambda_n^*}} \qquad (3.152)$$

Simplifying λ_{1n} by the use of equation (3.138) and substituting equation (3.152) into (3.151), the resulting equation can be solved for λ_n.

$$\lambda_n = \lambda_n^* \sqrt{\frac{1+\Pi_2}{\Pi_2}} \left[1 - \frac{\lambda_n^*}{2(1+\Pi_2)\Pi_2} \frac{1-(-1)^n\cos\sqrt{\lambda_n^*} - (-1)^n \frac{2}{\sqrt{\lambda_n^*}}\sin\sqrt{\lambda_n^*}}{1+(-1)^n\cos\sqrt{\lambda_n^*}} \Pi_1^{-1} \right.$$

$$\left. + O(\Pi_1^{-1.5}) \right] \; ; \quad n = 1,2,\ldots \qquad (3.153)$$

It is interesting that the asymptotic value

$$\lim_{\Pi_1 \to \infty} \lambda_n = \lambda_n^* \sqrt{\frac{1+\Pi_2}{\Pi_2}} \; ; \quad n = 1,2,\ldots \qquad (3.154)$$

can be explained directly by a physical consideration of the coupled shear wall. As mentioned earlier, when Π_1 increases, the stiffness of the spandrel systems becomes large compared to the stiffness of the walls. By making rigid spandrel connections the value of Π_1 becomes infinite, and looking at such a system should therefore yield the asymptotic values given above.

For a rigid spandrel system, the coupled shear wall will obey Euler-Bernoulli theory[31] with the moment of inertia and total cross-sectional area given by

$$\begin{aligned} A_T &= 2A_1 \\ I_T &= 2I_1 + 2A_1\left(\frac{a_1}{2}\right)^2 \end{aligned} \tag{3.155}$$

or, using equation (3.2)

$$I_T = 2I_1 \frac{1 + \Pi_2}{\Pi_2} \tag{3.156}$$

The eigenvalues for this system can be written as[31]

$$\lambda_n^* = \ell_1^2 \omega_n \sqrt{\frac{\rho_1 A_1 + \rho_3 A_3 \frac{\ell_3}{a_2}}{E_1 I_T}} \tag{3.157}$$

and by employing equations (3.3) and (3.156), equation (3.157) implies that

$$\lambda_n = \lambda_n^* \sqrt{\frac{1 + \Pi_2}{\Pi_2}} \quad ; \quad n = 1, 2 \tag{3.158}$$

in agreement with the asymptotic value, equation (3.154).

The mode shapes are obtained from equation (3.68) using equations (3.69), (3.44), (3.144), (3.146) and (3.83)

$$V_n(\xi) = (\cos p_1 + \cosh p_2)(\sin p_1\xi - \sinh p_2\xi)$$
$$- (\sin p_1 + \sinh p_2)(\cos p_1\xi - \cosh p_2\xi)$$
$$+ \frac{\beta}{\alpha}\Pi_1^{-1}\left[2\cosh p_2 \sin p_1\xi + (3\cos p_1 + \cosh p_2)\sinh p_2\xi\right.$$
$$\left. + \sinh p_2(\cos p_1\xi - \cosh p_2\xi)\right] + O(\Pi_1^{-1.5}) \qquad (3.159)$$

Finally, this equation can be written in terms of λ_n^* by the use of equations (3.146) and (3.151)

$$V_n(\xi) = (\cos\sqrt{\lambda_n^*} + \cosh\sqrt{\lambda_n^*})(\sin\sqrt{\lambda_n^*}\xi - \sinh\sqrt{\lambda_n^*}\xi)$$
$$- (\sin\sqrt{\lambda_n^*} + \sinh\sqrt{\lambda_n^*})(\cos\sqrt{\lambda_n^*}\xi - \cosh\sqrt{\lambda_n^*}\xi) + O(\Pi_1^{-1}) \; ; \; n=1,2,\ldots$$
(3.160)

The asymptotic mode shapes are again, by comparison with equation (B.8) in appendix B, the same as the mode shapes for an ordinary cantilever beam.

(d) Asymptotic Behavior when $\Pi_2 \to 0$

As mentioned in the introduction of this chapter, the case when $\Pi_2 \to 0$ cannot be solved in the same manner as the cases treated earlier. This fact can be seen from equation (3.88), which in this case can be expanded in a series of Π_2 as

$$\cos^2\phi = \frac{\Pi_1^6 + 9\lambda^2\Pi_1^4 + \frac{81}{4}\lambda^2\Pi_1^2}{27\lambda^6 + 27\lambda^4\Pi_1^2 + 9\lambda^2\Pi_1^4 + \Pi_1^6} + O(\Pi_2) \qquad (3.161)$$

From equation (3.161) it is clear that no simple form can be obtained for ϕ. This will complicate the expression for q_i and make the eigenvalue-equation intractable.

Another way to find the asymptotic behavior is the perturbation method[24]. It will prove to be a convenient method for this case, and also for one case in the next chapter.

The set of differential equations and boundary conditions, equations (3.23) and (3.24), can for the present case ($\Pi_3 = 0$) be written as

$$\left.\begin{aligned} &V'''' - \Pi_1 V'' + \Pi_1 U' - \lambda^2 V = 0 \\ &U'' + \Pi_1\Pi_2 V' - \Pi_1\Pi_2 U = 0 \end{aligned}\right\} \qquad \xi \in [0,1] \qquad (3.162)$$

$$\begin{aligned} &V(0) = V'(0) = U(0) = 0 \\ &V''(1) = V'''(1) - \Pi_1[V'(1) - U(1)] = U'(1) = 0 \end{aligned} \qquad (3.163)$$

When Π_2 is small, the solution will be assumed to have the form

$$\begin{aligned} V &= V_0 + V_1\Pi_2^{p_1} + O(\Pi_2^{p_1+p_2}) \\ U &= U_0 + U_1\Pi_2^{q_1} + O(\Pi_2^{q_1+q_2}) \\ \lambda &= \lambda_0 + \lambda_1\Pi_2^{r_1} + O(\Pi_2^{r_1+r_2}) \end{aligned} \qquad (3.164)$$

where the constants p_i, q_i and r_i are all positive, real numbers.

It can easily be proven that

$$p_i = r_i = q_i = 1; \quad i = 1,2 \tag{3.165}$$

by using a technique similar to the following derivations, and by noting, from equation (3.83), that if V_1 has the same form as V_0 it can be disregarded. Equations (3.164) can thus be written as

$$\begin{aligned} V &= V_0 + V_1\Pi_2 + O(\Pi_2^2) \\ U &= U_0 + U_1\Pi_2 + O(\Pi_2^2) \\ \lambda &= \lambda_0 + \lambda_1\Pi_2 + O(\Pi_2^2) \end{aligned} \tag{3.166}$$

Substituting these expressions into the differential equation (3.162), one obtains

$$\begin{aligned} &V_0'''' + \Pi_2 V_1'''' - \Pi_1 V_0'' - \Pi_1\Pi_2 V_1'' + \Pi_1 U_0' + \Pi_1\Pi_2 U_1' - \lambda_0^2 V_0 \\ &\qquad - 2\lambda_0\lambda_1\Pi_2 V_0 - \lambda_0^2\Pi_2 V_1 = O(\Pi_2^2) \\ &U_0'' + \Pi_2 U_1'' + \Pi_1\Pi_2 V_0' - \Pi_1\Pi_2 U_0 = O(\Pi_2^2) \end{aligned} \tag{3.167}$$

and it is clear that by repeatedly applying the limit $(\Pi_2 \to 0)$, the zeroeth and first order terms in Π_2 both must vanish giving

$$\left.\begin{aligned} O(\Pi_2^0): \quad V_0'''' - \Pi_1 V_0'' + \Pi_1 U_0' - \lambda_0^2 V_0 &= 0 \\ U_0'' &= 0 \end{aligned}\right\} \qquad \xi \in [0,1] \tag{3.168}$$

with

$$V_0(0) = V_0'(0) = U_0(0) = 0$$
$$V_0''(1) = V_0'''(1) - \Pi_1[V_0'(1) - U_0(1)] = U_0'(1) = 0 \tag{3.169}$$

$$0(\Pi_2^1): \quad \left.\begin{aligned} V_1'''' - \Pi_1 V_1'' + \Pi_1 U_1' - \lambda_0^2 V_1 &= 2\lambda_0\lambda_1 V_0 \\ U_1'' &= -\Pi_1(V_0' - U_o) \end{aligned}\right\} \quad \xi \in \langle 0,1\rangle \tag{3.170}$$

with

$$V_1(0) = V_1'(0) = U_1(0) = 0$$
$$V_1''(1) = V_1'''(1) - \Pi_1[V_1'(1) - U_1(1)] = U_1'(1) = 0 \tag{3.171}$$

The zeroeth order terms will be determined by solving the first system of differential equations and boundary conditions. Integrating the second equation in (3.168) twice and applying the appropriate boundary conditions,

$$U_0(\xi) = 0 \tag{3.172}$$

The first equation in (3.168) becomes

$$V_0'''' - \Pi_1 V_0'' - \lambda_0^2 V_0 = 0 \tag{3.173}$$

and the corresponding boundary conditions are

$$V_0(0) = V_0'(0) = V_0''(1) = V_0'''(1) - \Pi_1 V_0'(1) = 0 \tag{3.174}$$

This problem is treated in appendix C, and the solution is obtained from equation (C.7) and (C.8)

$$V_{0n}(\xi) = C\left[(p_1^2\cos p_1 + p_2^2\cosh p_2)(p_2\sin p_1\xi - p_1\sinh p_2\xi)\right.$$
$$\left. - p_1p_2(p_1\sin p_1 + p_2\sinh p_2)(\cos p_1\xi - \cosh p_2\xi)\right] \; ; \; n=1,2,\ldots \tag{3.175}$$

in which

$$p_1 = \sqrt{\frac{1}{2}\sqrt{\Pi_1^2 + 4\lambda_{0n}^2} - \frac{\Pi_1}{2}}$$
$$p_2 = \sqrt{\frac{1}{2}\sqrt{\Pi_1^2 + 4\lambda_{0n}^2} + \frac{\Pi_1}{2}} \tag{3.176}$$

C is any arbitrary constant, and λ_{0n} is the n'th eigenvalue for the zeroeth's approximation, determined by the equation

$$\lambda_{0n}^2(2 + 2\cos p_1\cosh p_2) + \lambda_{0n}\Pi_1\sin p_1\sinh p_2 + \Pi_1^2\cos p_1\cosh p_2 = 0 \tag{3.177}$$

The first order terms can be obtained by solving the differential equations in (3.170). Applying equations (3.172) and (3.175) the second equation in (3.170) reduces to

$$U_1''(\xi) = -\Pi_1 V_0'(\xi) \tag{3.178}$$

By integrating this equation and applying the boundary conditions (3.171), $U_1(\xi)$ is found to be

$$U_1(\xi) = \Pi_1 V_0(1)\cdot\xi + \frac{\Pi_1}{\lambda_{0n}^2}\left[V_0'''(0) - V_0'''(\xi) + \Pi_1 V_0'(\xi)\right] \tag{3.179}$$

Using this result in the first equation in (3.170) gives

$$V_1'''' - \Pi_1 V_1'' - \lambda_0^2 V_1 = (2\lambda_{1n}\lambda_{0n} + \Pi_1^2)V_0(\xi) - \Pi_1^2 V_0(1) \quad (3.180)$$

The particular solution to this equation is obtained by an inverse operator technique while the homogeneous solution will be of the same form as the zeroeth order solution. Adding these expressions and simplifying,

$$V_{1n}(\xi) = C_1 \sin p_1\xi + C_2 \cos p_1\xi + C_3 \sinh p_2\xi + C_4 \cosh p_2\xi + \frac{\Pi_1^2}{\lambda_{0n}^2} V_0(1) + K_n \xi\left[(\Pi_1^2 + 2\lambda_{0n}^2)V_0'(\xi) - \Pi_1 V_0'''(\xi)\right] \; ; \; n=1,2,\ldots \quad (3.181)$$

in which p_1 and p_2 are given by equation (3.176) and

$$K_n = \frac{2\lambda_{1n}\lambda_{0n} + \Pi_1^2}{2\lambda_{0n}^2(4\lambda_{0n}^2 + \Pi_1^2)} \; ; \; n = 1,2,\ldots \quad (3.182)$$

It should be observed that equation (3.181) has essentially six unknown quantities; C_1 through C_4, λ_1 and the constant C appearing in $V_0(1)$, $V_0'(\xi)$ and $V_0'''(\xi)$. The constant C can conveniently be absorbed into the constants C_1 through C_4, leaving only five unknowns.

The boundary conditions that $V_1(\xi)$ must satisfy are obtained from equation (3.171) using (3.169) and (3.179)

$$V_1(0) = V_1'(0) = V_1''(1) = 0$$
$$V_1'''(1) - \Pi_1 V_1'(1) = -\Pi_1^2 V_0(1) - \frac{\Pi_1^2}{\lambda_{0n}^2} V_0'''(0) \quad (3.183)$$

When these boundary conditions are applied to $V_1(\xi)$, four linear equations in C_1 through C_4 are obtained which can be written in matrix form as

$$A\underline{c} = \underline{b} \tag{3.184}$$

where

$$A = \begin{bmatrix} 0 & 1 & 0 & 1 \\ p_1 & 0 & p_2 & 0 \\ -p_1^2 \sin p_1 & -p_1^2 \cos p_1 & p_2^2 \sinh p_2 & p_2^2 \cosh p_2 \\ -p_1 p_2^2 \cos p_1 & p_1 p_2^2 \sin p_1 & p_2 p_1^2 \cosh p_2 & p_2 p_1^2 \sinh p_2 \end{bmatrix} \tag{3.185}$$

$\underline{c}$ is the vector containing the elements C_1 through C_4 and $\underline{b}$ is the vector given by

$$\underline{b} = \Pi_1 \begin{bmatrix} -\frac{\Pi_1}{\lambda_{0n}^2} V_0(1) \\ K_n V_0'''(0) \\ K_n \lambda_{0n}^2 [\, 2V_0(1) - V_0'(1)] \\ -K_n \lambda_{0n}^2 [\, V_0'(1) + (2\frac{\lambda_{0n}^2}{\Pi_1} + \Pi_1) V_0(1)] - \Pi_1 [\, V_0(1) + \frac{1}{\lambda_{0n}^2} V_0'''(0)] \end{bmatrix} \tag{3.186}$$

It is observed, by equations (3.176) and (3.177), that A is a singular matrix. Consequently, there will be a solution of equation (3.184) only if $\underline{b}$ possesses special properties, and these conditions on $\underline{b}$ will determine the unknown scalar quantity λ_1.

In order to find these relations for $\underline{b}$, let $\underline{y}$ be the solution to the homogeneous matrix equation

$$A^T\underline{y} = \underline{0} \tag{3.187}$$

(A^T is the transpose of A). Employing equations (3.184) and (3.187), the inner product[26] of $\underline{y}$ and $\underline{b}$ is evaluated as

$$(\underline{y},\underline{b}) = (\underline{y}, A\underline{c}) = (A^T\underline{y},\underline{c}) = (\underline{0},\underline{c}) \tag{3.188}$$

Hence

$$\sum_{i=1}^{4} y_i b_i = 0 \tag{3.189}$$

in which λ_1 is the only unknown quantity.

By solving equation (3.187), y_i is obtained as

$$\begin{bmatrix} y_1 \\ y_2 \\ y_3 \\ y_4 \end{bmatrix} = \text{const.} \begin{bmatrix} \lambda_{0n}^2 + p_1(p_2^3 \sin p_1 \sinh p_2 + p_1^3 \cos p_1 \cosh p_2) \\ p_1^3 \sin p_1 \cosh p_2 - p_2^3 \cos p_1 \sinh p_2 \\ p_2^2 \cos p_1 + p_1^2 \cosh p_2 \\ -(p_1 \sin p_1 + p_2 \sinh p_2) \end{bmatrix} \tag{3.190}$$

and by equations (3.186), (3.189) and (3.190), the scalar K_n is determined to be

$$K_n = \Pi_1^2\Big[y_1 V_{0n}(1) + y_4\{V_{0n}(1)\lambda_{0n}^2 + V_{0n}'''(0)\}\Big]\Big[\lambda_{0n}^2[\, y_2\Pi_1 V_{0n}'''(0)$$

$$+ y_3\lambda_{0n}^2\Pi_1\{2V_{0n}(1) - V_{0n}'(1)\}$$

$$- y_4\lambda_{0n}^2\{V_{0n}'(1)\Pi_1 + (\Pi_1^2+2\lambda_{0n}^2)V_{0n}(1)\}\ \Big]^{-1};\quad n = 1,2,\ldots \tag{3.191}$$

where, from equation (3.175)

$$V_{0n}(1) = C\sqrt{\Pi_1^2+4\lambda_{0n}^2}\,[\, p_2 \sin p_1 \cosh p_2 - p_1 \cos p_1 \sinh p_2]$$

$$V_{0n}'(1) = C\,\lambda_{0n}[\,-\Pi_1 + \Pi_1 \cos p_1 \cosh p_2 + 2\lambda_{0n}\sin p_1 \sinh p_2] \tag{3.192}$$

$$V_{0n}'''(0) = -C\lambda_{0n}\sqrt{\Pi_1^2+4\lambda_{0n}^2}\,[\, p_1^2 \cos p_1 + p_2^2 \cosh p_2]$$

λ_{1n} is finally obtained from equation (3.182)

$$\lambda_{1n} = \lambda_{0n}[\,4\lambda_{0n}^2 + \Pi_1^2]\,K_n - \frac{\Pi_1^2}{2\lambda_{0n}};\quad n = 1,2,\ldots \tag{3.193}$$

The first approximation to the mode shapes can now be found by solving equation (3.184) for $\underline{c}$ and applying the result to equation (3.181). With equation (3.189) satisfied, a solution to equation (3.184) of the form

$$\underline{c} = \begin{bmatrix} C_1 \\ C_2 \\ C_3 \\ C_4 \end{bmatrix} = h\underline{c_0} + \underline{c_1} \tag{3.194}$$

exists. h is any arbitrary constant, and $\underline{c_0}$ is the solution to the homogeneous matrix equation

$$A\,\underline{c_0} = \underline{0} \tag{3.195}$$

Hence, by equation (3.175) and (C.6) in appendix C, $\underline{c_0}$ is the vector solution giving the zeroeth order mode shapes. (This, in effect, was the result of the discussion in the introduction to this section, namely that the first approximation to the mode shapes could not be uniquely determined. Any addition of a constant multiplied by the zeroeth approximation would also yield the same total mode shapes.)

Because of the arbitrariness of h, and the fact that none of the elements of $\underline{c_0}$ are zero, one of the elements in $\underline{c}$ can be picked arbitrarily. Hence, without loss of generality, let

$$C_4 = 0 \tag{3.196}$$

Applying equations (3.184), (3.185), (3.186) and (3.196), C_1, C_2 and C_3 are given by

$$\begin{bmatrix} 0 & 1 & 0 \\ p_1 & 0 & p_2 \\ -p_1^2\sin p_1 & -p_1^2\cos p_1 & p_2^2\sinh p_2 \end{bmatrix} \begin{bmatrix} C_1 \\ C_2 \\ C_3 \end{bmatrix} = \frac{\Pi_1}{\lambda_{0n}^2} \begin{bmatrix} -\Pi_1 V_0(1) \\ K_n\lambda_{0n}^2 V_0'''(0) \\ K_n\lambda_{0n}^4 [2V_0(1) - V_0'(1)] \end{bmatrix} \tag{3.197}$$

Finally, the mode shapes when $\Pi_2 \to 0$ will be

$$V_n(\xi) = V_{0n}(\xi) + \Pi_2 V_{1n}(\xi) + O(\Pi_2^2) \tag{3.198}$$

where $V_{0n}(\xi)$ is given by equation (3.175) and $V_{1n}(\xi)$ by equations (3.181), (3.196) and (3.197).

3.4. Discussion on the General Solution

The object of this section is to discuss some of the results obtained in earlier sections and to present some general solutions for the eigenvalues. This will be done in the form of a number of graphs from which it will be possible to obtain approximate values for the eigenvalues given Π_1 and Π_2.

Figure 3.2 shows the general behavior of the first six eigenvalues as a function of Π_1 and Π_2. The values are obtained directly from the eigenvalue equation (3.66), with Π_2 taking on three different values believed to cover most cases of interest. Given any set of values for Π_1 and Π_2; Π_1 between 1.0 and 10,000, and Π_2 between 0.1 and 0.2, the eigenvalues can be obtained from this graph with less than 5% error. The natural frequencies of the coupled shear wall can then be calculated using equation (3.67)

$$\omega_n = \frac{\lambda_n}{\ell_1^2}\sqrt{\frac{E_1 I_1 a_2}{(\rho_1 A_1 a_2^{} + \frac{1}{2}\rho_3 \ell_3 A_3)}} \qquad (3.67)$$

Of special importance is the first natural frequency. Figure 3.3 gives more accurate result for this case and more values of Π_2 are included. Also included in the figure are the values for the asymptotic expansions when $\Pi_1 \to \infty$, as obtained in the previous section, equation (3.153), and when $\Pi_1 \to 0$, equation (3.140).

The importance of the asymptotic values can also be observed

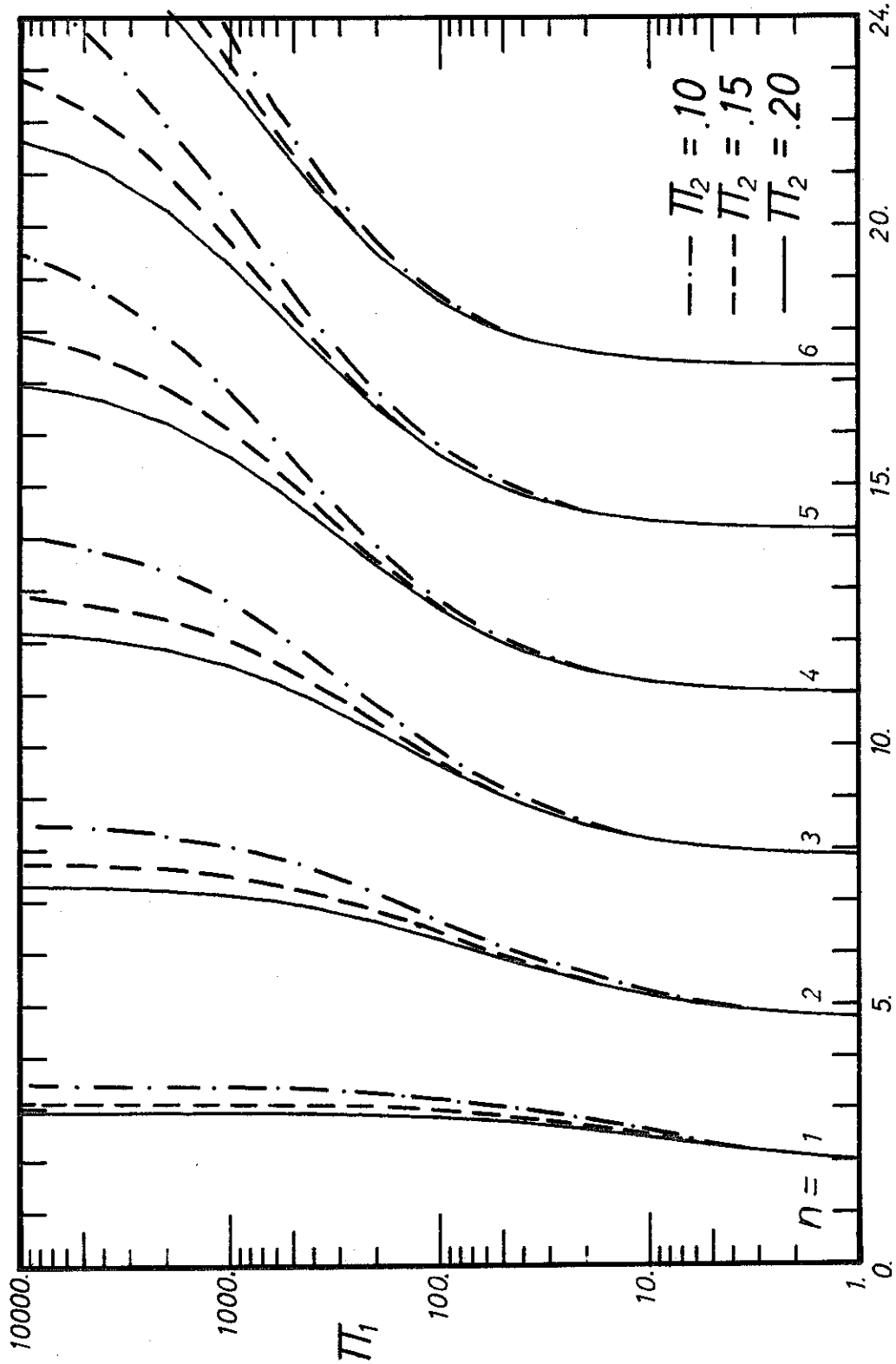

Fig. 3.2. First 6 Eigenvalues for Different Values of Π_2. $\Pi_3 = 0$

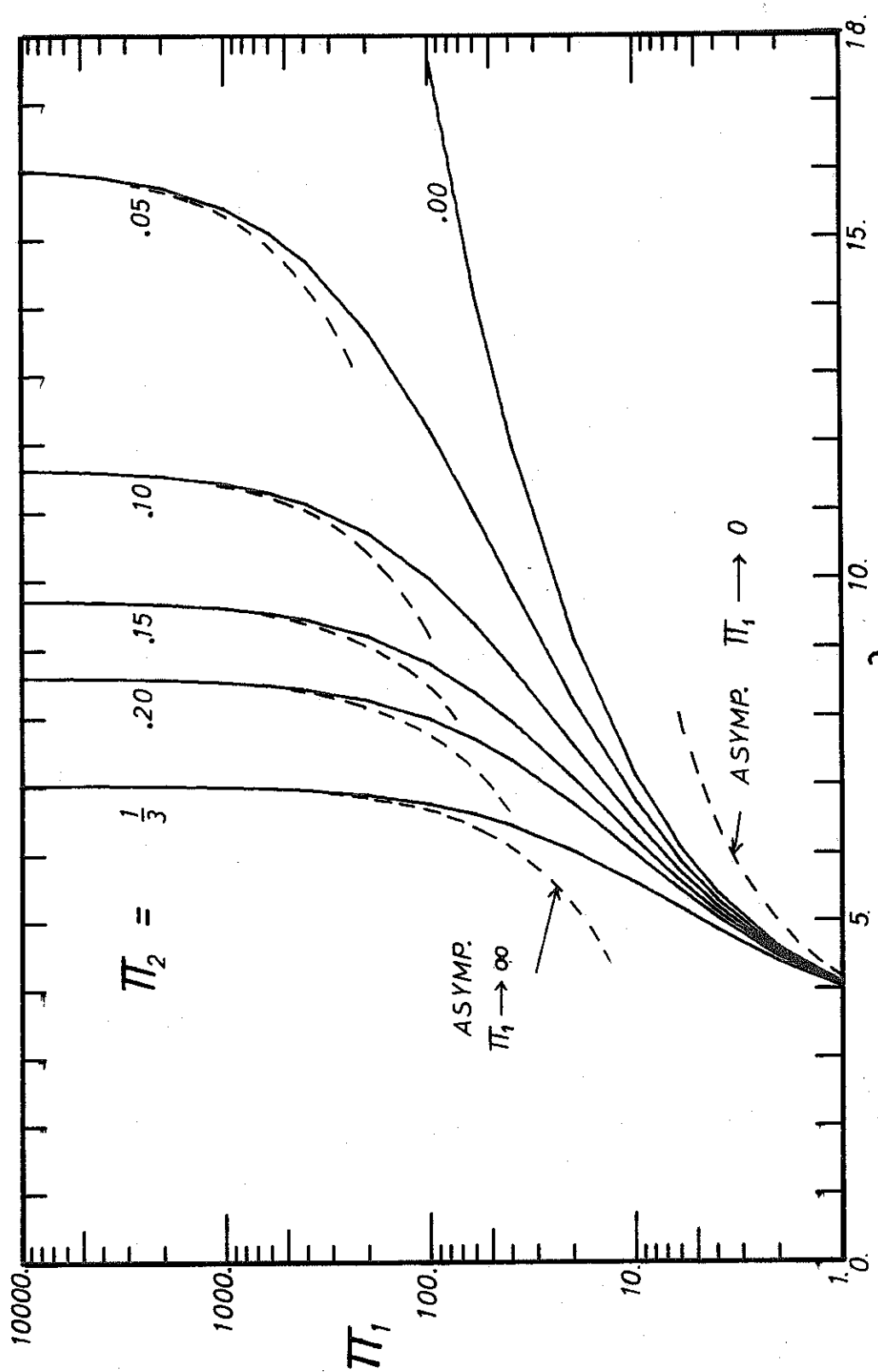

Fig. 3.3. First Eigenvalue Neglecting Vertical Inertia ($\Pi_3 = 0$)

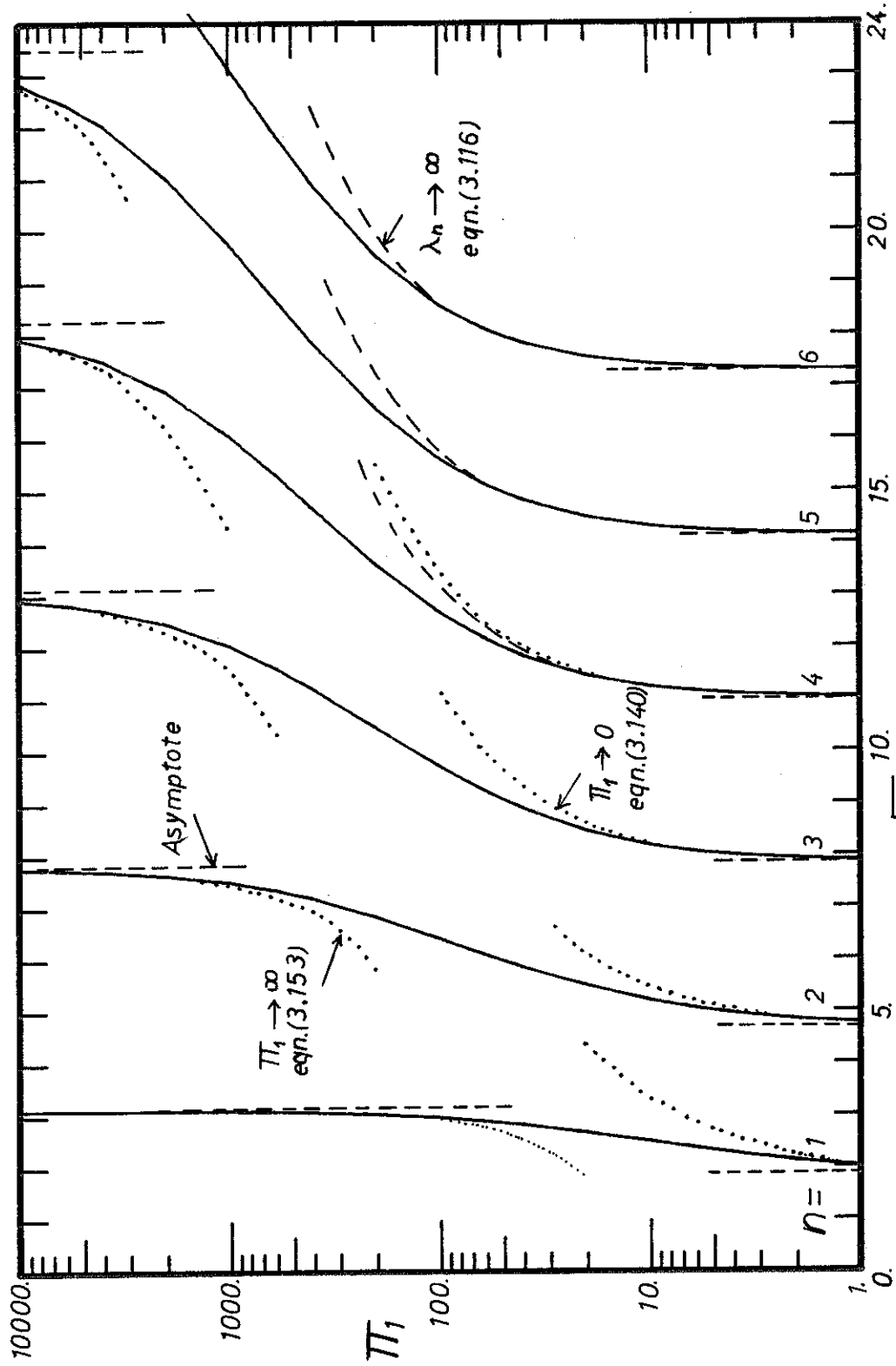

Fig. 3.4. Asymptotic Behavior as $\Pi_1 \to 0$, $\Pi_1 \to \infty$ and $\lambda_n \to \infty$ when $\Pi_2 = 0.15$

in Figure 3.4 which compares these values with the exact values for the case when $\Pi_2 = 0.15$. Both the asymptotic values (dashed lines) and the first approximation to the asymptotic values (dotted lines) are given, and the figure provides an indication of when the asymptotic expansions can be used, thereby simplifying the calculations considerably.

It can also be observed in Figure 3.4 what was indicated in previous sections about the convergence to the exact values, i.e., the convergence for large n, $\lambda_n \to \infty$, is slow for large Π_1, while the convergence for large Π_1 is slow for the larger eigenvalues.

The asymptotic expansion for the mode shapes showed that the modes approach those of an ordinary cantilever beam as $\lambda_n \to \infty$, as $\Pi_1 \to 0$ and as $\Pi_1 \to \infty$. The last two instances can be observed in Figure 3.5 where horizontal motion in the first mode is plotted for different values of Π_1.

The case for $\Pi_2 \to 0$ was not worked out in detail, although it was found (equation (3.175)) that the asymptotic mode shapes will be those found in appendix C when $\Pi_2 = 0$. Here it was observed that a sine-function (equation (C.34)) will be the dominating part as Π_1 becomes large. This feature can also be seen in Figure 3.6 which gives the first mode shape for different values of Π_2.

Although no proof is given, it appears from the figures and the asymptotic expansions that the actual mode shapes will be something between that of a cantilever beam and that of a shear beam (sine wave modes). Typically, the shape will closely resemble those

of the cantilever beam, but when Π_1 is large and Π_2 is small, the sine-wave will become more dominant.

For the higher eigenvalues, the mode shapes will again approach those of the cantilever beam, and again it can be observed (equation (3.119)) that a sine-term is added to the cantilever beam as a first approximation. An example will be given in chapter IV that will show this behavior.

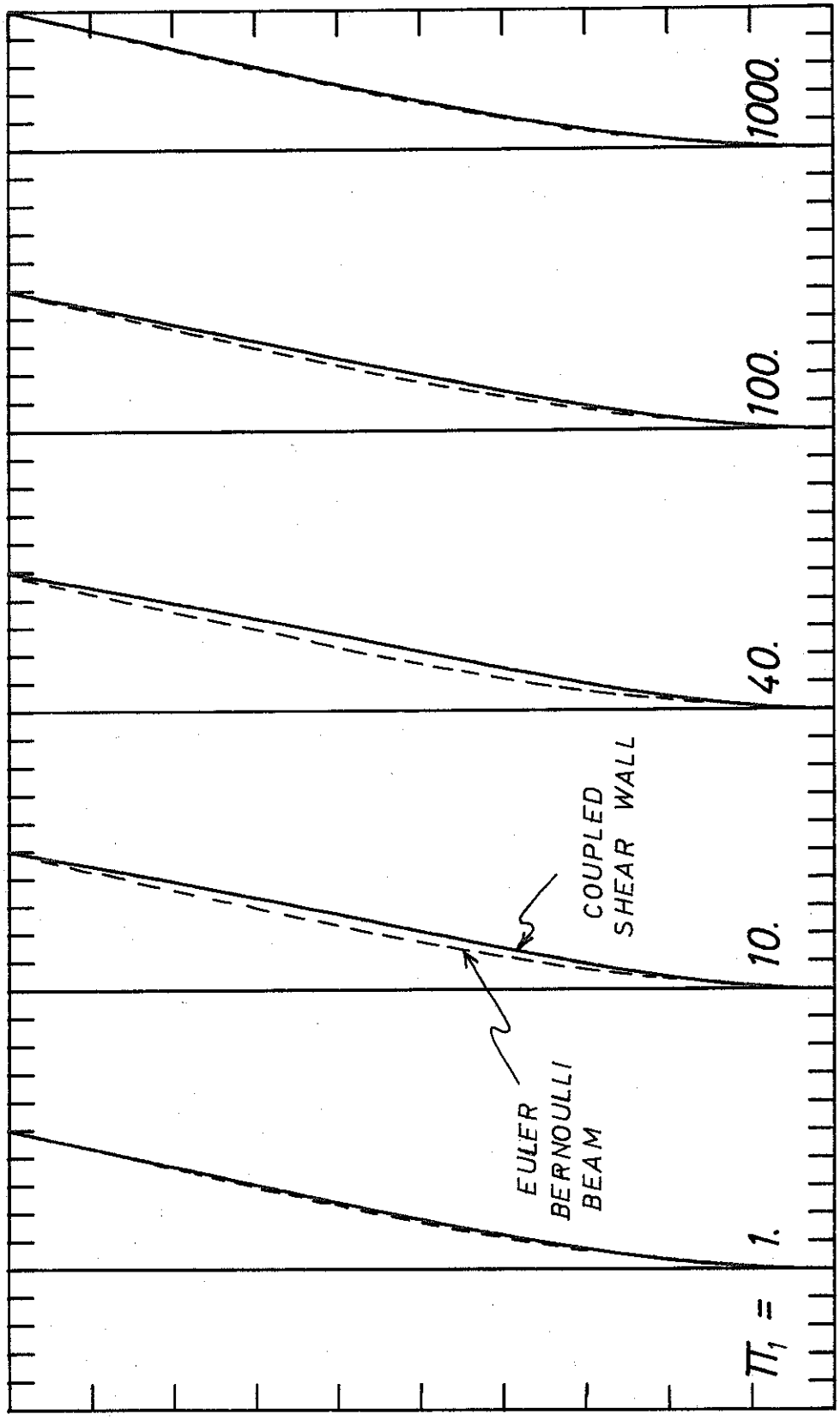

Fig. 3.5. First Mode Shape for Different Values of Π_1. $\Pi_2 = 0.10$, $\Pi_3 = 0$

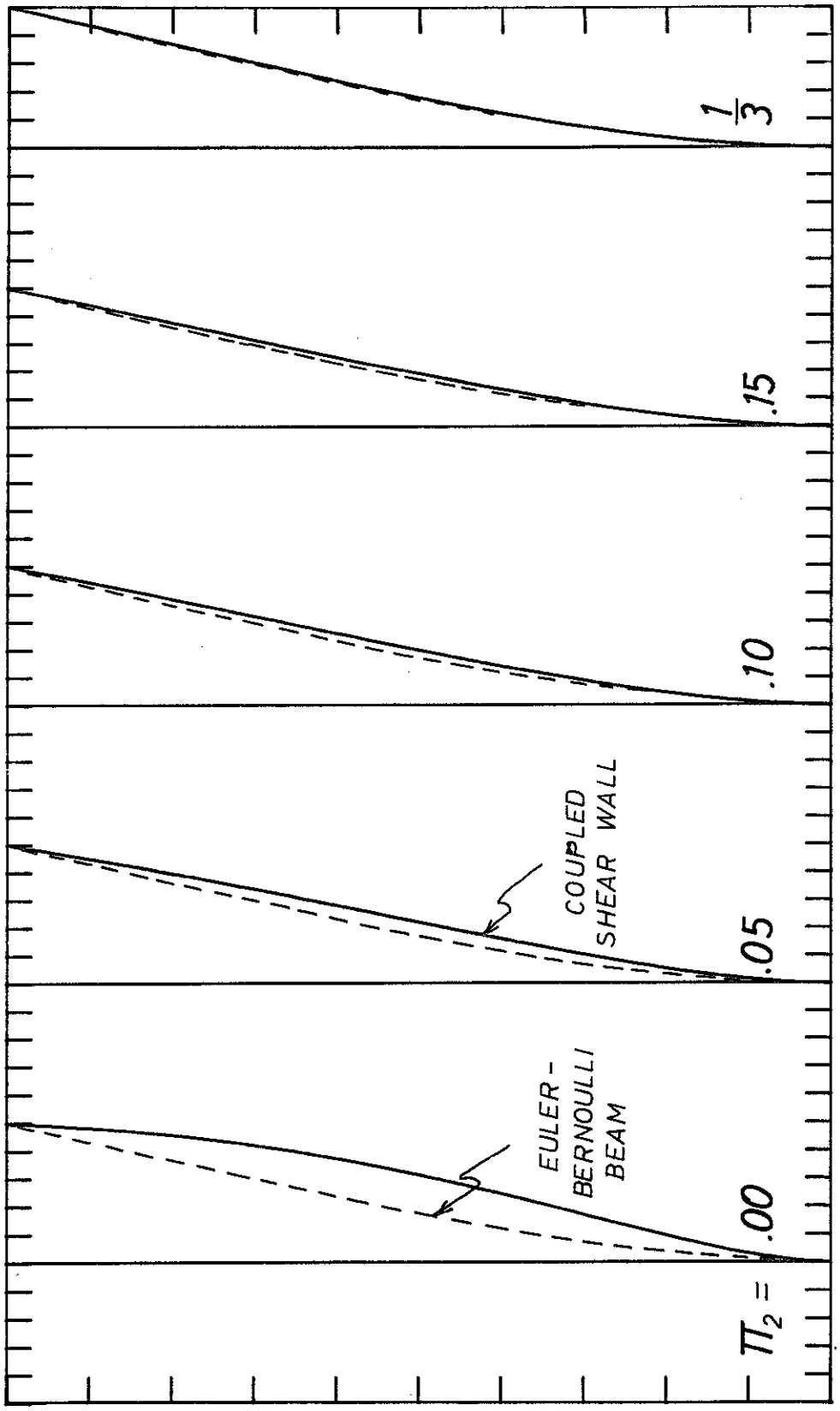

Fig. 3.6. First Mode Shape for Different Values of Π_2, $\Pi_1 = 100$, $\Pi_3 = 0$

CHAPTER IV

DYNAMIC ANALYSIS OF EQUAL-SIZED SHEAR WALLS INCLUDING VERTICAL INERTIA

When Π_3 was set equal to zero in chapter III, the effect of vertical inertia was eliminated. This assumption was based on the hypothesis that the lateral vibrations were of greatest interest and that the higher natural frequencies similarly were of lesser importance. As a result of setting $\Pi_3 = 0$, the eigenvalue equation was obtained in a fairly simple form, and the asymptotic expansions could be carried out in a straightforward manner. The object of this chapter is to examine the assumption that Π_3 vanishes, i.e., to compare results for $\Pi_3 \equiv 0$ and for $\Pi_3 \neq 0$.

It is found that when $\Pi_3 \neq 0$, there exists an increased number of eigenvalues in comparable frequency ranges, resulting from the fact that the eigenvalues associated with antisymmetrical longitudinal vibration will be obtained in addition to those associated with lateral vibration.

Section 4.1 gives equations for the eigenvalues and eigenvectors while some features of the asymptotic behavior are analyzed in section 4.2. Discussion of the general solution and of the effect of the vertical inertia is given in sections 4.3 and 4.4, while a numerical example is treated at the end of the chapter.

4.1. Derivation of Eigenvalue Equation and Mode Shapes

The assumption that $\Pi_3 = 0$ was not introduced, in section 3.1 of chapter III, so the results obtained there will be applicable in this case too. The characteristic equation will thus be as in equation (3.30).

$$q^3 - (\Pi_1 + \Pi_1\Pi_2 - \lambda^2\Pi_3)q^2 - \lambda^2(1 + \Pi_1\Pi_3)q + \lambda^2(\Pi_1\Pi_2 - \lambda^2\Pi_3) = 0 \quad (4.1)$$

Similar to the case in the last chapter, this equation will have three real and unequal roots in q if

$$\frac{b^2}{4} + \frac{a^3}{27} < 0 \quad (4.2)$$

where

$$a = -\frac{1}{3}[\,3(1 + \Pi_1\Pi_3)\lambda^2 + (\Pi_1 + \Pi_1\Pi_2 - \lambda^2\Pi_3)^2]$$

$$b = -\frac{1}{27}[\,2(\Pi_1 + \Pi_1\Pi_2 - \lambda^2\Pi_3)^3 + 9(\Pi_1 + \Pi_1\Pi_2 - \lambda^2\Pi_3)(1 + \Pi_1\Pi_3)\lambda^2 - 27(\Pi_1\Pi_2 - \lambda^2\Pi_3)\lambda^2] \quad (4.3)$$

After some algebra,

$$\frac{b^2}{4} + \frac{a^3}{27} = -\frac{\lambda^2}{108}\Big\{\Pi_1^4[\,4\Pi_2(1+\Pi_2)^3] + \Pi_1^2[\,(1 + 20\Pi_2 - 8\Pi_2^2) - 2(1+\Pi_2)(1+8\Pi_2^2)\Pi_1\Pi_3 + (1+\Pi_2)^2\Pi_1^2\Pi_3^2]\lambda^2 + [\,4 - 8(1-2\Pi_2)\Pi_1\Pi_3 + 2(1-2\Pi_2+12\Pi_2^2)\Pi_1^2\Pi_3^2 + 2(1-\Pi_2)\Pi_1^3\Pi_3^3]\lambda^4 + \Pi_3^2[\,-8 - 8(1-2\Pi_2)\Pi_1\Pi_3 + \Pi_1^2\Pi_3^2]\lambda^6 + 4\Pi_3^4\lambda^8\Big\} \quad (4.4)$$

Numerically, it can be shown that equation (4.4) is always negative

when

$$0 < \Pi_1 < 10^6$$
$$0 < \Pi_2 < 0.5 \qquad (4.5)$$
$$0 < \Pi_3 < 0.5$$

such that for values of Π_1, Π_2 and Π_3 within these limits, equation (4.1) will have three real roots. By application of Descartes Rule[34] it is found that when

$$\lambda^2 < \frac{\Pi_1 \Pi_2}{\Pi_3} \qquad (4.6)$$

equation (4.1) will have 2 positive and one negative roots, while when

$$\lambda^2 > \frac{\Pi_1 \Pi_2}{\Pi_3} \qquad (4.7)$$

equation (4.1) possesses 2 negative roots and one postive root. The limiting value between these two cases proves to be of interest, and will be defined by

$$\lambda_c^2 = \frac{\Pi_1 \Pi_2}{\Pi_3} \qquad (4.8)$$

The roots to equation (4.1) can, similar to equation (3.62), be written as

$$q_i = 2\sqrt{-\frac{a}{3}}\cos\left(\frac{\phi}{3} + \frac{2\pi i}{3}\right) + \frac{\Pi_1 + \Pi_1\Pi_2 - \lambda^2\Pi_3}{3}\ ;\ i = 1,2,3 \qquad (4.9)$$

in which

$$\phi = \cos^{-1}\left[\frac{3b}{2a}\sqrt{-\frac{3}{a}}\right]$$

and where a and b are as given in equation (4.3). Further, q_1 is defined such that

$$q_1 < q_2 < q_3 \tag{4.10}$$

which together with the above discussion implies that $q_1 < 0$, $q_3 > 0$, and that $q_2 > 0$ for $\lambda < \lambda_c$ and $q_2 < 0$ for $\lambda > \lambda_c$. With p_i defined as

$$p_i = \sqrt{|q_i|} \qquad i = 1,2,3 \tag{4.11}$$

the expressions for s_i and c_i, equation (3.40) can now be replaced by

$$\begin{aligned}
s_1(\xi) &= \frac{1}{p_1} \sin p_1\xi \\
s_2(\xi) &= \frac{1}{p_2} \sin\,(h)\, p_2\xi \equiv \begin{cases} \frac{1}{p_2} \sinh p_2\xi & ; \ \lambda < \lambda_c \\ \frac{1}{p_2} \sin p_2\xi & ; \ \lambda > \lambda_c \end{cases} \\
s_3(\xi) &= \frac{1}{p_3} \sinh p_3\xi \\
c_1(\xi) &= \cos p_1\xi \\
c_2(\xi) &= \cos\,(h)\, p_2\xi \equiv \begin{cases} \cosh p_2\xi & ; \ \lambda < \lambda_c \\ \cos p_2\xi & ; \ \lambda > \lambda_c \end{cases} \\
c_3(\xi) &= \cosh p_3\xi
\end{aligned} \tag{4.12}$$

With these substitutions, the eigenvalue equation (3.46) becomes

$$f(\lambda_n) = Q_2Q_3[\,2 + \frac{q_2+q_3}{p_2p_3}\sin(h)p_2\sinh p_3]\cos p_1$$

$$+ Q_3Q_1[\,2 + \frac{q_3+q_1}{p_3p_1}\sinh p_3\ \sin p_1]\cos(h)p_2$$

$$+ Q_1Q_2[\,2 + \frac{q_1+q_2}{p_1p_2}\sin p_1\sin(h)p_2]\cosh p_3$$

$$+ [\,Q_1^2+Q_2^2+Q_3^2]\cos p_1\cos(h)p_2\cosh p_3 = 0;\quad \lambda_n \neq \lambda_c \tag{4.13}$$

where Q_i are given by

$$Q_1 = (q_2 - q_3)(q_2q_3 + \lambda^2)$$

$$Q_2 = (q_3 - q_1)(q_3q_1 + \lambda^2) \tag{4.14}$$

$$Q_3 = (q_1 - q_2)(q_1q_2 + \lambda^2)$$

The derivation of the eigenvalue equation (3.46) was based on the assumptions that no roots of equation (4.1) were zero (equation (3.45)). When $\lambda = \lambda_c$ it can be observed from equation (4.1) that one of the roots is indeed zero, and the eigenvalue equation must be rederived for this special case. In any practical application, it is quite unlikely that an eigenvalue would equal λ_c, but this possibility is included for completeness.

For $\lambda = \lambda_c$ the eigenvalue equation can be derived by a technique similar to that in section 3.1, giving

$$q_1 \frac{Q_2}{\lambda_c^2}\left[2+\frac{q_3}{p_3}\sinh p_3\right]\cos p_1 - q_3 \frac{Q_2}{\lambda_c^2}\left[2+\frac{q_1}{p_1}\sin p_1\right]\cosh p_3$$

$$- q_1 q_3\left[2+\frac{q_1+q_3}{p_1 p_3}\sin p_1 \sinh p_3\right] + \left[q_1^2+q_3^2+\left(\frac{Q_2}{\lambda_c^2}\right)^2\right]\cos p_1 \cosh p_3$$

$$= 0 \quad ; \quad \lambda = \lambda_c \tag{4.15}$$

where q_1, q_3 and Q_2 can be obtained from equations (4.9) and (4.14) by replacing λ by λ_c. Because the cubic equation (4.1) becomes, in effect, a quadratic equation when $\lambda = \lambda_c$, q_1 and q_3 can be evaluated directly

$$q_1 = \frac{\Pi_1}{2} - \sqrt{\frac{\Pi_1^2}{4}+\frac{\Pi_1\Pi_2}{\Pi_3}(1+\Pi_1\Pi_3)}$$

$$q_3 = \frac{\Pi_1}{2} + \sqrt{\frac{\Pi_1^2}{4}+\frac{\Pi_1\Pi_2}{\Pi_3}(1+\Pi_1\Pi_3)} \tag{4.16}$$

The mode shapes associated with the eigenvalues are given by equation (3.53). Employing equations (4.12) and (3.51) the u- and v-displacements are obtained as follows.

$$U(\xi) = C\Big[\gamma_4(Q_1 D_1 \cos p_1\xi + Q_2 D_2 \cos(h) p_2\xi + Q_3 D_3 \cosh p_3\xi)$$

$$+\frac{D_1}{p_1}(\gamma_2-\gamma_3)\sin p_1\xi + \frac{D_2}{p_2}(\gamma_3-\gamma_1)\sin(h)p_2\xi + \frac{D_3}{p_3}(\gamma_1-\gamma_2)\sinh p_3\xi\Big] \tag{4.17}$$

$$V(\xi) = -\Pi_1 C\left[\gamma_4\left(\frac{Q_1 q_1}{p_1}\sin p_1\xi + \frac{Q_2 q_2}{p_2}\sin(h)p_2\xi + \frac{Q_3 q_3}{p_3}\sinh p_3\xi\right)\right.$$

$$\left. + (\gamma_2 - \gamma_3)\cos p_1\xi + (\gamma_3 - \gamma_1)\cos(h)p_2\xi + (\gamma_1 - \gamma_2)\cosh p_3\xi\right] \tag{4.18}$$

where

$$\gamma_1 = Q_2 Q_3\left[\frac{q_2}{p_2}\sin(h)p_2 - \frac{q_3}{p_3}\sinh p_3\right]\cos p_1$$

$$\gamma_2 = Q_3 Q_1\left[\frac{q_3}{p_3}\sinh p_3 - \frac{q_1}{p_1}\sin p_1\right]\cos(h)p_2 \tag{4.19}$$

$$\gamma_3 = Q_1 Q_2\left[\frac{q_1}{p_1}\sin p_1 - \frac{q_2}{p_2}\sin(h)p_2\right]\cosh p_3$$

$$\gamma_4 = Q_1\cos(h)p_2\cosh p_3 + Q_2\cosh p_3\cos p_1$$

$$+ Q_3\cos p_1\cos(h)p_2$$

and the values for D_i are given by equation (3.35). Equations (4.17) and (4.18)are valid only if $\lambda \neq \lambda_c$.

4.2. Asymptotic Behavior

The motive to study the asymptotic behavior for this extended case is again to obtain more understanding of the general eigenvalue problem, and to indicate regions where the asymptotic expansions are close approximations to the exact values. Three asymptotic behaviors will be analyzed: (a) when $\lambda_n \to \infty$, (b) when $\Pi_1 \to 0$ and (c) when $\Pi_1 \to \infty$. The case when $\Pi_2 \to 0$ does not have a physical

meaning unless $\Pi_3 \to 0$ and will consequently not be analyzed in this chapter.

The general discussion in section 3.3 applies to this chapter also, and the methods for obtaining the asymptotic expansions will be the same.

(a) Asymptotic Behavior when $\lambda_n \to \infty$

By the same procedure as given in section 3.3(a) the asymptotic values for q_i are obtained as

$$q_1 = -\Pi_3\lambda^2 + \Pi_1\Pi_2 - \frac{\Pi_1^2\Pi_2}{\Pi_3^2}\lambda^{-2} + O(\lambda^{-3})$$

$$q_2 = -\lambda + \frac{\Pi_1}{2} - \frac{\Pi_1^2}{8}\lambda^{-1} + \frac{\Pi_1^2\Pi_2}{2\Pi_3^2}\lambda^{-2} + O(\lambda^{-3}) \qquad (4.20)$$

$$q_3 = \lambda + \frac{\Pi_1}{2} + \frac{\Pi_1^2}{8}\lambda^{-1} + \frac{\Pi_1^2\Pi_2}{2\Pi_3^2}\lambda^{-2} + O(\lambda^{-3})$$

The eigenvalue equation will again be derived by assuming that $\lambda > 81$ so that

$$\sinh p_3 = \cosh p_3 + O(\lambda^{-2}) = \frac{1}{2}e^{p_3} + O(\lambda^{-2}) \qquad (4.21)$$

by equation (3.104). Substituting equations (4.20) and (4.21) into equation (4.13), the result can be written as

$$e^{p_3}\Omega_3^2\left[\cos p_1\left\{\cos p_2 + \Pi_1\lambda^{-1}(\cos p_2 + \frac{1}{2}\sin p_2) + O(\lambda^{-2})\right\} + O(\lambda^{-5.5})\right] = 0 \qquad (4.22)$$

The term $\Pi_1 \lambda^{-1} \cos p_2$ can again be neglected as explained in section 3.3, and equation (4.22) will thus imply that

$$\cos p_1 + O(\lambda^{-5.5}) = 0 \tag{4.23}$$

or that

$$\cos p_2 + \frac{1}{2} \Pi_1 \lambda^{-1} \sin p_2 + O(\lambda^{-2}) = 0 \tag{4.24}$$

From these two equations it is clear that there will exist two sets of eigenvalues, one set corresponding to the zeroes of equation (4.23) and the other set corresponding to the zeroes of equation (4.24). Later, when the mode shapes are determined, it will be seen that equation (4.23) determines the eigenvalues corresponding to principally u-motion while equation (4.24) determines the eigenvalues corresponding to principally v-motion.

By equations (4.20), (4.11) and (4.23) the eigenvalues can be obtained as follows.

$$\lambda_{un}^2 = \frac{(2n-1)^2}{4\Pi_3} \pi^2 + \frac{\Pi_1 \Pi_2}{\Pi_3} + O(\lambda^{-2}) \; ; \quad n \text{ large} \tag{4.25}$$

where the subscript u identifies the eigenvalues as those corresponding to principally u-motion.

The eigenvalues corresponding to the symmetrical longitudinal vibration, $\bar{u}$-motion, are obtained from equations (2.40) and (2.41). For fixed-free boundary conditions, the solution is given by[31]

$$\Pi_3 \lambda_{\bar{u}n}^2 = \left[\frac{2n - 1}{2} \pi\right]^2 \tag{4.26}$$

using equation (3.2) for the definition of Π_3.

By equations (4.8) and (4.26), λ_{un}^2, equation (4.25) can then be written as

$$\lambda_{un}^2 = \lambda_{\underline{un}}^2 + \lambda_c^2 + O(\lambda^{-2}) \tag{4.27}$$

This equation more clearly indicates that these eigenvalues correspond to u-motion. For example, as the spandrels get stiffer, i.e., Π_1 increases, the eigenvalues become larger without bounds. This is in agreement with physical consideration of the vertical antisymmetric vibration, but cannot be justified for the eigenvalues associated with lateral vibration.

The other set of eigenvalues is obtained from equations (4.24), (4.11) and (4.20).

$$\lambda_{vn} = \left(\frac{2n-1}{2}\pi\right)^2 + \frac{\Pi_1}{2} + O(\lambda_{vn}^{-1/2}) \tag{4.28}$$

This has the same form as was obtained in chapter III for lateral vibration (equation (3.116)), and it is concluded that the eigenvalues given in equation (4.28) are those corresponding to the v-motion. Thus, the eigenvalues are seen to separate for large λ. But, as was pointed out in chapter III, the convergence for the asymptotic expansions in q_i and λ_{vn} is slow for large values of Π_1, and the uncoupling effect is best observed for small values of Π_1.

The mode shapes associated with these eigenvalues is evaluated in a manner similar to the analysis in chapter III. The u-motion corresponding to the eigenvalues in equation (4.25) is derived using equations (4.23) and (4.17)

$$U_n(\xi) = \text{const}\left[\sin \frac{2n-1}{2} \pi\xi + O(\lambda_{un}^{-5.5}) \right] \qquad (4.29)$$

wherein it is seen that the convergence to the regular sine curve is very fast. Since the $O(\lambda_{un}^{-5.5})$ term also includes powers of Π_1, the fast convergence is again restricted to small values of Π_1.

The v-motion corresponding to the eigenvalues λ_{vn} is derived from equations (4.18), (4.24) and (3.83)

$$V(\xi) = \text{const}\left[\sin p_2\xi - \cos p_2\xi + e^{-p_3\xi} + (-1)^{n+1} e^{-p_3(1-\xi)} + \frac{\Pi_1}{2} \lambda_{vn}^{-1} \sin p_1\xi + O(\lambda_{vn}^{-2}) \right] \qquad (4.30)$$

This equation is exactly like equation (3.119), and when the values for p_2 and p_3 are substituted into this equation, equation (3.125) is obtained.

Thus the v-motion approaches the mode shapes of a cantilevered Euler-Bernoulli-beam as λ increases. It is seen that assuming $\Pi_3 = 0$ does not result in a loss of information about the asymptotic behavior of the eigenvalues and mode shapes of lateral vibration for large values of λ.

The analysis has shown, however, the existence of a set of eigenvalues and mode shapes associated with the u-motion, with the mode shapes asymptotically approaching those for the longitudinal vibrations of a bar. The eigenvalues approach those of the corresponding bar added by a constant proportional to the stiffness of the spandrels.

(b) Asymptotic Behavior when $\Pi_1 \to 0$

A regular perturbation method, as presented in chapter III for $\Pi_2 \to 0$ is applied here to the case $\Pi_1 \to 0$. Equation (3.23) can now be written as

$$V'''' - \Pi_1 V'' + \Pi_1 U' - \lambda^2 V = 0$$
$$U'' + \Pi_1 \Pi_2 V' - \Pi_1 \Pi_2 U + \mu^2 U = 0 \tag{4.31}$$

where

$$\mu^2 = \Pi_3 \lambda^2 \tag{4.32}$$

The boundary conditions corresponding to equation (4.31) are given by equation (3.24).

Assuming that the eigenvalues can be separated into two sets, μ_n and λ_n, corresponding to principally antisymmetrical longitudinal and symmetrical lateral motion, respectively, the perturbation method must be applied twice in order to obtain the eigenvalues and eigenvectors associated with both displacements. First, assume that the following perturbation scheme can be used for the case of predominantly vertical vibration

$$V^* = V_0^* + \Pi_1 V_1^* + O(\Pi_1^2)$$
$$U = U_0 + \Pi_1 U_1 + O(\Pi_1^2) \tag{4.33}$$
$$\mu^2 = \mu_0^2 + \Pi_1 \mu_1^2 + O(\Pi_1^2)$$

Substituting these expressions in equations (4.31) and (3.24) the terms

of the zeroeth and first order can be separated by repeatedly applying the limit $(\Pi_1 \to 0)$.

$O(\Pi_1^0)$:

$$V_0^{*''''} - \frac{\mu_0^2}{\Pi_3} V_0^* = 0 \tag{4.34a}$$

$$U_0'' + \mu_0^2 U_0 = 0 \tag{4.34b}$$

with the boundary conditions

$$V_0^*(0) = V_0^{*'}(0) = V_0^{*''}(1) = V_0^{*'''}(1) = 0$$

$$U_0(0) = U_0'(1) = 0 \tag{4.35}$$

$O(\Pi_1^1)$:

$$V_1^{*''''} - \frac{\mu_0^2}{\Pi_3} V_1^* = V_0^{*''} - U_0' + \frac{\mu_1^2}{\Pi_3} V_0^* \tag{4.36a}$$

$$U_1'' + \mu_0^2 U_1 = -\Pi_2 (V_0^{*'} - U_0) - \mu_1^2 U_0$$

with

$$V_1^*(0) = V_1^{*'}(0) = V_1^{*'}(1) = V_1^{*'''}(1) - V_0^{*'}(1) + U_0(1) = 0$$

$$U_1(0) = U_1'(1) = 0 \tag{4.37}$$

Solving equation (4.34b) subject to the appropriate boundary conditions gives

$$U_{0n}(\xi) = C_u \sin \mu_{0n} \xi \quad ; \quad n = 1, 2 \ldots \tag{4.38}$$

where C_u is a constant and

$$\mu_{0n} = \frac{2n - 1}{2}\pi \; ; \quad n = 1,2,... \tag{4.39}$$

Applying these results to equations (4.34a) and (4.35) the only possible solution for V_0^* is

$$V_0^*(\xi) = 0 \tag{4.40}$$

except when μ_{0n}^2 is such that

$$\Pi_3\mu_{0n}^2 = \lambda_m^{*2} \tag{4.41}$$

where λ_m^* is the eigenvalue for a cantilever beam (appendix B). This equation defines the condition for a degenerate case; i.e., two different mode shapes having the same natural frequencies.

Equations (4.38) and (4.40) can now be applied to (4.36), resulting in

$$V_1^{*\text{IV}} - \frac{\mu_{0n}^2}{\Pi_3} V_1^* = - C_u\mu_{0n}\cos \mu_{0n}\xi \tag{4.42a}$$

$$U_1'' + \mu_{0n}^2 U_1 = (\Pi_2 - \mu_1^2)C_u \sin \mu_{0n}\xi \tag{4.42b}$$

The solution to the second of these equations is

$$U_{1n}(\xi) = C_1 \sin \mu_{0n}\xi + C_2 \cos \mu_{0n}\xi - C_u \frac{\Pi_2 - \mu_{1n}^2}{2\mu_{0n}} \xi \cos \mu_{0n}\xi \; ;$$

$$n = 1,2... \tag{4.43}$$

where C_1 and C_2 are any arbitrary constants.

Applying the boundary conditions on U_1, equation (4.37), two equations for the two unknown quantities C_1 and C_2 are obtained.

$$C_2 = 0$$

$$\mu_{0n}\left[\cos \mu_{0n} C_1 - \sin \mu_{0n} C_2\right] + C_u \frac{\mu_{1n}^2 - \Pi_2}{2\mu_{0n}}\left[\cos \mu_{0n} - \mu_{0n} \sin \mu_{0n}\right] = 0 \tag{4.44}$$

Since $\cos \mu_{0n}$ equals zero by equation (4.39), equation (4.44) implies that

$$\mu_{1n}^2 = \Pi_2 \quad ; \quad n = 1,2,\ldots \tag{4.45}$$

and equation (4.43) can be written as

$$U_{1n}(\xi) = C_1 \sin \mu_{0n} \quad ; \quad n = 1,2,\ldots \tag{4.46}$$

The eigenvalues and mode shapes for the u-motion are thus given by substituting equations (4.38), (4.39), (4.45) and (4.46) into equation (4.33)

$$U_n(\xi) = C_u^* \sin \frac{2n-1}{2} \pi \xi + O(\Pi_1^2) \quad ; \quad n = 1,2,\ldots \tag{4.47}$$

$$\mu^2 = \left(\frac{2n-1}{2} \pi\right)^2 + \Pi_2 \Pi_1 + O(\Pi_1^2) \quad ; \quad n = 1,2,\ldots \tag{4.48}$$

It is observed that these values are equal to those obtained for the case when $\lambda_n \to \infty$, equations (4.25) and (4.29).

The case of lateral vibrations can be solved by assuming the following perturbation scheme.

$$V = V_0 + \Pi_1 V_1 + O(\Pi_1^2)$$

$$U^* = U_0^* + \Pi_1 U_1^* + O(\Pi_1^2) \tag{4.49}$$

$$\lambda^2 = \lambda_0^2 + \Pi_1 \lambda_1^2 + O(\Pi_1^2)$$

By substitution into equation (4.31), the zeroeth and first order terms can again be separated:

$O(\Pi_1^0)$:
$$V_0'''' - \lambda_0^2 V_0 = 0 \tag{4.50a}$$

$$U_0^{*''} + \Pi_3 \lambda_0^2 U_0^* = 0 \tag{4.50b}$$

$O(\Pi_1^1)$:
$$V_1'''' - \lambda_0^2 V_1 = V_0'' - U_0^{*'} + \lambda_1^2 V_0 \tag{4.51a}$$

$$U_1^{*''} + \Pi_3 \lambda_0^2 U_1^* = -\Pi_2 V_0' + \Pi_2 U_0^* - \Pi_3 \lambda_1^2 U_0^* \tag{4.51a}$$

Equation (4.50a) together with the appropriate boundary conditions obtained from equations (3.24) and (4.49) defines the regular vibration of a cantilever beam whose solution are given in appendix B, equation (B.8)

$$V_{0n}(\xi) = C_v \Big[(\cos\sqrt{\lambda_{0n}} + \cosh\sqrt{\lambda_{0n}})(\sin\sqrt{\lambda_{0n}}\xi - \sinh\sqrt{\lambda_{0n}}\xi) - (\sin\sqrt{\lambda_{0n}} + \sinh\sqrt{\lambda_{0n}})(\cos\sqrt{\lambda_{0n}}\xi - \cosh\sqrt{\lambda_{0n}}\xi)\Big] \quad ; \quad n = 1,2,\ldots \tag{4.52}$$

and where λ_{0n} is the solution to the equation

$$\cos\sqrt{\lambda_{0n}} \cosh\sqrt{\lambda_{0n}} + 1 = 0 \tag{4.53}$$

Under these conditions for λ_{0n}, equation (4.50b), together with the boundary conditions, gives only the trivial solution

$$U_0^*(\xi) = 0 \tag{4.54}$$

except for the degenerate case when equation (4.41) holds. Substituting equations (4.52) and (4.54) into (4.51a), the solution for $V_1(\xi)$ is given by

$$V_{1n}(\xi) = C_1 \sin\sqrt{\lambda_{0n}}\xi + C_2 \cos\sqrt{\lambda_{0n}}\xi + C_3 \sinh\sqrt{\lambda_{0n}}\xi$$
$$+ C_4 \cosh\sqrt{\lambda_{0n}}\xi + \frac{\xi}{4\lambda_{0n}^2}\left[\lambda_{1n}^2 V_{0n}'(\xi) + V_{0n}'''(\xi)\right] ;$$
$$n = 1, 2, \ldots \tag{4.55}$$

The boundary conditions for equation (4.55) are obtained from the first order terms when equation (4.49) is substituted into equation (3.24)

$$V_1(0) = V_1'(0) = V_1''(1) = V_1'''(1) - V_0'(1) = 0 \tag{4.56}$$

When these four conditions are applied to equation (4.55), a singular matrix equation, similar to equation (3.184) is obtained

$$\underline{Ac} = \underline{b} \tag{4.57}$$

where A is the singular matrix (by equation (4.53))

$$A = \begin{bmatrix} 0 & 1 & 0 & 1 \\ 1 & 0 & 1 & 0 \\ -\sin\sqrt{\lambda_{0n}} & -\cos\sqrt{\lambda_{0n}} & \sinh\sqrt{\lambda_{0n}} & \cosh\sqrt{\lambda_{0n}} \\ -\cos\sqrt{\lambda_{0n}} & \sin\sqrt{\lambda_{0n}} & \cosh\sqrt{\lambda_{0n}} & \sinh\sqrt{\lambda_{0n}} \end{bmatrix} \tag{4.58}$$

and $\underline{c}$ is the vector containing the four unknown C_i and

$$\underline{b} = -\frac{1}{4\lambda_{0n}^2\sqrt{\lambda_{0n}}} \begin{bmatrix} 0 \\ V_{0n}'''(0) \\ \lambda_{0n}\sqrt{\lambda_{0n}}(2V_{0n}(1)+V_{0n}'(1)) \\ \lambda_{0n}(\lambda_1^2 V_{0n}(1)-V_{0n}'(1)) \end{bmatrix} \tag{4.59}$$

Since A is singular, $\underline{b}$ must satisfy the condition (see section 3.3(d))

$$\sum_{i=1}^{4} b_i y_i = 0 \tag{4.60}$$

where y_i is the solution to

$$A^T \underline{y} = \underline{0} \tag{4.61}$$

Solving equation (4.61) for y_i and applying equation (4.60), λ_{1n}^2 is evaluated as

$$\lambda_{1n}^2 = \frac{\sqrt{\lambda_{0n}}\sin\sqrt{\lambda_{on}}\sinh\sqrt{\lambda_{0n}}\left[2(\sin\sqrt{\lambda_{0n}}+\sinh\sqrt{\lambda_{0n}})+\sqrt{\lambda_{0n}}(\cos\sqrt{\lambda_{0n}}+\cosh\sqrt{\lambda_{0n}})\right]}{(\sin\sqrt{\lambda_{0n}}+\sinh\sqrt{\lambda_{0n}})(\cosh\sqrt{\lambda_{0n}}\sin\sqrt{\lambda_{0n}}-\cos\sqrt{\lambda_{0n}}\sinh\sqrt{\lambda_{0n}})}$$

$$n = 1,2,\ldots \tag{4.62}$$

Finally, by equations (4.49), (4.53) and (4.62)

$$\lambda_n = \lambda_{0n} + \frac{(-1)^n - \cos\sqrt{\lambda_{0n}} - (2/\sqrt{\lambda_{0n}})\sin\sqrt{\lambda_{0n}}}{2(-1)^n + 2\cos\sqrt{\lambda_{0n}}}\,\Pi_1 + O(\Pi_1^2)\ ;$$

$$n = 1,2,\ldots \tag{4.63}$$

It can be observed, by comparing this equation with equation

(3.140), that the first two terms of λ_n are identical, implying that no new information is obtained by including Π_3 for the lateral vibration as $\Pi_1 \to 0$. By a procedure similar to that in section 3.3(d), the mode shapes can be obtained (to $O(\Pi_1^1)$) from equations (4.49), (4.52) and (4.55).

(c) Asymptotic Behavior when $\Pi_1 \to \infty$

This case is again solved by obtaining an expansion for the eigenvalues, equation (4.13). By equations (4.9) and (4.3), q_i is given by

$$\begin{aligned} q_1 &= -\alpha_1 - \alpha_2 + (\alpha_3 - \alpha_4)\Pi_1^{-1} + O(\Pi_1^{-2}) \\ q_2 &= \alpha_1 - \alpha_2 - (\alpha_3 + \alpha_4)\Pi_1^{-1} + O(\Pi_1^{-2}) \\ q_3 &= (1 + \Pi_2)\Pi_1 - 2\Pi_2\alpha_2 + 2\alpha_4\Pi_1^{-1} + O(\Pi_1^{-2}) \end{aligned} \tag{4.64}$$

in which

$$\begin{aligned} \alpha_1 &= \frac{\lambda}{2(1+\Pi_2)}\sqrt{4\Pi_2(1+\Pi_2)+\Pi_3^2\lambda^2} \\ \alpha_2 &= \frac{\Pi_3\lambda^2}{2(1+\Pi_2)} \\ \alpha_3 &= \frac{\Pi_3\lambda^3(1 + 5\Pi_2 + 4\Pi_2^2 - \Pi_2\Pi_3^2\lambda^2)}{2\sqrt{4\Pi_2(1+\Pi_2)+\Pi_3^2\lambda^2}\,(1 + \Pi_2^2)} \\ \alpha_4 &= \frac{\lambda^2}{2(1 + \Pi_2)^3}(1 + \Pi_2 + \Pi_2\Pi_3^2\lambda^2) \end{aligned} \tag{4.65}$$

It is observed that q_1 is negative while q_2 and q_3 are positive. Thus, in this case only one set of eigenvalues will be obtained,

which by equation (4.6) implies that this expansion is valid only as long as

$$\Pi_1 > \frac{\Pi_3}{\Pi_2}\lambda^2 \tag{4.66}$$

By substituting equation (4.64) into equations (4.14) and (4.13), the eigenvalue equation can be written in an asymptotic expansion. Setting the zeroeth-order term of this expansion equal to zero results in an equation for the asymptotic eigenvalues.

$$2 + (2+\gamma_1^2)\cos p_1 \cosh p_2 - \gamma_1 \sin p_1 \sinh p_2 = 0 \tag{4.67}$$

where

$$\gamma_1 = \frac{\Pi_3 \lambda_n}{\sqrt{\Pi_2(1+\Pi_2)}} \tag{4.68}$$

and p_1 and p_2 are given by equations (4.64), (4.65) and (4.11)

$$\begin{aligned} p_1^2 &= \gamma_1^2 \frac{\Pi_2}{2\Pi_3}\left[\sqrt{1+4\gamma_1^{-2}}+1\right] \\ p_2^2 &= \gamma_1^2 \frac{\Pi_2}{2\Pi_3}\left[\sqrt{1+4\gamma_1^{-2}}-1\right] \end{aligned} \tag{4.69}$$

No closed form solution of equation (4.67) is obtained, but for given values of Π_2 and Π_3, numerical methods will give the asymptotic eigenvalues. When λ_n becomes very large, such that $\Pi_3\lambda_n >> 1$, an asymptotic expression of equation (4.67) yields the following result.

$$\lim_{\substack{\Pi_1 \to \infty \\ n \to \infty}} \lambda_n = \sqrt{\frac{1+\Pi_2}{\Pi_3}}\ \frac{2n-1}{2}\pi \tag{4.70}$$

For comparison, the similar case when $\Pi_3 = 0$ can be evaluated from equations (3.154) and (B.13) in appendix B

$$\lim_{\substack{\Pi_1 \to \infty \\ n \to \infty \\ \Pi_3 = 0}} \lambda_n = \sqrt{\frac{1+\Pi_2}{\Pi_2}}\left(\frac{2n-1}{2}\pi\right)^2 \tag{4.71}$$

From these two expressions it is seen that the asymptotic values of λ_n when n is large are substantially different when Π_3 is included in the analysis.

For small values of λ, $\lambda\Pi_3 \ll 1$, a similar asymptotic expansion of equation (4.67) yields

$$\lim_{\substack{\Pi_1 \to \infty \\ \lambda_n \to 0}} \lambda_n = \sqrt{\frac{1+\Pi_2}{\Pi_2}}\ \lambda_n^* \tag{4.72}$$

which is the asymptotic value for the lower frequencies obtained in chapter III, equation (3.154).

In chapter III, the asymptotes of the eigenvalues when $\Pi_1 \to \infty$ were also found from a physical consideration by letting the spandrels become rigid. Since inertia of longitudinal motion has been included in the analysis in this chapter, it is natural to seek the eigenvalues to

a beam with rigid spandrels within the Timoshenko theory of beam vibration[31], excluding the effect of shear. Using equations (3.155) and (3.156) for the properties of such a beam, the eigenvalue equation in the Timoshenko theory neglecting shear reduces to[31]

$$2 + (2+\gamma_2^2) \cos \bar{p}_1 \cosh \bar{p}_2 - \gamma_2 \sin \bar{p}_1 \sinh \bar{p}_2 = 0 \qquad (4.73)$$

in which

$$\gamma_2 = \omega \sqrt{\frac{\rho I_T}{E_1 A_T}} = \gamma_1 \cdot k_0$$

$$\bar{p}_1^{\,2} = \gamma_2^2 \frac{\Pi_2}{2\Pi_3} \frac{k_0}{1+\Pi_2} \left[\sqrt{1 + 4\gamma_2^{-2}} + 1 \right] \qquad (4.74)$$

$$\bar{p}_2^{\,2} = \gamma_2^2 \frac{\Pi_2}{2\Pi_3} \frac{k_0}{1+\Pi_2} \left[\sqrt{1 + 4\gamma_2^{-2}} - 1 \right]$$

$$k_0 = \frac{\rho_1 A_1 a_2 + \rho_3 A_3 \ell_3}{\rho_1 A_1 a_2 + k_u \rho_3 A_3 \ell_3}$$

The small differences in equations (4.73) and (4.67) are due to the fact that the kinetic energy due to rotary motion in the two walls and the spandrels is neglected in equation (4.67), an error which becomes smaller when Π_2 and the spandrel mass decreases. Overall, the two equations are similar, and it can be concluded within the errors specified that as Π_1 becomes large, the eigenvalues for the coupled shear wall asymptotically approaches those of a Timoshenko beam, with shearing deformations excluded.

4.3 Discussion of the General Solution

When the inertia associated with u-motion was included in the analysis, the eigenvalue equation (4.13) changed in general character as λ increased. That is, when $\lambda < \lambda_c$ there were four hyperbolic (sinh and cosh) and two circular (sin and cos) functions in the eigenvalue equation, while when $\lambda > \lambda_c$ two of the hyperbolic terms became circular functions (equation (4.12)), resulting in a total of four circular and two hyperbolic functions for this case. Since the hyperbolic functions are sign definite while the circular functions change sign for increasing values, the change of the character of the solution at $\lambda = \lambda_c$ indicates that a new set of zeros to the eigenvalue equation develops for eigenvalues larger than λ_c. This set of eigenvalues was observed in section 4.2 to be associated with vertical, antisymmetric vibrations. In the asymptotic cases when $n \to \infty$ and when $\Pi_1 \to 0$, the motion connected with u- and v-displacement became uncoupled, resulting in two distinct sets of eigenvalues. This behavior is clearly indicated in figure 4.1 which gives the eigenvalues as a function of Π_1, with Π_2 and Π_3 constant. Π_3 is chosen close to the value given in equation (3.18), as the maximum it can have under the stated assumptions, so that both the extreme cases can be viewed. (The other extreme, $\Pi_3 = 0$, is seen in figure 3.2). Because shearing deformations were excluded from the analysis, the higher eigenvalues presented in figures 4.1 and 4.2 are not physically realistic, but are included so general trends in the results can be viewed. The curve $\lambda = \lambda_c$ separates the figure into two regions where either one or two sets of eigenvalues exists.

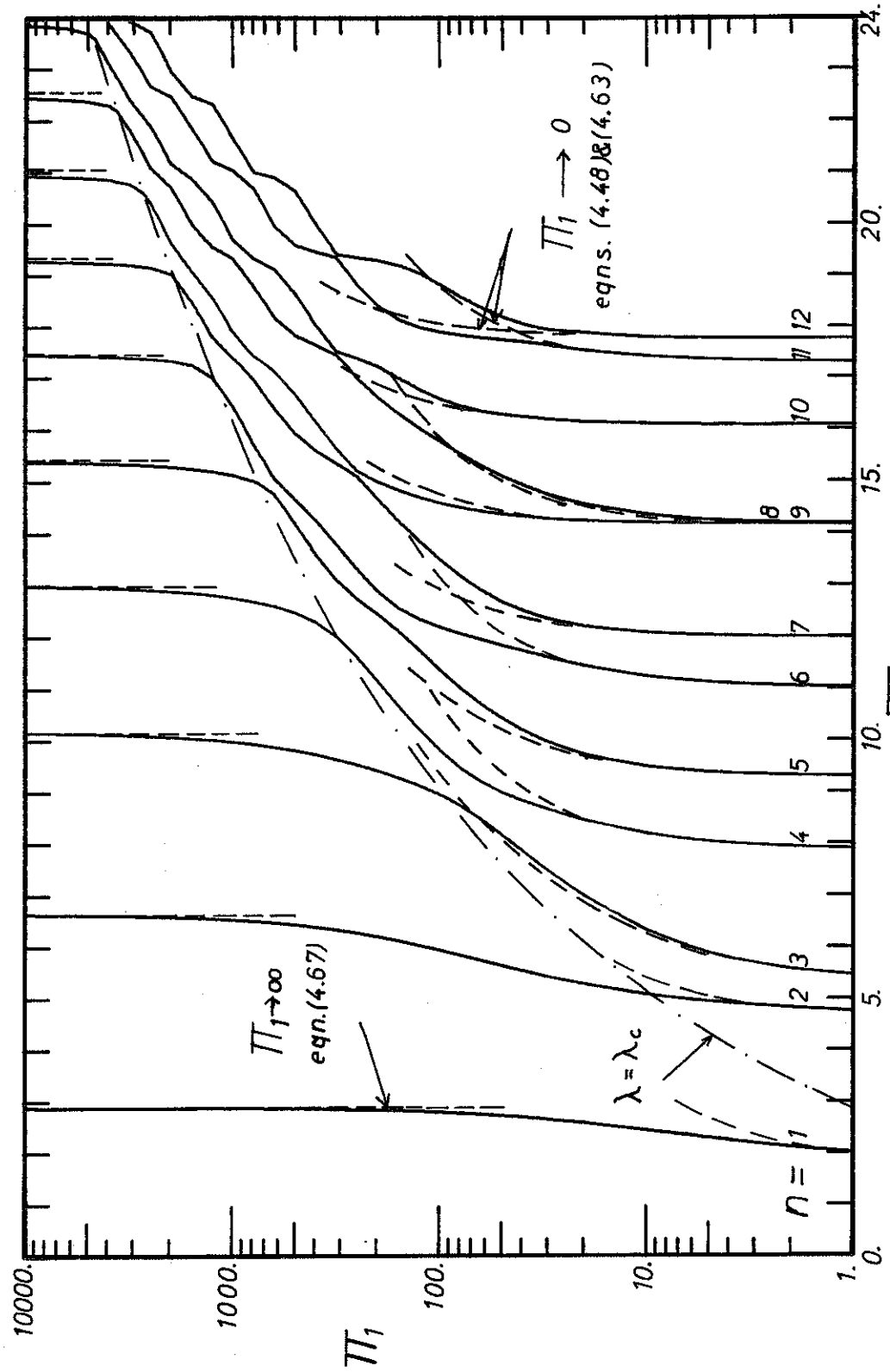

Fig. 4.1. First 12 Eigenvalues when $\Pi_2 = 0.2$, $\Pi_3 = 0.003$.

Also plotted on the figure are the asymptotic values for λ_n as $\Pi_1 \to \infty$, obtained from equation (4.67), and the values obtained as $\Pi_1 \to 0$, equations (4.48), (4.32) and (4.63). The convergence to the eigenvalues when $\Pi_1 \to \infty$ is seen to be much faster than was observed in chapter III when $\Pi_3 = 0$.

For small Π_1, when the two sets of eigenvalues become uncoupled, the figure shows that the eighth and ninth eigenvalues almost overlap. From equations (4.48), (4.32) and (4.53) the asymptotic values are given by

$$\lambda_8 = \lambda_{v5} = \lambda_5^* = 199.8595$$
$$\lambda_9 = \lambda_{u4} = \left(\frac{8-1}{2}\pi\right)\frac{1}{\sqrt{\Pi_3}} = 200.7508 \qquad (4.77)$$

where the notation indicates that the asymptotes are for the fifth and fourth eigenvalues, associated with v- and u-motion, respectively.

To complete the picture, the eigenvalues corresponding to $\bar{u}$- and $\bar{v}$-motion should also be included in figure 4.1. It was found in chapter II that the differential equation for these displacements uncoupled from the other equations, and the corresponding eigenvalues reflect this fact. The eigenvalues for $\bar{u}$-motion were given in equation (4.26), and since they are independent of Π_1, they will appear as straight vertical lines on figure 4.1, coinciding with the asymptotic values for λ_{un} as $\Pi_1 \to 0$.

The behavior of the mode shapes cannot be illustrated as easily, but the asymptotic expansions indicated that the lateral com-

ponents of the mode shapes were close to those obtained when $\Pi_3 = 0$, and the longitudinal mode shapes (u-displacement) were close to a regular sine wave. For the eigenvalues away from the asymptotic limits, coupling of horizontal and vertical motions in the mode shapes will be more apparent, and this will be indicated in the example given in section 4.5.

4.4. Discussion of the Effect of Vertical Inertia

It was observed in earlier sections that two major differences were introduced by including vertical inertia: (1) the additional eigenvalues and (2) the reduction of the numerical values for the higher eigenvalues as Π_1 increases. These effects can also be observed by comparing figures 4.1 ($\Pi_3 \neq 0$) and 3.2 ($\Pi_3 = 0$).

In figure 4.2 the eigenvalues for the case when $\Pi_2 = 0.1$ and $\Pi_3 = 0.001$ are shown together with the simplified case when $\Pi_3 = 0$ (dashed lines). Also shown in the figure (dotted lines) are the eigenvalues obtained when V is set equal to zero. These eigenvalues are easily evaluated from equation (3.23) together with the fixed-free boundary conditions on U; giving

$$\Pi_3 \lambda_{un}^2 = \left[\frac{2n-1}{2}\pi\right]^2 + \Pi_1 \Pi_2 \quad ; \quad n = 1, 2, \ldots \tag{4.78}$$

In the asymptotic cases, when $\Pi_1 \to 0$ and when $\lambda_n \to \infty$, the first approximations to the eigenvalues associated with longitudinal motion (equations (4.25), (4.32) and (4.48)), had the same form as equation (4.78). Equation (4.78) also proves to be good approximation

for the eigenvalues away from the asymptotic limits. This is observed in figure 4.2 as well as in the example treated in the next section.

Figures 4.1 and 4.2 were obtained for fixed values of Π_2 and Π_3, but because of the form of the equations, similar behavior is expected for other values of Π_2 and Π_3. It is therefore reasonable to conclude that as long Π_1 is small, the simplified cases ($\Pi_3 = 0$ and $V = 0$) give good approximations for the eigenvalues. For larger values of Π_1, figures 4.1 and 4.2 indicates that taking Π_3 equal to zero results in large errors in the eigenvalues, with increasing errors for higher eigenvalues. In fact, only the first eigenvalue is close to the general case while errors of about 10% are obtained in the second and third eigenvalue if vertical inertia is neglected.

It can therefore be concluded that if only the first eigenvalue is to be determined, or if the spandrels are weak (small Π_1), then the vertical inertia can be neglected. Otherwise, the assumption that $\Pi_3 = 0$ results in large errors.

Computationally, there are no major differences in calculating the eigenvalues for the two cases, and it is therefore recommendable to include the vertical inertia in all calculations where doubt might arise.

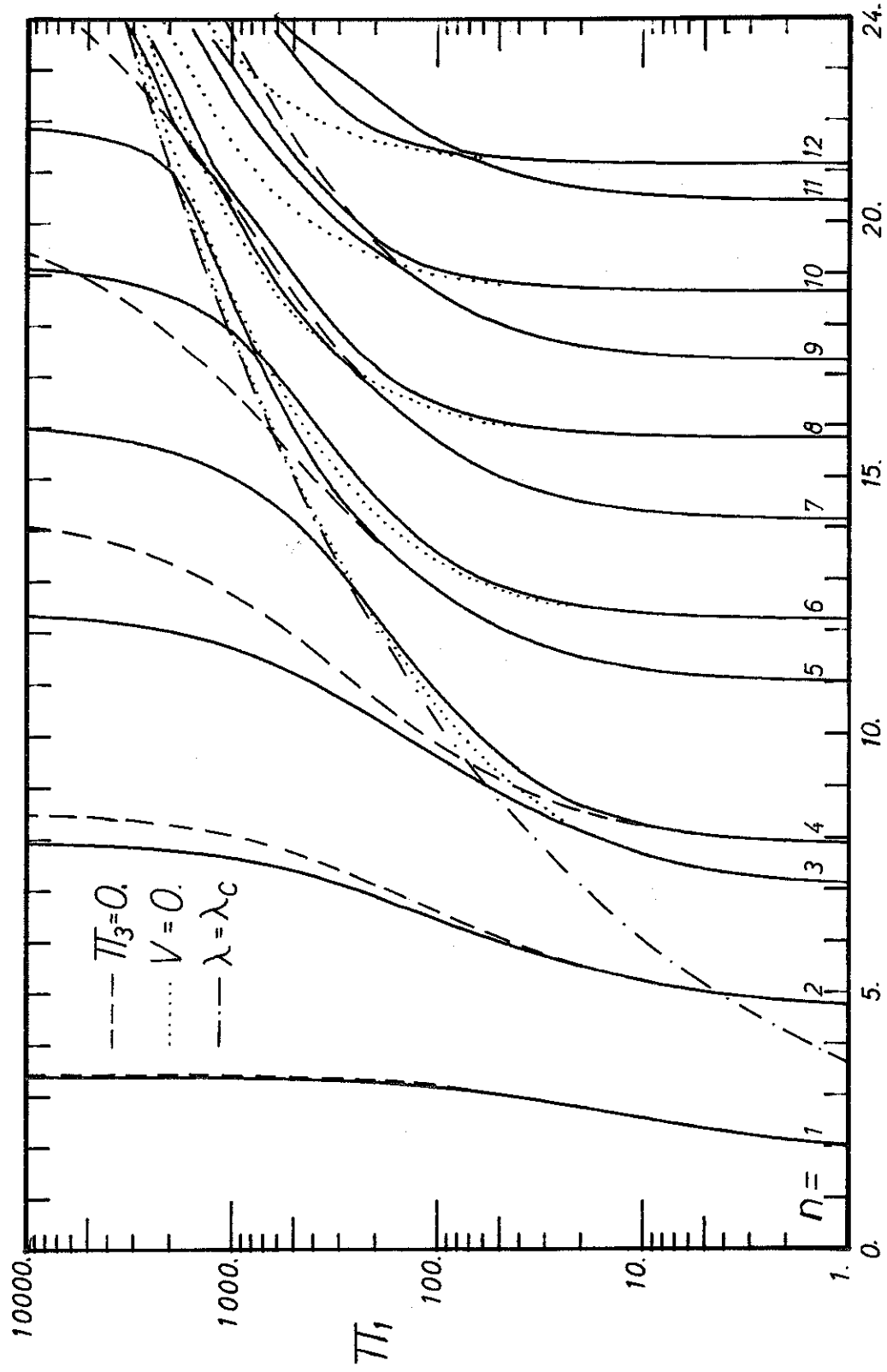

Fig. 4.2. First 12 Eigenvalues when $\Pi_2 = 0.1$, $\Pi_3 = 0.001$.

4.5. Numerical Example

In order to illustrate some of the analytical results and to give a specific presentation of the differences arising from excluding the vertical inertia, a numerical example is presented. The numerical values for this example are taken from the plans of the McKinley and 1200L apartment buildings in Anchorage, Alaska[17]. A picture of the McKinley building is shown in figure 1.1, and referring to equations (2.2) and (2.3) for the definition of the dimensions, the following set of values are used for this example

$$\begin{aligned} a_1 &= 18' & I_3 &= \tfrac{8}{3} t \ ft^3 \\ a_2 &= 8.5' & A_1 &= 12t \ ft \\ \ell_1 &= 14a_2 & A_3 &= 2t \ ft \\ \ell_3 &= 6' & k &= 1.2 \\ I_1 &= 144t \ ft^3 \end{aligned} \tag{4.79}$$

where t is the thickness of the reinforced concrete shear wall. The spandrels are of the same material as the walls, so the material properties will be taken as[18,32]

$$\begin{aligned} E_1 &= E_3 = 4.64 \cdot 10^8 \ \text{lbs ft}^{-2} \\ \rho_1 &= \rho_2 = 4.5 \ \text{lbs sec}^2 \ \text{ft}^{-4} \\ G_3 &= E_3/2 \end{aligned} \tag{4.80}$$

From equations (2.35) and (2.36) the values of k_u and β are given by

$$\beta^2 = 2.0667$$
$$k_u = 0.20115 \tag{4.81}$$

With these dimensions, the parameters defined in equation (3.2) become

$$\Pi_1 = 134.355$$
$$\Pi_2 = 0.148148 \tag{4.82}$$
$$\Pi_3 = 0.00081926$$

and similarly, equation (3.3) reduces to

$$\omega_n = 2.4140\ \lambda_n \tag{4.83}$$

The eigenvalues for this example are obtained for two cases: (a) when vertical inertia is neglected (table 4.1); (b) when it is included (table 4.2) in the analysis. For the first case, the eigenvalues are obtained from equation (3.66) and are presented in table 4.1. Also given in the table are the values obtained by the asymptotic expansions, $\Pi_1 \rightarrow \infty$ and $n \rightarrow \infty$, and the eigenvalues for the simplified cases when $\Pi_2 = 0$ and when $\Pi_1 = 0$. It is seen that the first eigenvalue given by the asymptotic behavior when $\Pi_1 \rightarrow \infty$ lies within 3% of the correct value, and starting at the fifth eigenvalue, the asymptotic values for higher eigenvalues lie within 4% of those for the more generalized case. The simplified cases are included to illustrate the fact that the values obtained by these assumptions are poor approximations for the actual eigenvalues, especially the more

TABLE 4.1

Eigenvalues When Vertical Inertia is Neglected

Eigenvalue number n	Eigenvalue eq.(3.66) λ_n	$\frac{\lambda_n}{\lambda_1}$	Asymptotic values $\Pi_1 \to \infty$ eq.(3.153)	Asymptotic values $n \to \infty$ eq.(3.116)	Simplified cases $\Pi_2 = 0$ (U=0) eq.(C.7)	Simplified cases $\Pi_1 = 0$ eq.(B.7)
1	9.028	1.00	8.79		20.07	3.516
2	43.50	4.82	17.83		63.53	22.03
3	100.82	11.17		128.86	116.19	61.70
4	170.57	18.89		188.08	182.38	120.90
5	256.29	28.39		265.73	264.95	199.86
6	358.91	39.76		365.73	365.53	298.56
7	479.92	53.16		484.17	484.97	416.99
8	619.67	68.64		622.34	623.69	555.17
9	778.69	86.26		780.25	781.89	713.08
10	957.06	106.01		957.91	959.70	890.73

TABLE 4.2

Eigenvalues When Vertical Inertia is Included

Eigenvalue number			Eigenvalues eq. (4.13)		$\frac{\lambda_i}{\lambda_1}$	Asymptotic values			Simplified cases	
i	m	n	u-motion λ_{um}	v-motion λ_{vn}		$\Pi_1 \to \infty$ eq. (4.67)	$\lambda_{vn} \to \infty$ eq. (4.28)	$\lambda_{um} \to \infty$ eq. (4.25)	v=0 eq. (4.78)	$\Pi_3=0$ eq. (3.66)
1		1		8.948	1.00	9.66				9.028
2		2		41.90	4.68	56.48				43.50
3		3		97.05	10.85	143.93	128.86			100.82
4	1*		154.06		17.23			164.77		
5		4*		185.07	20.69		188.08			170.57
6	2		225.55		25.23			226.06		
7		5		263.74	29.48		267.04			256.29
8	3		316.80		35.44			314.66		
9		6		362.99	40.57		365.73			358.91
10	4		416.93		46.64			413.37		
11		7		481.33	53.80		484.17			479.92
12	5		520.85		58.27			516.42		
13		8*		618.69	69.15		622.34			619.67
14	6*		627.15		70.16			621.66		

*indicates strong coupling of eigenmodes

important, lower values.

Table 4.2 gives the eigenvalues obtained by including vertical inertia, equation (4.13). The eigenvalues are divided into two sets corresponding to the dominant motion (u- or v-motion) of vibration, and a star indicates where the coupling between vertical and horizontal motion is strong. The appropriate asymptotic values and the two simplified cases ($\Pi_3 = 0$ and $v = 0$) are included for comparison. It is observed that, with the possible exception of λ_4 and λ_5, the simplified cases give very satisfactory results.

The mode shapes corresponding to some of the eigenvalues given in tables 4.1 and 4.2 are plotted in figures 4.3, 4.4 and 4.5. Figure 4.3 gives the first three lateral mode shapes for four cases: (1) An Euler-Bernoulli cantilever beam ($\Pi_1 = 0$) (dotted lines), (2) Coupled shear walls with vertical motion neglected ($\Pi_2 = 0$) (dashed-dotted line), (3) Coupled shear walls with vertical inertia neglected ($\Pi_3 = 0$) (dashed line) and (4) Coupled shear walls with vertical inertia included (solid line). The figure clearly indicates the necessity of including vertical motion in order to get a close representation of the actual mode shapes. The difference between the cases (3) and (4) is much smaller; this is to be expected since Π_3 is relatively small in this example.

Figure 4.4 shows the first five lateral mode shapes when $\Pi_3 = 0$. The physical displacements, $\hat{V}$ (solid lines) and $\hat{U}$ (dashed lines), equation (3.71), are plotted so that the actual difference between the lateral and longitudinal displacements can be viewed. The figure shows that the maximum $\hat{U}$-displacement is about 10%

of the maximum $\hat{V}$-displacement for the first mode, and about 30% for the other four modes shown, clearly indicating the importance of vertical motion in the analysis, and suggesting that the vertical inertia also should be included.

Figure 4.5 gives the first ten mode shapes when the vertical inertia is included in the analysis. Again, the physical displacements are plotted, and it is observed, that for most modes, the dominant motion is obvious, and by this figure, the separation of the eigenvalues into two sets as done in table 4.2, is justified.

By comparing figures 4.4 and 4.5, the obvious difference is the addition of the predominantly vertical modes appearing as the 4^{th}, 6^{th}, 8^{th} and 10^{th} natural modes in figure 4.5. The other mode shapes have a dominant lateral displacement, and the similarity with the mode shapes in figure 4.4 is quite clear. With a closer look though, the $\hat{U}$-displacement for even these cases are larger when vertical inertia is included, figure 4.5.

It can also be observed that the mode shapes obtained for this example are in good agreement with what was derived for the asymptotic behavior as $n \rightarrow \infty$, for example, the ninth mode shape in figure 4.5 has a form close to the sixth mode for an Euler-Bernoulli beam (figure B.1) while the tenth mode shape is almost a perfect sine wave as was predicted in equation (4.29).

Finally, this example gave a good indication on how important it was to include vertical motion in the analysis, while, by including the vertical inertia term, relatively small corrections were obtained

for the eigenvalues and mode shapes associated with principally lateral motion.

The above discussion has concentrated on the mechanics of coupled shear walls as such. For application to buildings, such as the structure from which the example was drawn, it should be recalled that the exclusion of shearing deformation and other limitations restricts the application of the results to about the first three modes of vibration.

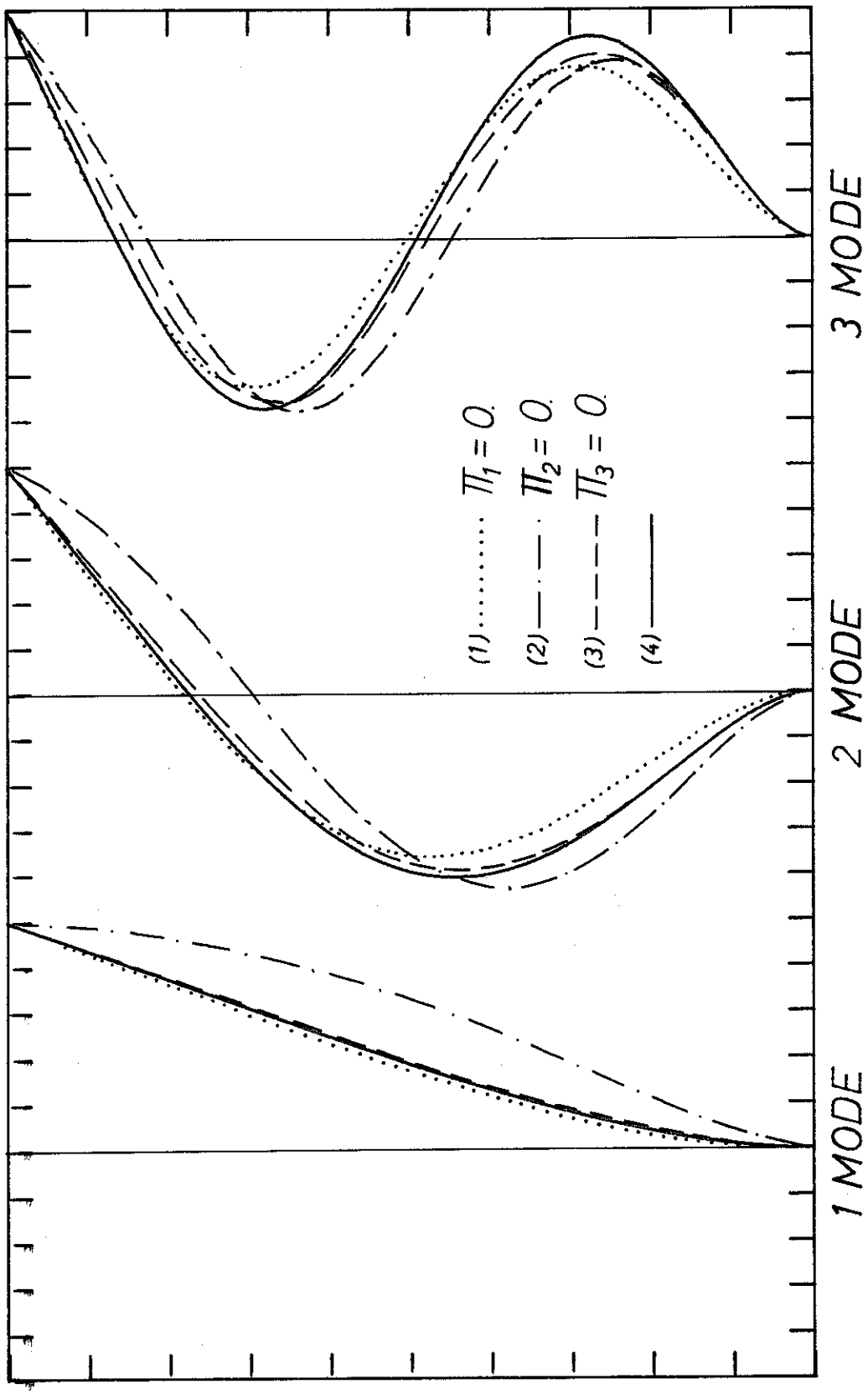

Fig. 4.3. First 3 Lateral Mode Shapes for the Example

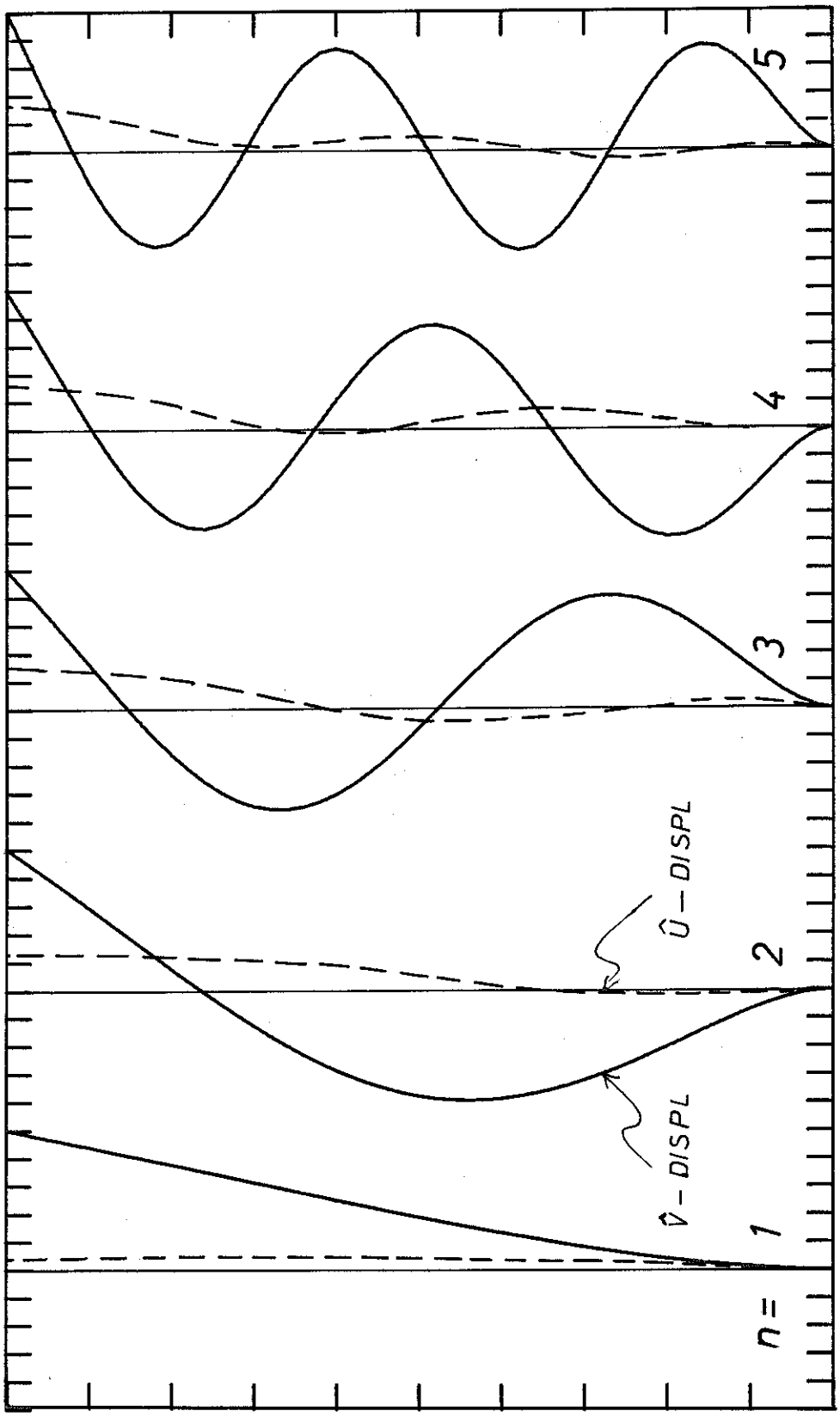

Fig. 4.4. First 5 Mode Shapes for the Example Neglecting Vertical Inertia

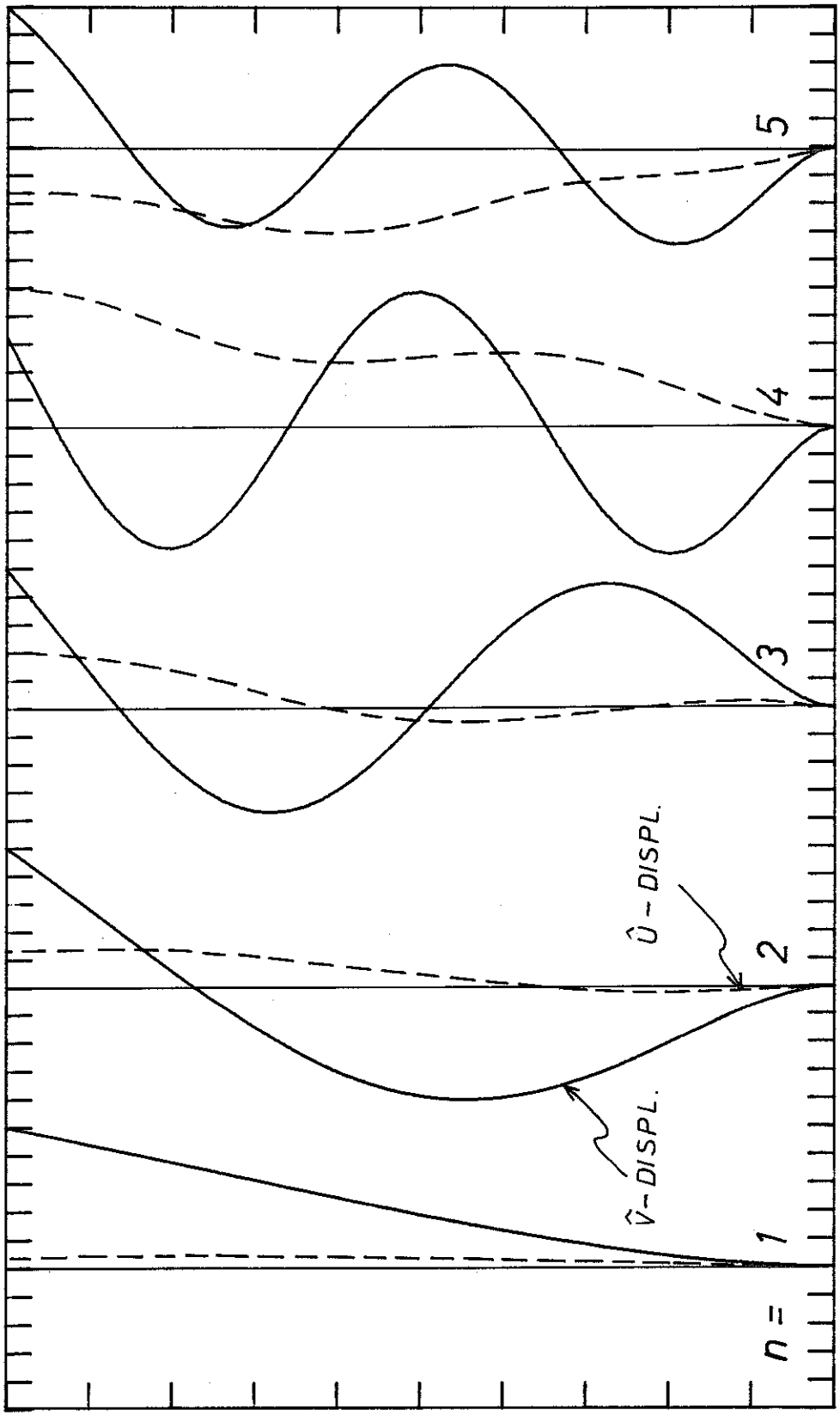

Fig. 4.5(a). First 10 Mode Shapes for the Example

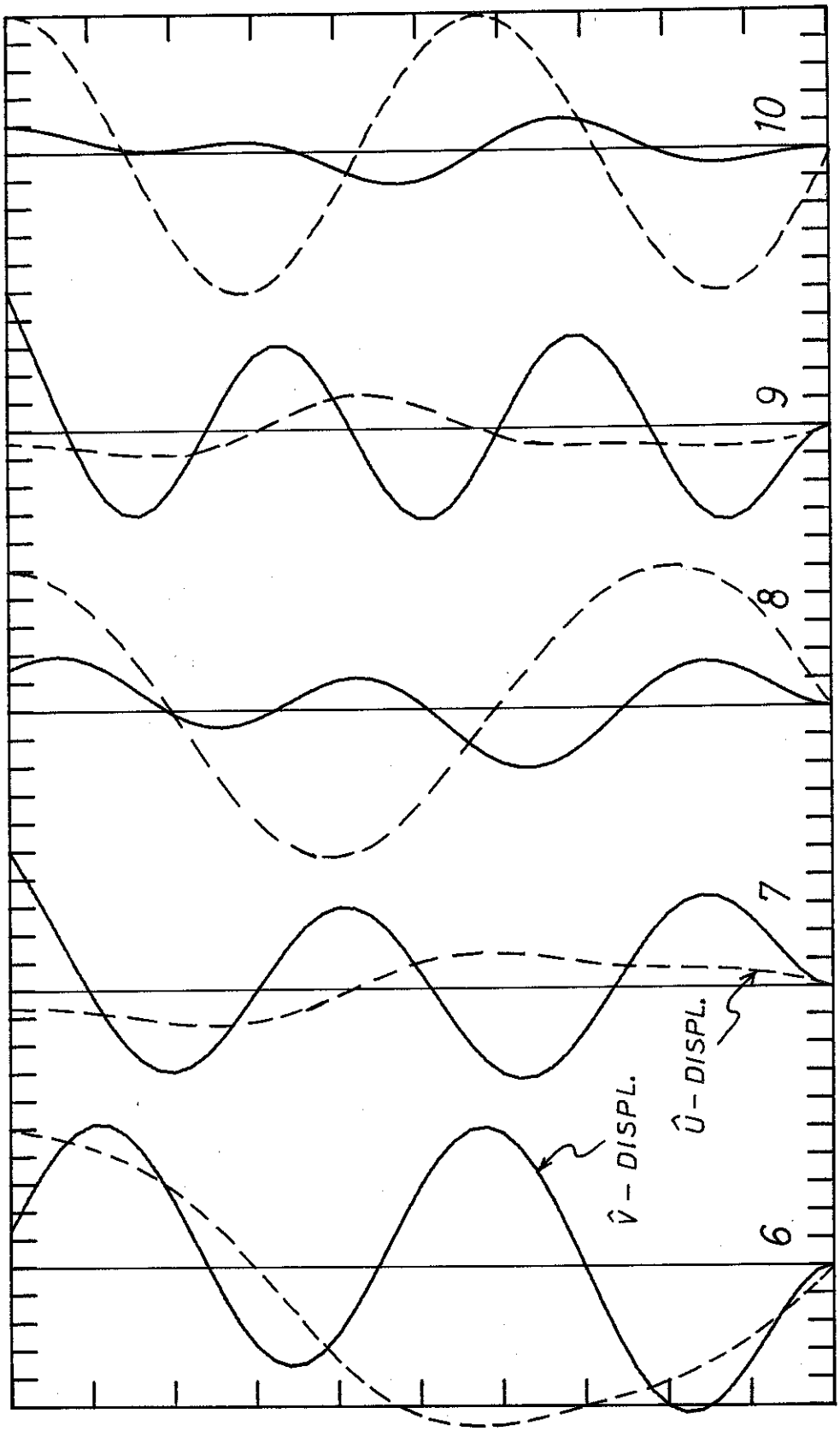

Fig. 4.5(b). First 10 Mode Shapes for the Example

CHAPTER V

SANDWICH BEAM THEORY

A sandwich beam (see figure 5.1) consists of two comparatively thin faces of a strong material, and a core, usually light weight and comparatively weak, which is sandwiched between the stiffer elements. The advantage of this construction is the large moment of inertia of the section, obtained by spacing the two faces far apart.

The object of this chapter is to show that the differential equations for a sandwich beam in many cases, to be specified, are of the same form as those of the coupled shear wall, and the analysis can in these cases be carried out exactly as done in earlier chapters.

In section 5.1, the differential equations for a sandwich beam are derived. For this derivation, the core is assumed to be made of an isotropic material. For many sandwich beams, especially those with metal honeycomb or corrugated cores, the assumption of isotropy is highly unjustified. For these cases it is usually assumed that Young's Modulus is different for the longitudinal and lateral directions and that the deformations in these directions are independent of each other. (In effect, Poisson's ratio is set equal to zero.)

The differential equations and boundary conditions will be derived for the isotropic case, with an approach similar to that used for the coupled shear wall. After the general equations are formulated, reductions to sandwich beams with constant properties, and finally to equal faces are performed. For the sandwich beams with

orthotropic cores the differential equations and boundary conditions are easily deduced from the isotropic case, and this procedure is indicated at the end of section 5.1, and performed for the case of constant, equal faces.

Section 5.2 discusses the similarities and differences between coupled shear walls and sandwich beams. It is found that for many cases, the differential equations have the same form, and the analysis of coupled shear walls performed in earlier chapters hence will apply to the sandwich beams as well.

5.1. Derivation of Differential Equations and Boundary Conditions

The notation used in this chapter follows that defined in chapter II for the coupled shear wall. The two faces will thus be defined by equation (2.2), and for generality, all properties except ℓ_1 are functions of x, the longitudinal coordinate.

For this analysis, the core is taken to be an isotropic medium, and the properties can hence be defined as

$$\begin{aligned} \rho_c &= \rho_c(x) = \text{mass density} \\ A_c &= A_c(x) = \text{cross sectional area} \\ \nu_c &= \nu_c(x) = \text{Poisson's ratio} \\ G_c &= G_c(x) = \text{shear modulus} \\ \ell_c &= \ell_c(x) = \text{depth} \\ t_c &= t_c(x) = \text{width} \end{aligned} \tag{5.1}$$

As indicated in equation (5.1), ℓ_c can be a function of x for this analysis (contrary to the assumption for the coupled shear wall).

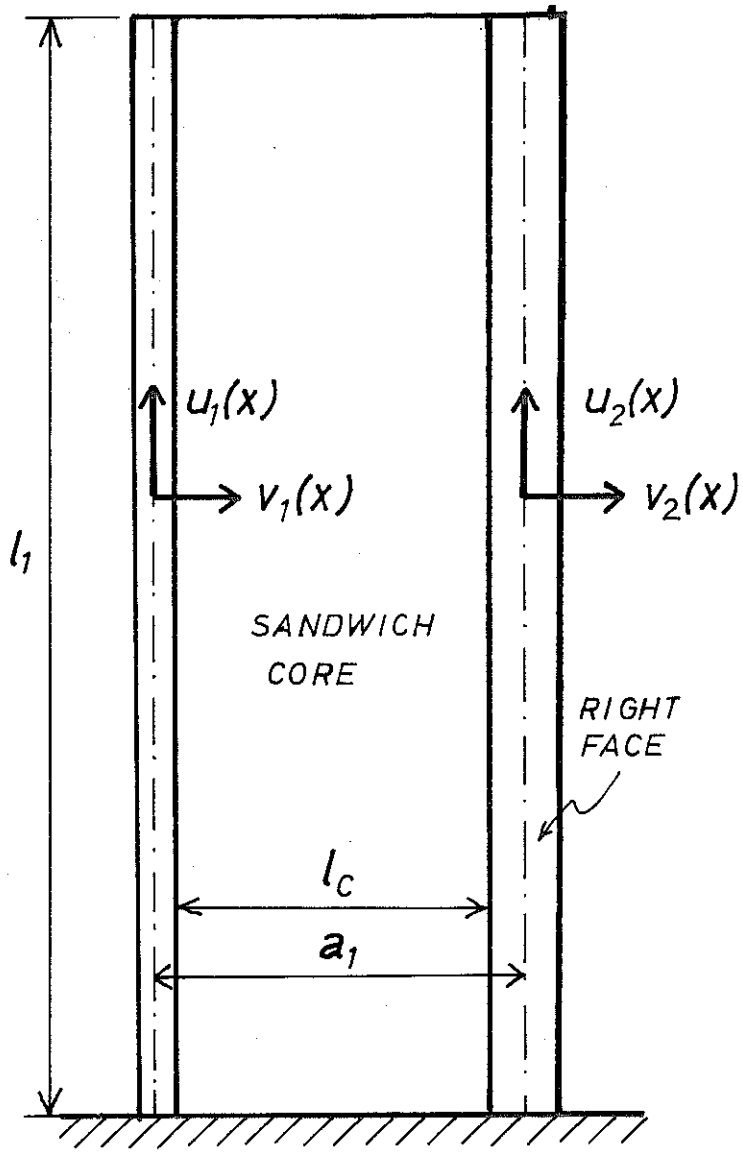

Fig. 5.1. Sandwich Beam

For the orthotropic case, the properties of the core will be as defined in equation (5.1), with the exception that ν_c is set equal to zero, and Young's Modulus will be defined as

$$E_{cx} = E_{cx}(x) = \text{Young's Modulus, longitudinal direction}$$
$$E_{cy} = E_{cy}(x) = \text{Young's Modulus, lateral direction} \qquad (5.2)$$

The distance between the neutral axis of the two beams is given by (see figure 5.1)

$$a_1 = d_1 + d_2 + \ell_c \qquad (5.3)$$

The displacements u_i and v_i, $i = 1,2$ are defined as in chapter II. Hence u_1 and u_2 are the longitudinal displacements while v_1 and v_2 are the lateral displacements of the left ($i = 1$) and right ($i = 2$) face, respectively.

The faces will be subject to the same assumptions as the walls in the coupled shear wall, i.e., bending and axial deformations of the faces are included in the analysis while shearing deformations are neglected. The main assumption for the core, both in the isotropic and orthotropic case, is that plane sections remain plane. This assumption implies that the core deforms mainly in shear, while bending deformations are excluded.

Kinetic Energy

The kinetic energy in the sandwich beam is obtained by considering the faces and the core separately. For the faces, the kinetic energy is[23]

$$T_B = \frac{1}{2}\int_0^{\ell_1} \left\{\rho_1 A_1\left[\left(\frac{\partial u_1}{\partial t}\right)^2 + \left(\frac{\partial v_1}{\partial t}\right)^2\right] + \rho_2 A_2\left[\left(\frac{\partial u_2}{\partial t}\right)^2 + \left(\frac{\partial v_2}{\partial t}\right)^2\right]\right\} dx \qquad (5.4)$$

The lateral and longitudinal deflections of the core are functions both of the x- and y-coordinates (see figure 5.2), and since plane sections remain plane, the variation in the deformations must be linear in y, giving

$$\begin{aligned} v_c(x,y) &= v_1(x) + \frac{y}{\ell_c}\left[v_2(x) - v_1(x)\right] \\ u_c(x,y) &= u_1(x) + \frac{y}{\ell_c}\left[u_2(x) - u_1(x)\right] \end{aligned} \qquad (5.5)$$

The kinetic energy of the core must be integrated over both coordinates

$$T_c = \frac{1}{2}\int_{x=0}^{\ell_1}\int_{y=0}^{\ell_c} \rho_c t_c \left\{\left[\frac{\partial}{\partial t}\left(u_1 + \frac{y}{\ell_c}(u_2 - u_1)\right)\right]^2 + \left[\frac{\partial}{\partial t}\left(v_1 + \frac{u}{\ell_c}(v_2 - v_1)\right)\right]^2\right\} dx\, dy \qquad (5.6)$$

Carrying out the integration for the y-coordinate and noting that

$$A_c = \ell_c t_c \qquad (5.7)$$

equation (5.6) reduces to

$$T_c = \frac{1}{2}\int_0^{\ell_1} \rho_c A_c \left[\frac{1}{3}\left(\frac{\partial u_2}{\partial t} - \frac{\partial u_1}{\partial t}\right)^2 + \frac{\partial u_1}{\partial t}\frac{\partial u_2}{\partial t} + \frac{1}{3}\left(\frac{\partial v_2}{\partial t} - \frac{\partial v_1}{\partial t}\right)^2 + \frac{\partial v_1}{\partial t}\frac{\partial v_2}{\partial t}\right] dx \qquad (5.8)$$

The total kinetic energy is obtained by adding the expressions in equations (5.4) and (5.8).

Strain Energy

When bending and axial deformations are considered for the two faces, the strain energy will be given by equation (2.16).

Under the hypothesis of an isotropic core material, the strain energy in the core will be obtained by integrating the strain energy density for a two-dimensional material in plane stress[33]

$$U_c = G_c \int_v \left[\frac{1}{1-\nu_c}(\epsilon_x^2 + \epsilon_y^2 + 2\nu_c \epsilon_x \epsilon_y) + \frac{1}{2}\gamma_{xy}^2\right] dv \qquad (5.9)$$

The normal strains ϵ_x and ϵ_y and the shearing strain γ_{xy} are obtained under the assumptions that the core deforms into straight lines. From figure 5.2 these strains can be evaluated as

$$\epsilon_x = \frac{\partial u_1}{\partial x} - \frac{y}{\ell_c}\left(\frac{\partial u_1}{\partial x} - \frac{\partial u_2}{\partial x}\right) \quad ; \quad y \in [0, \ell_c]$$

$$\epsilon_y = \frac{v_2 - v_1}{\ell_c} \qquad (5.10)$$

$$\gamma_{xy} = \gamma_v + \gamma_u = \frac{a_1}{2\ell_c}\left(\frac{\partial v_1}{\partial x} + \frac{\partial v_2}{\partial x}\right) + \frac{u_2 - u_1}{\ell_c}$$

Substituting these expressions into equation (5.9) and integrating over the y-coordinate,

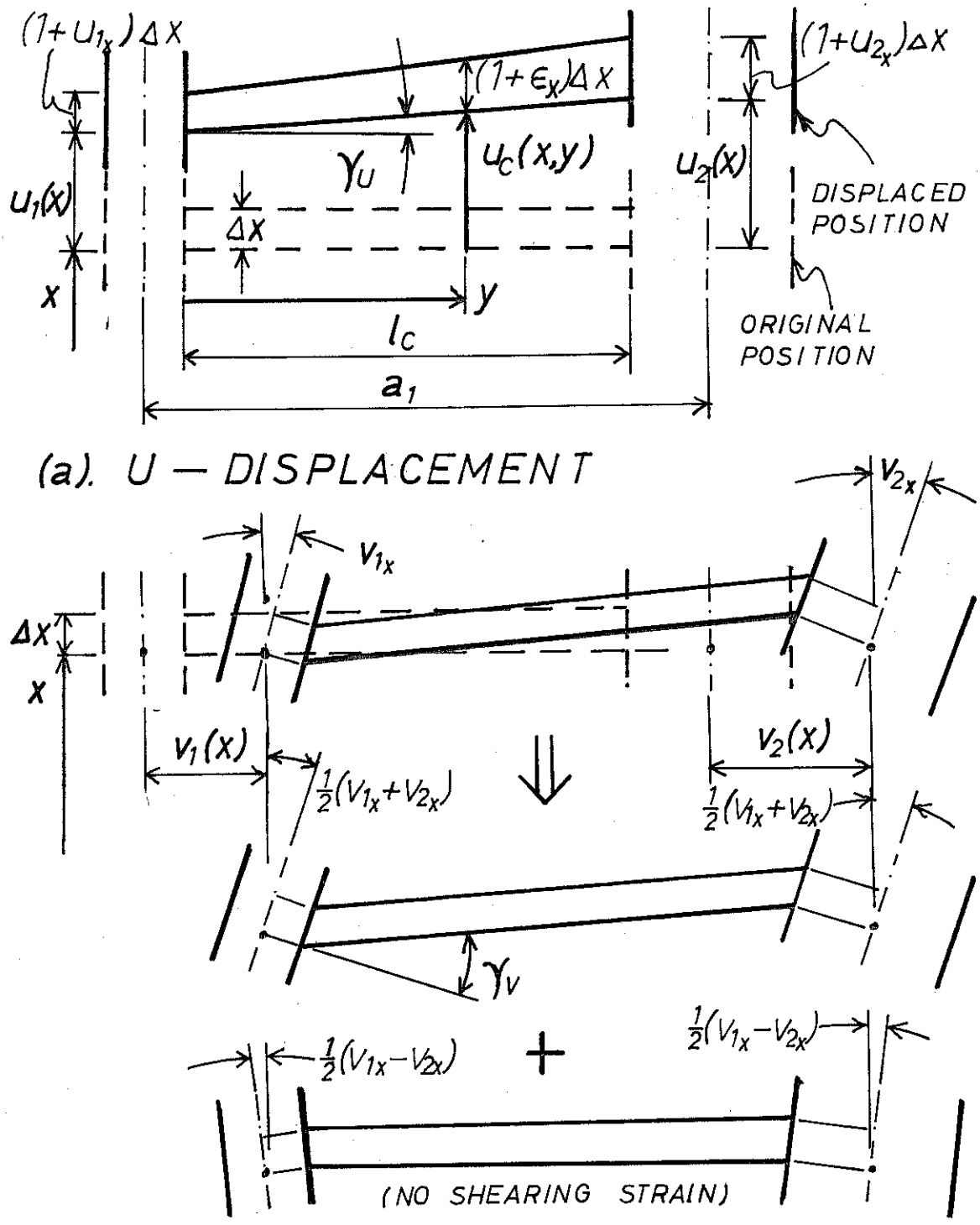

Fig. 5.2 Displacement of the Core at Position x

$$U_c = G_c A_c \int_0^{\ell_1} \left\{ \frac{1}{1-\nu_c} \left[\left(\frac{v_2 - v_1}{\ell_c} \right)^2 + \frac{1}{3} \left(\frac{\partial u_1}{\partial x} - \frac{\partial u_2}{\partial x} \right)^2 + \frac{\partial u_1}{\partial x} \frac{\partial u_2}{\partial x} \right.\right.$$

$$\left.\left. + \nu_c \left(\frac{v_2 - v_1}{\ell_c} \right) \left(\frac{\partial u_1}{\partial x} + \frac{\partial u_2}{\partial x} \right) \right] + \frac{1}{2} \left[\frac{a_1}{2\ell_c} \left(\frac{\partial v_1}{\partial x} + \frac{\partial v_2}{\partial x} \right) + \frac{u_2 - u_1}{\ell_c} \right]^2 \right\} dx \tag{5.11}$$

The differential equations and boundary conditions are then evaluated by using Hamilton's Principle. By equation (2.1)

$$\delta \int_{t_0}^{t_1} (T_B + T_c - U_1 - U_c)\, dt = 0 \tag{5.12}$$

Substituting equations (5.4), (5.8), (2.16) and (5.11) into equation (5.12) and performing the variation in the displacement variables, the following differential equations are obtained.

$$- \rho_1 A_1 \frac{\partial^2 u_1}{\partial t^2} - \frac{1}{6} \rho_c A_c \left(2 \frac{\partial^2 u_1}{\partial t^2} + \frac{\partial^2 u_2}{\partial t^2} \right) + \frac{\partial}{\partial x} \left[E_1 A_1 \frac{\partial u_1}{\partial x} \right]$$

$$+ \frac{\partial}{\partial x} \left[\frac{G_c A_c}{\ell_c (1-\nu_c)} \left\{ \frac{\ell_c}{3} \left(2 \frac{\partial u_1}{\partial x} + \frac{\partial u_2}{\partial x} \right) + \nu_c (v_2 - v_1) \right\} \right]$$

$$+ \frac{G_c A_c}{\ell_c} \left[\frac{a_1}{2\ell_c} \left(\frac{\partial v_1}{\partial x} + \frac{\partial v_2}{\partial x} \right) + \frac{u_2 - u_1}{\ell_c} \right] = 0 \tag{5.13a}$$

$$-\rho_2 A_2 \frac{\partial^2 u_2}{\partial t^2} - \frac{\rho_c A_c}{6}\left(2\frac{\partial^2 u_2}{\partial t^2} + \frac{\partial^2 u_1}{\partial t^2}\right) + \frac{\partial}{\partial x}\left[E_2 A_2 \frac{\partial u_2}{\partial x}\right]$$

$$+ \frac{\partial}{\partial x}\left[\frac{G_c A_c}{\ell_c(1-\nu_c)}\left\{\frac{\ell_c}{3}\left(2\frac{\partial u_2}{\partial x} + \frac{\partial u_1}{\partial x}\right) + \nu_c(v_2 - v_1)\right\}\right]$$

$$- \frac{G_c A_c}{\ell_c}\left[\frac{a_1}{2\ell_c}\left(\frac{\partial v_1}{\partial x} + \frac{\partial v_2}{\partial x}\right) + \frac{u_2 - u_1}{\ell_c}\right] = 0 \qquad (5.13b)$$

$$-\rho_1 A_1 \frac{\partial^2 v_1}{\partial t^2} - \frac{\rho_c A_c}{6}\left(2\frac{\partial^2 v_1}{\partial t^2} + \frac{\partial^2 v_2}{\partial t^2}\right) - \frac{\partial^2}{\partial x^2}\left[E_1 I_1 \frac{\partial^2 v_1}{\partial x^2}\right]$$

$$+ \frac{G_c A_c}{\ell_c(1-\nu_c)}\left[\frac{2(v_2 - v_1)}{\ell_c} + \nu_c\left(\frac{\partial u_1}{\partial x} + \frac{\partial u_2}{\partial x}\right)\right]$$

$$+ \frac{\partial}{\partial x}\left[\frac{G_c A_c a_1}{2\ell_c}\left\{\frac{a_1}{2\ell_c}\left(\frac{\partial v_1}{\partial x} + \frac{\partial v_2}{\partial x}\right) + \frac{u_2 - u_1}{\ell_c}\right\}\right] = 0 \qquad (5.13c)$$

$$-\rho_2 A_2 \frac{\partial^2 v_2}{\partial t^2} - \frac{\rho_c A_c}{6}\left(2\frac{\partial^2 v_2}{\partial t^2} + \frac{\partial^2 v_1}{\partial t^2}\right) - \frac{\partial^2}{\partial x^2}\left[E_2 I_2 \frac{\partial^2 v_2}{\partial x^2}\right]$$

$$- \frac{G_c A_c}{\ell_c(1-\nu_c)}\left[\frac{2(v_2 - v_1)}{\ell_c} + \nu_c\left(\frac{\partial u_1}{\partial x} + \frac{\partial u_2}{\partial x}\right)\right]$$

$$+ \frac{\partial}{\partial x}\left[\frac{G_c A_c a_1}{2\ell_c}\left\{\frac{a_1}{2\ell_c}\left(\frac{\partial v_1}{\partial x} + \frac{\partial v_2}{\partial x}\right) + \frac{u_2 - u_1}{\ell_c}\right\}\right] = 0 \qquad (5.13d)$$

The boundary condition at $x = 0$ and $x = \ell_1$ corresponding to these differential equations are also obtained from equation (5.12).

$$E_1A_1 \frac{\partial u_1}{\partial x} + \frac{G_cA_c}{\ell_c(1-\nu_c)}\left[\frac{\ell_c}{3}\left(2\frac{\partial u_1}{\partial x}+\frac{\partial u_2}{\partial x}\right) + \nu_c(v_2-v_1)\right] = 0; \quad \text{or} \quad u_1 = 0 \tag{5.14a}$$

$$E_2A_2 \frac{\partial u_2}{\partial x} + \frac{G_cA_c}{\ell_c(1-\nu_c)}\left[\frac{\ell_c}{3}\left(2\frac{\partial u_2}{\partial x}+\frac{\partial u_1}{\partial x}\right) + \nu_c(v_2-v_1)\right] = 0; \quad \text{or} \quad u_2 = 0 \tag{5.14b}$$

$$E_1I_1 \frac{\partial^2 v_1}{\partial x^2} = 0 \quad ; \quad \text{or} \quad \frac{\partial v_1}{\partial x} = 0 \tag{5.14c}$$

$$\frac{\partial}{\partial x}\left[E_1I_1 \frac{\partial^2 v_1}{\partial x^2}\right] - \frac{G_cA_ca_1}{2\ell_c^2}\left[\frac{a_1}{2}\left(\frac{\partial v_1}{\partial x}+\frac{\partial v_2}{\partial x}\right) + u_2 - u_1\right] = 0; \quad \text{or} \quad v_1 = 0 \tag{5.14d}$$

$$E_2I_2 \frac{\partial^2 v_2}{\partial x^2} = 0 \quad ; \quad \text{or} \quad \frac{\partial v_2}{\partial x} = 0 \tag{5.14e}$$

$$\frac{\partial}{\partial x}\left[E_2I_2 \frac{\partial^2 v_2}{\partial x^2}\right] - \frac{G_cA_ca_1}{2\ell_c^2}\left[\frac{a_1}{2}\left(\frac{\partial v_1}{\partial x}+\frac{\partial v_2}{\partial x}\right) + u_2 - u_1\right] = 0; \quad \text{or} \quad v_2 = 0 \tag{5.14f}$$

Reduction to Constant Properties

The differential equations for the uniform sandwich beam are determined by considering all dimensions and material properties to be constant along the height of the beam. Also, by introducing new displacement variables, $\bar{u}$, $\hat{u}$, $\bar{v}$ and $\hat{v}$ as defined in equation (2.33), equation (5.13) can be reduced to the following form.

$$-\frac{1}{2}(\rho_1 A_1+\rho_2 A_2)\bar{u}_{tt}-\frac{1}{2}(\rho_1 A_1-\rho_2 A_2)\hat{u}_{tt}-\frac{1}{2}\rho_c A_c \bar{u}_{tt}+\frac{1}{2}(E_1 A_1+E_2 A_2)\bar{u}_{xx}$$

$$+\frac{1}{2}(E_1 A_1-E_2 A_2)\hat{u}_{xx}+\frac{G_c A_c}{\ell_c(1-\nu_c)}(\ell_c \bar{u}_{xx}-2\nu_c \bar{v}_x)=0 \qquad (5.15a)$$

$$-\frac{1}{2}(\rho_1 A_1+\rho_2 A_2)\hat{u}_{tt}-\frac{1}{2}(\rho_1 A_1-\rho_2 A_2)\bar{u}_{tt}-\frac{1}{6}\rho_c A_c \hat{u}_{tt}+\frac{1}{2}(E_1 A_1+E_2 A_2)\hat{u}_{xx}$$

$$+\frac{1}{2}(E_1 A_1-E_2 A_2)\bar{u}_{xx}+\frac{G_c A_c}{3(1-\nu_c)}\hat{u}_{xx}+\frac{G_c A_c}{\ell_c^2}(a_1 \hat{v}_x-2\hat{u})=0 \qquad (5.15b)$$

$$-\frac{1}{2}(\rho_1 A_1+\rho_2 A_2)\hat{v}_{tt}-\frac{1}{2}(\rho_1 A_1-\rho_2 A_2)\bar{v}_{tt}-\frac{1}{2}\rho_c A_c \hat{v}_{tt}-\frac{1}{2}(E_1 I_1+E_2 I_2)\hat{v}_{xxxx}$$

$$-\frac{1}{2}(E_1 I_1-E_2 I_2)\bar{v}_{xxxx}+\frac{G_c A_c a_1}{2\ell_c^2}(a_1 \hat{v}_{xx}-2\hat{u}_x)=0 \qquad (5.15c)$$

$$-\frac{1}{2}(\rho_1 A_1+\rho_2 A_2)\bar{v}_{tt}-\frac{1}{2}(\rho_1 A_1-\rho_2 A_2)\hat{v}_{tt}-\frac{1}{6}\rho_c A_c \bar{v}_{tt}-\frac{1}{2}(E_1 I_1+E_2 I_2)\bar{v}_{xxxx}$$

$$-\frac{1}{2}(E_1 I_1-E_2 I_2)\hat{v}_{xxxx}-2\frac{G_c A_c}{\ell_c^2(1-\nu_c)}(2\bar{v}-\nu_c \ell_c \bar{u}_x)=0 \qquad (5.15d)$$

The corresponding boundary conditions at $x = 0$ and $x = \ell_1$ are evaluated from equation (5.14).

$$\frac{1}{2}(E_1 A_1+E_2 A_2)\bar{u}_x+\frac{1}{2}(E_1 A_1-E_2 A_2)\hat{u}_x+\frac{G_c A_c}{\ell_c(1-\nu_c)}(\ell_c \bar{u}_x-2\nu_c \bar{v})=0\ ;$$

$$\text{or } \bar{u}=0 \qquad (5.16a)$$

$$\frac{1}{2}(E_1A_1+E_2A_2)\hat{u}_x+\frac{1}{2}(E_1A_1-E_2A_2)\bar{u}_x+\frac{G_cA_c}{3(1-\nu_c)}\hat{u}_x=0;\quad \text{or}\quad \hat{u}=0 \tag{5.16b}$$

$$\frac{1}{2}(E_1I_1+E_2I_2)\bar{v}_{xx}+\frac{1}{2}(E_1I_1-E_2I_2)\hat{v}_{xx}=0\ ;\quad \text{or}\quad \bar{v}_x=0 \tag{5.16c}$$

$$\frac{1}{2}(E_1I_1+E_2I_2)\hat{v}_{xx}+\frac{1}{2}(E_1I_1-E_2I_2)\bar{v}_{xx}=0;\quad \text{or}\quad \hat{v}_x=0 \tag{5.16d}$$

$$\frac{1}{2}(E_1I_1+E_2I_2)\hat{v}_{xxx}+\frac{1}{2}(E_1I_1-E_2I_2)\bar{v}_{xxx}-\frac{G_cA_ca_1}{2\ell_c^2}(a_1\hat{v}_x-2\hat{u})=0\ ;$$
$$\text{or}\quad \hat{v}=0 \tag{5.16e}$$

$$\frac{1}{2}(E_1I_1+E_2I_2)\bar{v}_{xxx}+\frac{1}{2}(E_1I_1-E_2I_2)\hat{v}_{xxx}=0\ ;\quad \text{or}\quad \bar{v}=0 \tag{5.16f}$$

Reduction to the Case of Equal, Constant Faces

When the two faces are identical, the differential equations as well as the boundary conditions will uncouple. From equations (5.15a) and (5.15d)

$$-(\rho_1A_1+\frac{1}{2}\rho_cA_c)\bar{u}_{tt}+E_1A_1\bar{u}_{xx}+\frac{G_cA_c}{\ell_c(1-\nu_c)}(\ell_c\bar{u}_{xx}-2\nu_c\bar{v}_x)=0 \tag{5.17a}$$

$$-(\rho_1A_1+\frac{1}{6}\rho_cA_c)\bar{v}_{tt}-E_1I_1\bar{v}_{xxxx}-\frac{2G_cA_c}{\ell_c^2(1-\nu_c)}(2\bar{v}-\nu_c\ell_c\bar{u}_x)=0 \tag{5.17b}$$

where subscript one now refers to both faces. The corresponding boundary conditions at $x=0$ and $x=\ell_1$ are given by equations (5.16a), (5.16c) and (5.16f):

$$E_1 A_1 \bar{u}_x + \frac{G_c A_c}{\ell_c (1-\nu_c)} (\ell_c \bar{u}_x - 2\nu_c \bar{v}) = 0 \; ; \quad \text{or} \quad \bar{u} = 0 \tag{5.18a}$$

$$\bar{v}_{xx} = 0 \; ; \quad \text{or} \quad \bar{v}_x = 0 \tag{5.18b}$$

$$\bar{v}_{xxx} = 0 \; ; \quad \text{or} \quad \bar{v} = 0 \tag{5.18c}$$

The displacements $\bar{u}$ and $\bar{v}$ remain coupled in the differential equations as well as the boundary conditions, but they have become uncoupled from the two other displacements, $\hat{u}$ and $\hat{v}$.

As in the case of the coupled shear wall, the motions described by $\hat{u}$ and $\hat{v}$ are of most practical importance. From equations (5.15b) and (5.15c)

$$-(\rho_1 A_1 + \tfrac{1}{6}\rho_c A_c)\hat{u}_{tt} + \left(E_1 A_1 + \frac{G_c A_c}{3(1-\nu_c)}\right)\hat{u}_{xx} + \frac{G_c A_c}{\ell_c^2}(a_1 \hat{v}_x - 2\hat{u}) = 0 \tag{5.19a}$$

$$-(\rho_1 A_1 + \tfrac{1}{2}\rho_c A_c)\hat{v}_{tt} - E_1 I_1 \hat{v}_{xxxx} + \frac{G_c A_c a_1}{2\ell_c^2}(a_1 \hat{v}_{xx} - 2\hat{u}_x) = 0 \tag{5.19b}$$

The associated boundary conditions are obtained from equations (5.16b), (5.16d) and (5.16e)

$$\hat{u}_x = 0 \; ; \quad \text{or} \quad \hat{u} = 0$$

$$\hat{v}_{xx} = 0 \; ; \quad \text{or} \quad \hat{v}_x = 0 \qquad \text{at } x = 0, \ell_1 \tag{5.20}$$

$$E_1 I_1 \hat{v}_{xxx} - \frac{G_c A_c a_1}{2\ell_c^2}(a_1 \hat{v}_x - 2\hat{u}) = 0 \; ; \quad \text{or} \quad \hat{v} = 0$$

Orthotropic Core Material

All differential equations and boundary conditions derived earlier in this section can be reduced to the case of orthotropic core material when (1) the term $G_c/(1-\nu_c)$ is replaced by $E_{cx}/2$ or $E_{cy}/2$ depending upon whether the term $G_c/(1-\nu_c)$ is multiplied by functions of u_i or v_i, respectively, and (2) when ν_c is set equal to zero.

For the case of equal, constant faces, equations (5.17a) and (5.18a) reduce to

$$-(\rho_1 A_1 + \tfrac{1}{2}\rho_c A_c)\bar{u}_{tt} + \left(E_1 A_1 + \frac{E_{cx} A_c}{2}\right)\bar{u}_{xx} = 0 \qquad (5.21)$$

with

$$\bar{u}_x = 0 \;\; ; \;\; \text{or} \;\; \bar{u} = 0 \;\; ; \;\; \text{at} \;\; x = 0, \ell_1 \qquad (5.22)$$

Similarly, equations (5.17b), (5.18b) and (5.18c) become

$$-(\rho_1 A_1 + \tfrac{1}{6}\rho_c A_c)\bar{v}_{tt} - E_1 I_1 \bar{v}_{xxxx} - \frac{2E_{cy} A_c}{\ell_c^2}\bar{v} = 0 \qquad (5.23)$$

with

$$\begin{aligned} &\bar{v}_{xx} = 0 \;\; ; \;\; \text{or} \;\; \bar{v}_x = 0 \\ &\qquad\qquad\qquad\qquad\qquad\qquad \text{at} \;\; x = 0, \ell_1 \\ &\bar{v}_{xxxx} = 0 \; ; \;\; \text{or} \;\; \bar{v} = 0 \end{aligned} \qquad (5.24)$$

Hence, the $\bar{v}$- and $\bar{u}$-motions have now uncoupled completely into differential equations and boundary conditions similar to those obtained in chapter II, equations (2.40) through (2.43).

The equations for the coupled $\hat{u}$- and $\hat{v}$-displacements remain

the same for the orthotropic case with the exception of equation (5.19a) which now is given by

$$-(\rho_1 A_1 + \frac{1}{6}\rho_c A_c)\hat{u}_{tt} + \left(E_1 A_1 + \frac{E_{cx} A_c}{6}\right)\hat{u}_{xx} + \frac{G_c A_c}{\ell_c^2}(a_1 \hat{v}_x - 2\hat{u}) = 0 \tag{5.25}$$

5.2. Similarities with Coupled Shear Walls

Some similarities could be pointed out for the most general differential equations derived, when the properties of the coupled shear wall and the sandwich beam change over the height of the structure (equations (2.32) and (5.13)). However, for most applications, the structures with constant property are of most importance, and this section only deals with those cases.

Constant, Unequal Beams or Faces

Comparing equation (5.15) to (2.34) it is observed that most differences will be eliminated if the sandwich structure has an orthotropic core ($\nu_c = 0$). In fact, if

$$d_1 = d_2 \tag{5.26}$$

then the two sets of differential equations ((2.34) and (5.15)) and boundary conditions (equations (2.35) and (5.16)) would have the same form, with one exception: Equation (2.34d) has a term $\bar{v}_{xx}$ which does not occur in equation (5.15d). This is due to the bending rigidity of the spandrel system which is not included in the sandwich core.

On the other hand, if one can assume that

$$\overline{v}(x) = 0 \tag{5.27}$$

in addition to equation (5.26), then equations (2.34d) and (5.15d) drop out of the analysis, and the two sets of differential equations and boundary conditions are equal for the isotropic core as well as for the orthotropic core.

The assumption of no antisymmetrical lateral motion, equation (5.27), is often made in sandwich construction where the core stiffness in the lateral direction is much larger than in the longitudinal.

Constant, Equal Beams or Faces

For the sandwich beam with an isotropic core, the motions $\overline{u}$ and $\overline{v}$ are coupled together, but if ν_c is set equal to zero as in the case with the orthotropic core, $\overline{v}$- and $\overline{u}$-motions do uncouple in the differential equations as well as in the boundary conditions. It is then observed that the equations for the symmetrical longitudinal motion, $\overline{u}$, have the same form in the coupled shear wall, equations (2.40) and (2.41) as in the sandwich beam, equations (5.21) and (5.22).

The differential equations and the boundary conditions for the antisymmetrical lateral motion, $\overline{v}$, are different for the two cases. Again, this difference comes from the fact that the spandrel system admits bending deformations which are neglected in the sandwich core.

The two remaining displacement variables, $\hat{u}$ and $\hat{v}$, are coupled together in the differential equations as well as in the boundary conditions, but the form of these equations, (2.44), (2.45), (5.19), (5.20) and (5.25), are the same with the exception of the constant

coefficients. Hence, for these displacements, which are of most practical importance, the theory of coupled shear walls and sandwich beams, both for isotropic and orthotropic cores are the same.

If the displacements $\hat{u}$ and $\hat{v}$, and the coordinates x and t, are made dimensionless by equation (3.1), then the differential equations for a sandwich beam, equation (5.19), become

$$\begin{aligned} &v_{\xi\xi\xi\xi} - \Pi_1^* v_{\xi\xi} + \Pi_1^* u_\xi + \lambda^{*2} v_{\tau\tau} = 0 \\ &u_{\xi\xi} + \Pi_1^* \Pi_2^* v_\xi - \Pi_1^* \Pi_2^* u - \Pi_3^* \lambda^{*2} u_{\tau\tau} = 0 \end{aligned} \qquad \xi,\ \xi \in \langle 0,1 \rangle \quad (5.28)$$

in which

$$\begin{aligned} \Pi_1^* &= \frac{G_c A_c a_1^2 \ell_1^2}{2 E_1 I_1 \ell_c^2} \\ \Pi_2^* &= \frac{4 I_1}{A_1 a_1^2 \gamma} \\ \Pi_3^* &= \frac{I_1}{A_1 \ell_1^2 \gamma} \cdot \frac{\rho_1 A_1 + \frac{1}{6} \rho_c A_c}{\rho_1 A_1 + \frac{1}{2} \rho_c A_c} \\ \lambda^{*2} &= \frac{(\rho_1 A_1 + \frac{1}{2} \rho_c A_c) \ell_1^4 \omega^2}{E_1 I_1} \end{aligned} \qquad (5.29)$$

and where γ is given by

$$\gamma = 1 + \frac{G_c A_c}{3 E_1 I_1 (1 - \nu_c)} \qquad (5.30)$$

for the sandwich beam with an isotropic core and by

$$\gamma = 1 + \frac{E_{cx} A_c}{6 E_1 A_1} \tag{5.31}$$

for the sandwich beam with orthotropic core.

Similarly, the boundary conditions associated with the differential equations (5.28) are obtained using equations (5.20) and (3.1)

$$\begin{aligned} &u_\xi = 0 \ ; \quad \text{or} \quad u = 0 \\ &v_{\xi\xi} = 0 \ ; \quad \text{or} \quad v_\xi = 0 \qquad\qquad \xi = 0.1 \\ &v_{\xi\xi\xi} - \Pi_1^*(v_\xi - u) = 0 \ ; \quad \text{or} \quad v = 0 \end{aligned} \tag{5.32}$$

The differential equations (5.28) and the corresponding boundary conditions, equation (5.32) are the same as for the coupled shear wall, equations (3.4) and (2.45). Hence, all the analysis carried out for the coupled shear walls, in statics as well as dynamics, apply to the sandwich beams as well, and vice-versa.

The dimensionless parameters defined in equation (5.29) are similar to those for the coupled shear wall, equations (3.2) and (3.3). Essentually, Π_1 can be reduced to Π_1^* if the spandrels are assumed to deform in shear only. This is seen by comparing equations (3.12) and (5.29).

For a sandwich beam with rectangular faces,

$$\begin{aligned} A_1 &= t_c \cdot t \\ I_1 &= \frac{1}{12} t_c t^3 \end{aligned} \tag{5.33}$$

where

$$t = 2d_1 = 2d_2 \tag{5.34}$$

and t_c is the thickness of the sandwich beam. From equation (5.3) and (5.34)

$$a_1 = \ell_c + t \tag{5.35}$$

Using equations (5.33) and (5.35), Π_1^*, equation (5.29) can be written as

$$\Pi_1^* = 6\left(\frac{G_c}{E_1}\right)\left(1 + \frac{t}{\ell_c}\right)^2\left(\frac{\ell_c}{t}\right)\left(\frac{\ell_1}{t}\right)^2 \tag{5.36}$$

and the numerical values for Π_1^* appears to lie between 1 and 10,000, similar to what was found for Π_1.

The only difference between Π_2 and Π_2^* is the quantity γ. For many sandwich beams, particularly those with orthotropic cores, γ is usually set equal to unity[35-37] (by assuming that $E_{cx} << E_1$). By this assumption, Π_2 and Π_2^* are identical, but the typical values of Π_2^* will be different from the typical values of Π_2. In the coupled shear wall, the distances between the walls tend to be small so that the full advantage of the shear walls can be obtained. This results in fairly high values for Π_2 (see figure 3.1). For the sandwich beam, the core exists to place the faces far apart, and Π_2^* will then become very small. If the faces of the sandwich beam have a rectangular cross section, Π_2^*, equation (5.29) can be reduced employing equations (5.33) and (5.35)

$$\Pi_2^* = \frac{1}{3}\left(\frac{t}{\ell_c + t}\right)^2 \tag{5.37}$$

This equation for Π_2^* shows that the numerical values may be much less than 0.01, values which seem uncommon for coupled shear walls. For these low values of Π_2^*, the asymptotic analysis given in chapter III for the case when $\Pi_2 \rightarrow 0$, will become very useful.

Π_3^* and Π_3 are, for all practical purposes identical, as long as γ is unity, and equation (3.18) which gives 1/300 as an upper bound for Π_3 applies to Π_3^* also.

CHAPTER VI

CONCLUSIONS AND RECOMMENDATIONS

Conclusions

In the formulation of the basic dynamic problem of the thesis, it was found more useful to obtain the differential equations in terms of displacement variables rather than the variables used in most previous studies. Further, the energy approach for deriving these equations seems to be well suited to extensions of the coupled shear wall theory. Since the differential equations were derived for a general coupled shear wall, they can easily be applied to static and dynamic analyses of structures with unequal walls, or to structures with walls and spandrels varying along the height. The main restrictions in the analysis were that the opening between the walls was kept constant and that each spandrel was uniform.

The main portion of the thesis treated the free vibrations of the practically important case in which the walls are equal. By a transformation of displacement variables, the differential equations and the boundary conditions uncoupled for this case into three sets of new equations, in which two were less important for most applications. The last set of equations, containing the symmetrical lateral and antisymmetrical longitudinal displacements, was made dimensionless by introducing a dimensionless frequency and three parameters containing the properties of the coupled shear wall. The equation for the natural frequencies (eigenvalues) was obtained, and the eigenvalues can be found directly from figures 3.2 and 3.3 when

vertical inertia is neglected, or from figures 4.1 and 4.2 when it is included in the analysis.

These eigenvalue plots, figure 3.3 in particular, also portray the general stiffness of the coupled shear wall as a function of the wall properties: the higher the first frequency, the stiffer the structure. Hence, figure 3.3 can be helpful in the design of coupled shear walls for static loads. For example, it can be observed (in figure 3.3), that after some value, where the curves become almost vertical for increasing π_1, the coupled shear wall becomes only slightly stiffer from increases in the stiffness of the spandrels.

The importance of including vertical motion has been stated repeatedly in the earlier chapters. By including vertical inertia too, smaller, but in some cases significant differences in the results were obtained, as stated in Chapter IV, Section 4.4.

Asymptotic analyses of the frequencies and mode shapes showed that for thin spandrels, the coupled shear wall behaved as a simple Euler-Bernoulli cantilever beam. When the stiffness of the spandrels increased, the asymptotic values obtained were different depending upon whether or not vertical inertia was included in the analysis: in the first (and most general) case, the asymptotic values for the frequencies were found to be, in essence, those obtained by the Timoshenko theory of beam vibration excluding shearing deformation, under the assumptions that the spandrels were rigid.

One asymptotic result that was not investigated, but is easily deduced from the other results, is the case where the

openings in the coupled shear wall fill up, i.e., when the coupled shear wall reduces to a wide cantilever wall. From figure 1.2 it is observed that there are two ways to approach this limit: (1) when the spandrels increase in depth, and (2) when the distance between the two walls decreases. Asymptotically, these two cases will give different results; in case (1) the medium between the two walls is still considered to be composed of independently acting laminae. In case (2) the laminar system collapses (as $\pi_2 \to \frac{1}{3}$ (for rectangular walls) and $\pi_1 \to \infty$), and it is easily shown that for this last case, the frequencies and mode shapes will asymptotically approach the case of a regular wide wall.

For the asymptotic behavior when the frequencies became large, it was observed in Chapter IV that the mode shapes corresponding to the lateral and longitudinal antisymmetrical motion uncoupled, asymptotically approaching the mode shapes for a cantilever beam and the longitudinal vibration of a bar, respectively. The corresponding frequencies asymptotically approached those for the cantilever beam (for the lateral motion) and the longitudinal vibration of a bar (for the longitudinal motion), but both asymptotes are increased by constants directly proportional to the relative stiffness of the spandrels.

The analysis of sandwich beams was carried out in a way similar to that for coupled shear walls, with the object of Chapter V to show that the two theories were similar for constant, equal or unequal walls and faces. Because of the similarities

between the two theories, new information might be obtained for the coupled shear wall theory by examining the research efforts in the sandwich beam theory, and vice versa.

Recommendation for Future Work

Regarding future study, the theory and analysis presented in this thesis can easily be extended to new and related fields of interest.

1. Applying the energy method by which the present set of differential equations were derived, shear walls with several bands of openings can be analyzed for static or dynamic behavior. For example, three walls symmetrically coupled together will, in the dynamic case, reduce essentially to the equal wall case treated in this thesis, and four or five wall symmetric systems will be similar to the unequal wall case. Because of the similarities between coupled shear walls and sandwich beams, the extension of the theory to include more walls is also applicable to layered sandwich construction where two or more cores are sandwiched between thinner and stronger material.

2. In most shear wall buildings, the variation of structural and material properties along the height of the building is relatively small, and has usually been neglected. Nevertheless, in some structures the properties of the walls could change considerably, and for these instances an extension of the given analysis would be appropriate.

3. As mentioned in the introduction, the dynamics and statics of coupled shear wall buildings have been the object of considerable study in the last few years. Further study in this field seems to be important, and the energy approach given in this thesis is well suited for such investigations.

4. In the theory of sandwich beams, other boundary conditions than the one treated would be of interest. These problems can be solved by extending the analysis given in this thesis.

APPENDIX A

STRAIN ENERGY IN A COMBINED SHEAR AND BENDING BEAM SUBJECT TO DEFORMATIONS AT ONE END

The properties of the beam are taken as E, Young's Modulus, G, shear modulus, A, area, I, moment of inertia, ℓ, length and A^*, composite cross section of the beam defined by[23]

$$A^* = \frac{A}{k} \tag{A.1}$$

where k is given in equation (2.25).

The total lateral deflection of the beam, v(x), consists of two parts,

$$v(x) = v_b(x) + v_s(x) \tag{A.2}$$

where $v_b(x)$ and $v_s(x)$ are the deformations due to bending and shear, respectively. u(x) will denote the longitudinal deformations of the centerline and x is the coordinate along the beam as shown in Figure A.1. Also shown in the figure are the generalized forces at the left end: V_o, shear; N_o, axial force; and M_o, moment.

Assuming small deflections, the governing differential equations are[23]

$$\frac{d^2 v_b}{dx^2} = \frac{M(x)}{EI} \tag{A.3}$$

$$\frac{dv_s}{dx} = -\frac{V(x)}{GA^*} \tag{A.4}$$

$$\frac{du}{dx} = \frac{N(x)}{EA} \tag{A.5}$$

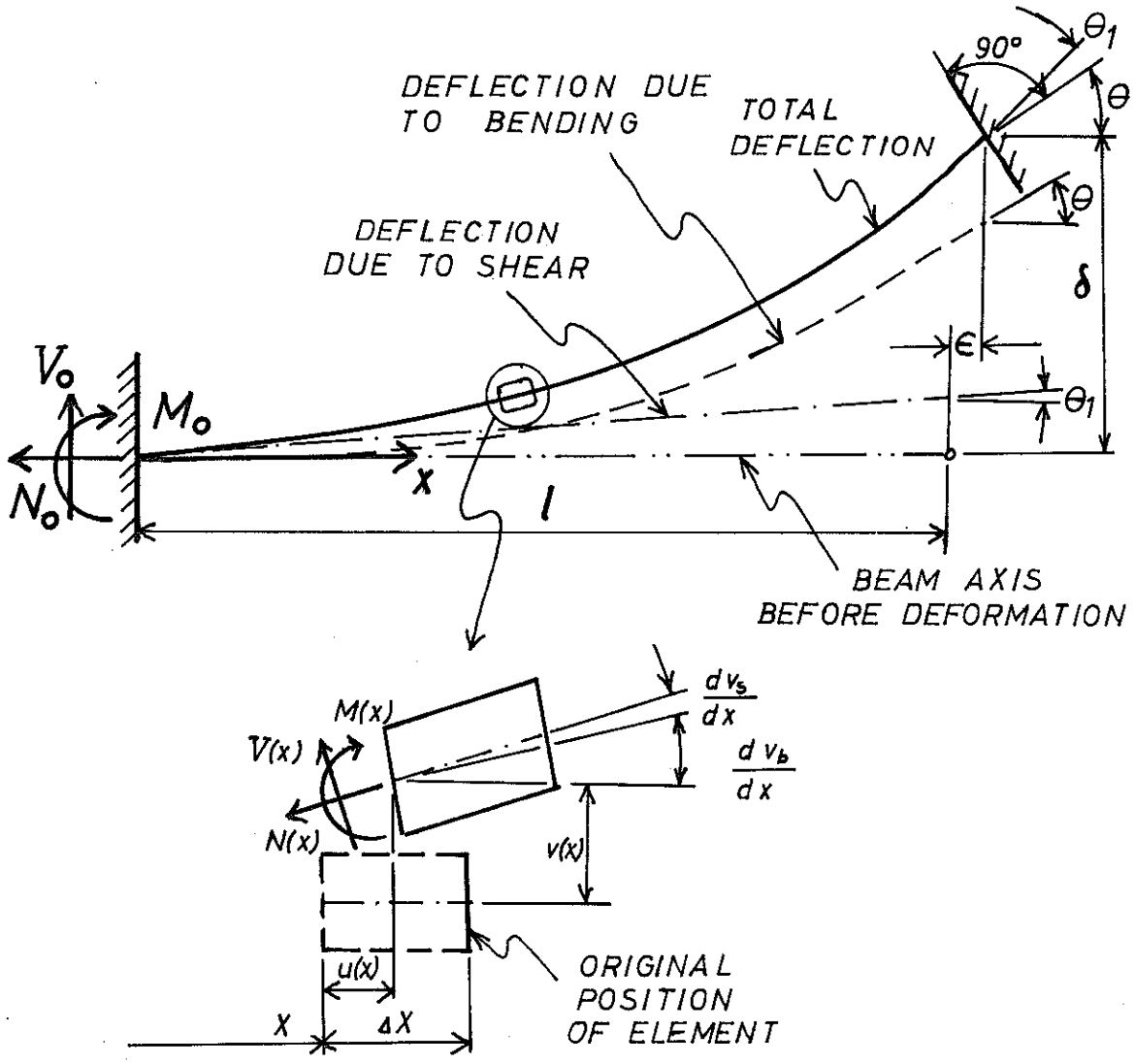

Fig. A.1. Notation and Geometry of a Beam

where the forces in the beam at position x can be obtained from Figure A.1. Neglecting higher order terms,

$$N(x) = N_o \tag{A.6}$$

$$V(x) = V_o \tag{A.7}$$

$$M(x) = M_o + V_o x \tag{A.8}$$

The differential equation can now be obtained in the variable $v(x)$. From equations (A.2), (A.3), (A.6) and (A.7)

$$\frac{d^2v}{dx^2} = \frac{1}{EI}(M_o + V_o x) \tag{A.9}$$

The boundary conditions associated with this equation are indicated in Figure A.1, and can be given by

$$\begin{aligned} v\big|_{x=0} &= 0 \\ \frac{dv}{dx}\Big|_{x=0} &= \frac{dv_s(0)}{dx} = -\frac{V_o}{GA^*} \\ v\big|_{x=\ell} &= \delta \\ \frac{dv}{dx}\Big|_{x=\ell} &= \theta - \frac{V_o}{GA^*} \end{aligned} \tag{A.10}$$

Integrating equation (A.9) twice and applying the boundary conditions (A.10), two equations for the two unknown quantities M_o and V_o are obtained, and M_o and V_o are subsequently evaluated

$$M_o = \frac{EI}{\ell^2\beta^2}\left[6\delta - (3-\beta^2)\theta\ell\right] \tag{A.11}$$

$$V_o = \frac{EI}{\ell^2\beta^2}\left[-12\,\frac{\delta}{\ell} + 6\theta\right] \tag{A.12}$$

where

$$\beta^2 = 1 + \frac{12\ EI}{\ell^2 GA^*} \tag{A.13}$$

The expression for N_o is obtained by solving equation (A.5) subject to the boundary conditions

$$\left.\begin{aligned} u\,|_{x=0} &= 0 \\ u\,|_{x=\ell} &= \epsilon \end{aligned}\right\} \tag{A.14}$$

giving

$$N_o = \frac{EA}{\ell}\,\epsilon \tag{A.15}$$

The total strain energy in the beam can now be evaluated[23]

$$U = \int_0^\ell \frac{N(x)^2 dx}{2\ EI} + \int_0^\ell \frac{M(x)^2 dx}{2\ EI} + \int_0^\ell \frac{V(x)^2 dx}{2\ GA^*} \tag{A.16}$$

where the different terms are the strain energy due to axial, bending and shearing forces, respectively. Making use of equations (A.6), (A.7), (A.8), (A.11), (A.12) and (A.15), the integration of equation (A.16) can be carried out to yield the final expression for the strain energy in terms of the right end ($x = \ell$) deflections.

$$V = \frac{6\ EI}{\ell^3\beta^2}\left[\delta^2 - \theta\delta\ell + \frac{1}{12}(3+\beta^2)\theta^2\ell^2\right] + \frac{EA}{2\ell}\,\epsilon^2 \tag{A.17}$$

APPENDIX B

ASYMPTOTIC EIGENVALUES AND EIGENVECTORS FOR A CANTILEVER BEAM

In the notation of equation (3.4) the Euler-Bernoulli Beam equation can be written as

$$v_{\xi\xi\xi\xi} + \lambda^{*2} v_{\tau\tau} = 0 \tag{B.1}$$

in which

$$\lambda^{*2} = \frac{\rho A \ell^4}{EI} \omega^2 \tag{B.2}$$

ρ is the mass density, A is the cross sectional area, E is Young's modulus, I is the moment of inertia, ω is the frequency of oscillation and ℓ is the length of the beam. The boundary conditions for a cantilever beam

$$v(0) = v_{\xi}(0) = v_{\xi\xi}(1) = v_{\xi\xi\xi}(1) = 0 \tag{B.3}$$

are similar to those given for the lateral displacement in equation (3.8). Assuming a solution of the form

$$v(\xi, \tau) = V(\xi) e^{i\tau} \tag{B.4}$$

to equation (B.1), the solution can be written as

$$V(\xi) = C_1 \sin\sqrt{\lambda^*}\xi + C_2 \cos\sqrt{\lambda^*}\xi + C_3 \sinh\sqrt{\lambda^*}\xi + C_4 \cosh\sqrt{\lambda^*}\xi \tag{B.5}$$

in terms of the four constants C_i. When this equation is employed in the boundary conditions, equation (B.3), the eigenvalue equation becomes

$$\cosh \sqrt{\lambda_n^*} \cos \sqrt{\lambda_n^*} + 1 = 0 \tag{B.6}$$

which can be solved numerically to yield the following results.

$$\begin{aligned} \lambda_1^* &= 3.51602 \\ \lambda_2^* &= 22.03449 \\ \lambda_3^* &= 61.69721 \\ \lambda_4^* &= 120.90192 \\ \lambda_5^* &= 199.8595 \\ \lambda_n^* &\doteq \left[\frac{2n-1}{2}\pi\right]^2 \; ; \quad n \geq 6 \end{aligned} \tag{B.7}$$

Further, the mode shapes at these eigenvalues are given by

$$V_n(\xi) = C\left[(\cosh\sqrt{\lambda_n^*}\xi - \cos\sqrt{\lambda_n^*}\xi) - q(\lambda_n^*)(\sinh\sqrt{\lambda_n^*}\xi - \sin\sqrt{\lambda_n^*}\xi)\right] ; \quad n = 1,2,\ldots \tag{B.8}$$

in which

$$q(\lambda_n^*) = \frac{\cosh\sqrt{\lambda_n^*} + \cos\sqrt{\lambda_n^*}}{\sin\sqrt{\lambda_n^*} + \sinh\sqrt{\lambda_n^*}} = \frac{\sin\sqrt{\lambda_n^*}}{(-1)^{n+1} - \cos\sqrt{\lambda_n^*}} \tag{B.9}$$

using equation (B.6).

Asymptotic Behavior

When λ_n^* is larger than 81, equation (3.105) implies thaw

$$\cosh\sqrt{\lambda_n^*} = \frac{1}{2} e^{\sqrt{\lambda_n^*}} + O(\lambda_n^{*-2}) \tag{B.10}$$

such that equation (B.6) can be written as

$$\frac{1}{2} e^{\sqrt{\lambda_n^*}} \left[\cos\sqrt{\lambda_n^*}(1 + O(\lambda_n^{*-2})) + O(\lambda_n^{*-2})\right] = 0 \tag{B.11}$$

or

$$\cos\sqrt{\lambda_n^*} = O(\lambda_n^{*-2}) \tag{B.12}$$

Solving equation (B.12) gives

$$\lambda_n^* = \left[\frac{2n-1}{2}\pi\right]^2 + O(\lambda_n^{*-1}) \tag{B.13}$$

in agreement with equation (B.7). Furthermore, from equations (B.9) and (B.13)

$$\frac{1}{q(\lambda_n^*)} = 1 + 2e^{-\sqrt{\lambda_n^*}} \sin\sqrt{\lambda_n^*} + O(\lambda_n^{*-4}) \tag{B.14}$$

and the mode shapes, equation (B.8) become

$$V(\xi) = C \cdot q(\lambda_n^*)\left[e^{-\sqrt{\lambda_n^*}\xi} + (-1)^{n+1} e^{-\sqrt{\lambda_n^*}(1-\xi)} + \sin\sqrt{\lambda_n^*}\,\xi - \cos\sqrt{\lambda_n^*}\,\xi + O(\lambda_n^{*-2})\right] \tag{B.15}$$

Noting that

$$\sin\sqrt{\lambda_n^*}\xi - \cos\sqrt{\lambda_n^*}\xi = \sqrt{2}\,\sin(\sqrt{\lambda_n^*}\xi - \frac{\pi}{4}) \qquad \text{(B.16)}$$

the asymptotic expression for the mode shape as n becomes large is

$$V_n(\xi) = \text{const.}\left[e^{-\sqrt{\lambda_n^*}\xi} + (-1)^{n+1}e^{-\sqrt{\lambda_n^*}(1-\xi)} + \sqrt{2}\,\sin(\sqrt{\lambda_n^*}\xi - \frac{\pi}{4})\right] \qquad \text{(B.17)}$$

Figure B.1 shows a plot of this asymptotic mode shape when $n = 6$, including the contributions of the individual terms.

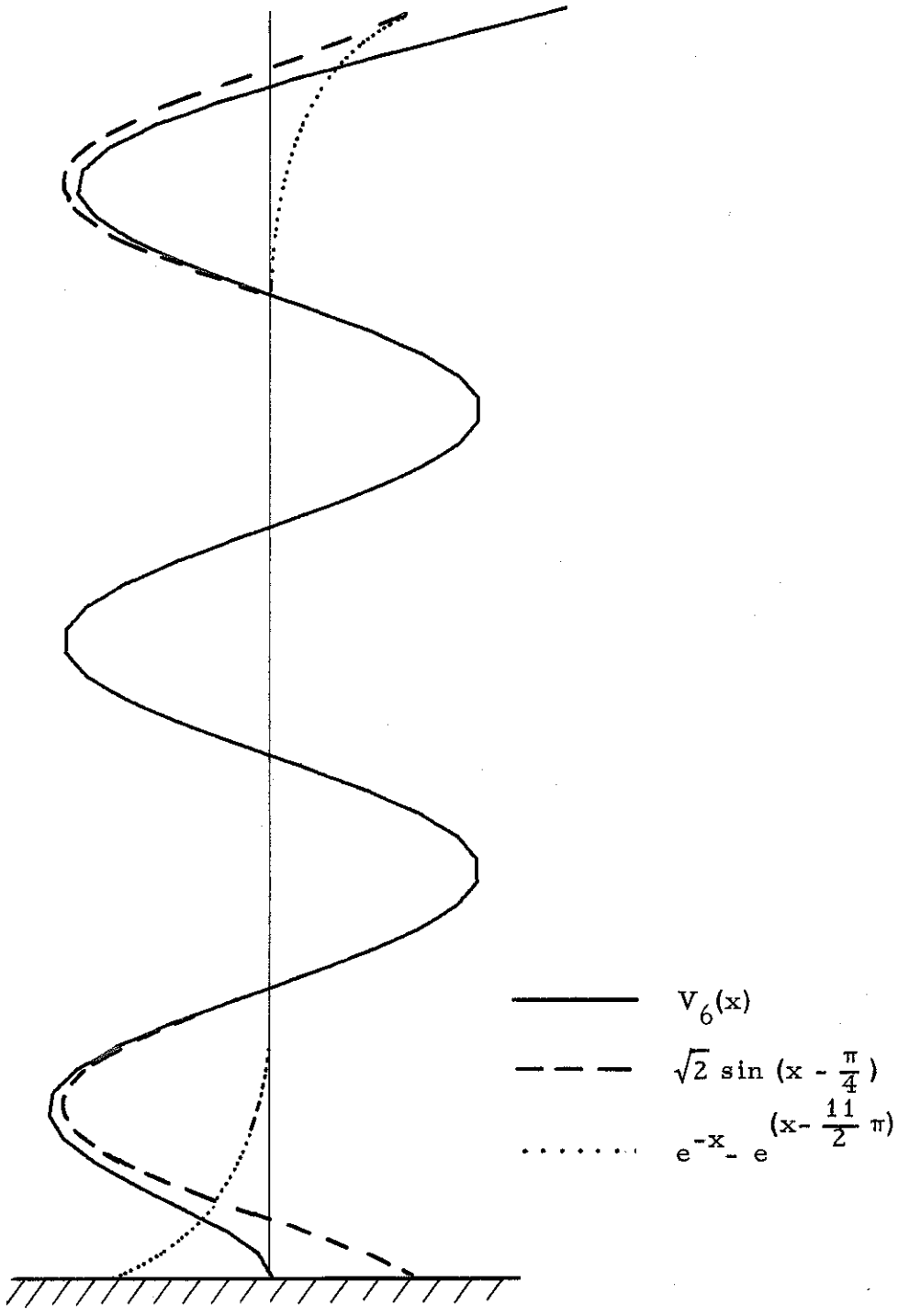

Fig. B.1. Asymptotic 6^{th} Mode Shape, Euler-Bernoulli Beam

APPENDIX C

EIGENVALUES AND EIGENVECTORS FOR A COUPLED SHEAR WALL WITH NO VERTICAL MOTION

The differential equation is obtained from equation (3.4) when u is set equal to zero.

$$v_{\xi\xi\xi\xi} - \Pi_1 v_{\xi\xi} + \bar{\lambda}^2 v_{\tau\tau} = 0 \tag{C.1}$$

and the corresponding boundary conditions will be

$$\begin{aligned} v(0,\tau) &= 0 \\ v_{\xi}(0,\tau) &= 0 \\ v_{\xi\xi}(1,\tau) &= 0 \\ v_{\xi\xi\xi}(1,\tau) &= \Pi_1 v_{\xi}(1,\tau) \end{aligned} \tag{C.2}$$

as can be verified from equation (3.8). Assuming an oscillatory solution to equation (C.1), v can be obtained as

$$v(\xi,\tau) = V(\xi)e^{i\tau} \tag{C.3}$$

where

$$V(\xi) = C_1 \sin p_1\xi + C_2 \cos p_1\xi + C_3 \sinh p_2\xi + C_4 \cosh p_2\xi \tag{C.4}$$

in which

$$p_1 = \sqrt{\sqrt{\left(\frac{\Pi_1}{2}\right)^2 + \bar{\lambda}^2} - \frac{\Pi_1}{2}}$$

$$p_2 = \sqrt{\sqrt{\left(\frac{\Pi_1}{2}\right)^2 + \bar{\lambda}^2} + \frac{\Pi_2}{2}} \qquad \text{(C.5)}$$

Applying the boundary conditions to equation (C.4), four homogeneous equations in C_i are obtained

$$\begin{bmatrix} 0 & 1 & 0 & 1 \\ p_1 & 0 & p_2 & 0 \\ -p_1^2 \sin p_1 & -p_1^2 \cos p_1 & p_2^2 \sinh p_2 & p_2^2 \cosh p_2 \\ -p_1 p_2^2 \cos p_1 & p_1 p_2^2 \sin p_1 & p_2 p_1^2 \cosh p_2 & p_2 p_1^2 \sinh p_2 \end{bmatrix} \begin{bmatrix} C_1 \\ C_2 \\ C_3 \\ C_4 \end{bmatrix} = \begin{bmatrix} 0 \\ 0 \\ 0 \\ 0 \end{bmatrix} \qquad \text{(C.6)}$$

and for nontrivial solutions, the determinant of the matrix is set equal to zero giving the eigenvalue equation

$$\bar{\lambda}_n^2 (2 + 2\cos p_1 \cosh p_2) + \bar{\lambda}_n \Pi_1 \sin p_1 \sinh p_2 + \Pi_1^2 \cos p_1 \cosh p_2 = 0 \qquad \text{(C.7)}$$

It is observed that the eigenvalues given by this equation will be functions of the parameter Π_1, and solutions can best be obtained by some numerical procedure.

The mode shapes corresponding to these eigenvalues are obtained by solving equation (C.6) for C_i and substituting the values back into equation (C.4), giving

$$V_n(\xi) = C\Big[(p_1^2\cos p_1 + p_2^2\cosh p_2)(p_2\sin p_1\xi - p_1\sinh p_2\xi)$$

$$- p_1p_2(p_1\sin p_1 + p_2\sinh p_2)(\cos p_1\xi - \cosh p_1\xi)\Big] \quad (C.8)$$

where C is a constant and, following equation (C.5)

$$p_1 = \left[\left\{\left(\frac{\Pi_1}{2}\right)^2 + \bar{\lambda}_n^2\right\}^{\frac{1}{2}} - \frac{\Pi_1}{2}\right]^{\frac{1}{2}}$$

$$p_2 = \left[\left\{\left(\frac{\Pi_1}{2}\right)^2 + \bar{\lambda}_n^2\right\}^{\frac{1}{2}} + \frac{\Pi_1}{2}\right]^{\frac{1}{2}} \quad (C.9)$$

Asymptotic Behavior

(a) $\Pi_1 \to 0$

From Equation (C.9),

$$p_1 = \sqrt{\bar{\lambda}_n} - \frac{\Pi_1}{4}\bar{\lambda}_n^{-\frac{1}{2}} + O(\Pi_1^2)$$

$$p_2 = \sqrt{\bar{\lambda}_n} + \frac{\Pi_1}{4}\bar{\lambda}_n^{-\frac{1}{2}} + O(\Pi_1^2) \quad (C.10)$$

Substituting this in equation (C.7) leads to

$$(2 + 2\cos\sqrt{\bar{\lambda}_n}\cosh\sqrt{\bar{\lambda}_n}) + \frac{\Pi_1}{\bar{\lambda}_n}\sin\sqrt{\bar{\lambda}_n}\sinh\sqrt{\bar{\lambda}_n} + \frac{\Pi_1}{2\sqrt{\bar{\lambda}_n}}(\sin\sqrt{\bar{\lambda}_n}\cosh\sqrt{\bar{\lambda}_n}$$

$$+ \cos\sqrt{\bar{\lambda}_n}\sinh\sqrt{\bar{\lambda}_n}) + O(\Pi_1^2) = 0 \quad (C.11)$$

which can be solved for $\bar{\lambda}_n$ by letting

$$\bar{\lambda}_n = \bar{\lambda}_n^* + \Pi_1\lambda_{1n} + O(\Pi_1^2) \quad (C.12)$$

and setting terms of equal order equal to zero. By this procedure $\overline{\lambda}_n$ is found to be

$$\overline{\lambda}_n = \lambda_n^* + \frac{(-1)^n - \cos\sqrt{\lambda_n^*} - (2/\sqrt{\lambda_n^*})\sin\sqrt{\lambda_n^*}}{2(-1)^n + 2\cos\sqrt{\lambda_n^*}} \Pi_1 + O(\Pi_1^2) \; ; \quad n = 1, 2, \ldots \tag{C.13}$$

where λ_n^* is the solution to the transcendental equation

$$1 + \cos\sqrt{\lambda_n^*}\cosh\sqrt{\lambda_n^*} = 0 \tag{C.14}$$

Numerical values of λ_n^* are given in appendix B, equation (B.7). The mode shapes are obtained by substituting equation (C.10) into (C.8)

$$\begin{aligned} V_n(\xi) = p_1\overline{\lambda}_n \Big[& (\cos p_1 + \cosh p_2)(\sin p_1\xi - \sinh p_2\xi) \\ & - (\sin p_1 + \sinh p_2)(\cos p_1\xi - \cosh p_2\xi) \\ & + \frac{\Pi_1}{2\overline{\lambda}_n} \Big\{ 2\cosh p_2 \sin p_1\xi + (\cos p_1 - \cosh p_2)\sinh p_2\xi \\ & - \sinh p_2(\cos p_1\xi - \cosh p_2\xi) \Big\} + O(\Pi_1^2) \Big] \end{aligned} \tag{C.15}$$

and by use of equations (C.10), (C.13) and (C.14)

$$\begin{aligned} \lim_{\Pi_1 \to 0} V_n(\xi) = \text{const.} \Big[& \cosh\sqrt{\lambda_n^*}\,\xi - \cos\sqrt{\lambda_n^*}\,\xi \\ & - \frac{\sin\sqrt{\lambda_n^*}}{(-1)^{n+1} - \cos\sqrt{\lambda_n^*}} (\sinh\sqrt{\lambda_n^*}\,\xi - \sin\sqrt{\lambda_n^*}\,\xi) \Big]; \\ & n = 1, 2, \ldots \end{aligned} \tag{C.16}$$

This equation is similar to equation (B.15) in appendix B, showing that the mode shapes asymptotically approch those of an ordinary cantilever beam.

(b) $\bar{\lambda}_n \to \infty$

From equation (C.9)

$$p_1 = \sqrt{\bar{\lambda}_n} - \frac{\Pi_1}{4}\bar{\lambda}_n^{-\frac{1}{2}} + O(\bar{\lambda}_n^{-3/2})$$
$$p_2 = \bar{\lambda}_n^{\frac{1}{2}} + \frac{\Pi_1}{4}\bar{\lambda}_n^{-\frac{1}{2}} + O(\bar{\lambda}_n^{-3/2}) \qquad (C.17)$$

If $\bar{\lambda}_n > 81$,

$$e^{-\sqrt{\bar{\lambda}_n}} \leq O(\bar{\lambda}_n^{-2}) \qquad (C.18)$$

such that the eigenvalue equation (C.7) reduces to

$$\bar{\lambda}_n^2 \cdot \tfrac{1}{2} e^{p_2}\left[2\cos p_1 + \frac{\Pi_1}{\bar{\lambda}_n}\sin p_1 + O(\bar{\lambda}_n^{-2})\right] = 0 \qquad (C.19)$$

which implies that

$$p_1 = \left(\frac{2n-1}{2}\pi\right) + \frac{\Pi_1}{2}\bar{\lambda}_n^{-1} + O(\bar{\lambda}_n^{-2}) \qquad (C.20)$$

Equating this expression with that of p_1 in equation (C.17) will give the asymptotic value for the eigenvalue,

$$\bar{\lambda}_n = \left(\frac{2n-1}{2}\pi\right)^2 + \frac{\Pi_1}{2} + O(\bar{\lambda}_n^{-\frac{1}{2}}) \;;\; \text{as} \;\; n \to \infty \qquad (C.21)$$

The mode shapes for this case are obtained by substituting equations (C.17) and (C.21) in equation (C.8) and making use of (C.18)

$$V_n(\xi) = \tfrac{1}{2}p_1 e^{p_2}\bar{\lambda}_n C\Big[\ \sin p_1\xi\ -\ \cos p_1\xi\ +(-1)^{n+1}e^{-p_2(1-\xi)}\ +e^{-p_2\xi}$$

$$+\frac{\Pi_1}{2}\bar{\lambda}_n^{-1}\Big\{2\sin p_1\xi\ -\ \cos p_1\xi\ +e^{-p_2\xi}+(-1)^{n+1}e^{-p_2(1-\xi)}\Big\}$$

$$+\ O(\bar{\lambda}_n^{-2})\Big] \qquad \text{(C.22)}$$

or, by letting

$$C = \frac{2e^{-p_2}}{p_1\bar{\lambda}_n}\left(1\ -\ \frac{\Pi_1}{2}\bar{\lambda}_n^{-1}\right) \qquad \text{(C.23)}$$

$$V_n(\xi) = \sin p_1\xi\ -\ \cos p_1\xi\ +(-1)^{n+1}e^{-p_2(1-\xi)}\ +e^{-p_2\xi}$$

$$+\ \frac{\Pi_1}{2}\bar{\lambda}_n^{-4}\sin p_1\xi\ +O(\bar{\lambda}_n^{-2}) \qquad \text{(C.24)}$$

Applying equations (C.17) and (C.21), the asymptotic mode shapes become

$$\lim_{\lambda_n\to\infty} V_n(\xi) = \sin\frac{2n-1}{2}\pi\xi\ -\ \cos\frac{2n-1}{2}\pi\xi\ +e^{-\frac{2n-1}{2}\pi\xi}$$

$$+(-1)^{n+1}e^{-\frac{2n-1}{2}\pi(1-\xi)} \qquad \text{(C.25)}$$

(c) $\Pi_1 \to \infty$

From equation (C.9):

$$p_1 = \bar{\lambda}_n\,\Pi_1^{-\frac{1}{2}} + O(\Pi_1^{-5/2})$$

$$p_2 = \Pi_1^{\frac{1}{2}} - \frac{\bar{\lambda}_n^2}{2}\Pi_1^{-3/2} + O(\Pi_1^{-7/2}) \qquad \text{(C.26)}$$

Requiring that $\Pi_1 > 81$

$$e^{-\sqrt{\Pi_1}} \leq O(\Pi_1^{-2}) \tag{C.27}$$

equation (C.7) can be written asymptotically as

$$\Pi_1^2 \tfrac{1}{2} e^{p_2} \left[\cos p_1 + \frac{\bar{\lambda}_n}{\Pi_1} \sin p_1 + O(\Pi_1^{-2})\right] = 0 \tag{C.28}$$

Hence

$$\cos p_1 + \frac{\bar{\lambda}_n}{\Pi_1} \sin p_1 = O(\Pi_1^{-2}) \tag{C.29}$$

which can easily be solved for p_1,

$$p_1 = \frac{2n-1}{2}\pi + \bar{\lambda}_n \Pi_1^{-1} + O(\Pi_1^{-2}) \tag{C.30}$$

Equating this equation to the value for p_1 given in equation (C.26), the asymptotic eigenvalues are found to be

$$\bar{\lambda}_n = \frac{2n-1}{2}\pi\,(\sqrt{\Pi_1} + 1) + O(\Pi_1^{-\frac{1}{2}}); \quad n = 1, 2, \ldots \tag{C.31}$$

Similar to earlier cases, the mode shape is obtained as

$$V(\xi) = \tfrac{1}{2} C e^{p_2} p_2^3 \left[\sin p_1\xi - \bar{\lambda}_n \Pi_1^{-1}(\cos p_1\xi - e^{-p_2\xi}) + O(\Pi_1^{-2})\right] \tag{C.32}$$

Letting

$$C = \frac{2e^{-p_2}}{p_2^3} \tag{C.33}$$

and substituting the values for p_1 and p_2 gives the final result

$$V_n(\xi) = \sin\frac{2n-1}{2}\pi\xi - \bar{\lambda}_n \Pi_1^{-1}\left[(1-\xi)\cos\frac{2n-1}{2}\pi\xi - e^{-\sqrt{\Pi_1}\xi}\right]$$

$$+ O(\Pi_1^{-2}) \quad ; \quad n = 1,2,\ldots \qquad \text{(C.34)}$$

References

1. Chitty, L., "On the Cantilever Composed of a Series of Parallel Beams Interconnected by Cross Bars," Phil. Mag. (London) V. 38, Oct., 1947.

2. Chitty, L., and Wan, Wen-Yuh, "Tall Building Structures Under Wind Load," Proceedings 7th International Congress for Applied Mechanics, London, England, V. 1, Paper No. 22, 1948, pp. 254-268.

3. Beck, H., "Contribution to the Analysis of Coupled Shear Walls," Journal of the American Concrete Institute, Detroit, Mich., V. 59, 1962, pp. 1055-1069.

4. Rosman, R., "Approximate Analysis of Shear Walls Subject to Lateral Loads," Journal of the American Concrete Institute, Detroit, Mich., V. 61, 1964, pp. 717-732.

5. Burns, R. J., "An Approximate Method of Analysing Coupled Shear Walls Subject to Triangular Loading," Proceedings of the Third World Conf. on Earthquake Engineering, New Zealand, Jan., 1965.

6. Coull, A., and Choudhury, J. R., "Stresses and Deflections in Coupled Shear Walls," Journal of the American Concrete Institute, V. 64, No. 2, pp. 65-72.

7. Coull, A., and Stafford Smith, B., "Analysis of Shear Wall Structures," Proceedings of a Symposium on Tall Buildings, Univ. of Southampton, 1966, Pergamon Press.

8. Coull, A., and Puri, R. D., "Analysis of Pierced Shear Walls," Journal of the Structural Division, ASCE, V. 94, No. ST1, Proc. Paper 5710, Jan., 1968, pp. 71-82.

9. Traum, E. E., "Multi-Story Pierced Shear Walls of Variable Cross-Section," Proceedings of a Symposium on Tall Buildings, Univ. of Southampton, edited by A. Coull and E. Stafford Smith, 1966, Pergamon Press.

10. Barnard, P. R., and Schwaighofer, J., "The Interaction of Shear Walls Connected Solely Through Slabs," Proceedings of a Symposium on Tall Buildings, Univ. of Southampton, England, 1966, Pergamon Press.

11. Sensmeier, Paul E., "An Analytical and Experimental Study of Shear Walls with Openings," Thesis, Purdue Univ., Lafayette, Indiana, June, 1967.

12. Tso, W. K., "General Analysis of Coupled Symmetrical Shear Walls," Report, Department of Civil Engineering and Engineering Mechanics, McMaster University, Hamilton, Ontario, Canada.

13. Tso, W.K., and Chan, H. B., "Dynamic Analysis of Plane Coupled Shear Walls," Journal of the Engineering Mechanics Division, ASCE, V. 97, No. EM1, Proc. Paper 7899, Feb., 1971, pp. 33-48/

14. Tani, S., Sakurai, J., and Iguchi, M., "An Approximate Method of Static and Dynamic Analysis of Core-Wall Buildings," Proceedings of the Fourth World Conference on Earthquake Engineering, Santiago, Chile, 1969.

15. Habip, L.M., "A Survey of Modern Developments in the Analysis of Sandwich Structures," Applied Mechanics Review, V. 18, No. 2, 1965, pp. 93-98.

16. Kanai, K., Tajimi, M., Osawa, Y., and Kobayashi, H., "Dynamic Characteristics of Buildings with Pure Laminae-Type Construction," Architectural and Structural Engineering Series, V. 1, "Earthquake Engineering," pp. 111-122, Shokokusha, Tokyo, Japan, 1968 (in Japanese).

17. Jennings, P. C., "Vertical Shear Failure of Coupled Shear Walls in the Alaskan Earthquake," Proceedings of the Japan Earthquake Engineering Symposium, Tokyo, Japan, 1966, pp. 379-384.

18. Troxell, G. E., and Davis, H. E., "Composition and Properties of Concrete," McGraw-Hill Book Company, New York, 1956.

19. Abrahamowitz, M., and Stegun, I. A., "Handbook of Mathematical Functions," Seventh Printing, May, 1968. National Bureau of Standards.

20. Gurfinkel, G., "Simple Method of Analysis of Vierendeel Structures," Journal of the Structural Division, ASCE, V. 93, No. ST3, Proc. Paper 5296, June, 1967.

21. Girijavallabhan, C. V., "Analysis of Shear Walls with Openings," Journal of the Structural Division, ASCE, V. 95, No. ST10, Proc. Paper 6824, Oct., 1969.

22. Courant, R., and Hilbert, D., "Methods of Mathematical Physics," V.I, Chap. IV, Wiley, Dec. 1966.

23. Gere, J. M., "Statically Determinate Structures," Handbook of Engineering Materials," edited by W. Flügge, McGraw-Hill, New York, 1962.

24. Cole, Julian D., "Perturbation Methods in Applied Mathematics," Blaisdell Publ. Co., 1968.

25. Nelson, Alfred L., Folley, Karl W., and Coral, Max, "Differential Equations," D. C. Heath and Company, Boston, Second Edition, 1960.

26. Bellman, Richard, "Introduction to Matrix Analysis," McGraw-Hill, New York, 1960.

27. Isaacson, Eugene, and Keller, Herbert B., "Analysis of Numerical Methods," Wiley & Sons, New York, 1966.

28. Hahne, H. V., "Bending of Beams," Handbook of Engineering Mechanics," edited by W. Flügge, McGraw-Hill, New York, 1962.

29. Kantorovich, L. V., and Krylov, V. I., "Approximate Methods of Higher Analysis," Interscience Publishers, Inc., 1964.

30. Hetenyi, M., "Beams on Elastic Foundations," Handbook of Engineering Mechanics, edited by W. Flügge, McGraw-Hill, 1962.

31. Young, D., "Continuous Systems," Handbook of Engineering Mechanics, edited by W. Flügge, McGraw-Hill, 1962.

32. ACI Standard Building Code Requirements for Reinforced Concrete, June, 1963.

33. Marguerre, K., "Elasticity, Basic Concepts," Handbook of Engineering Mechanics, edited by W. Flügge, McGraw-Hill, 1962.

34. Arnold, F. R., "Algebra," Handbook of Engineering Mechanics, edited by W. Flügge, McGraw-Hill, 1962.

35. Hoff, N. J., "The Analysis of Structures," Wiley & Sons, New York, 1956.

36. Plantema, F. J., "Sandwich Constructions," Wiley & Sons, New York, 1966.

37. Allen, H. G., "Analysis and Design of Structural Sandwich Panels," Pergamon Press, 1969.

38. Pauley, T., "The Coupling of Reinforced Concrete Shear Walls," Proceedings of the Fourth World Conference on Earthquake Engineering, Santiago Chile, Jan. 1969.

39. Coull, A., and Irwin, A. W., "Analysis of Load Distribution in Multistory Shear Wall Structures," The Structural Engineer, V. 48, No. 8, Aug. 1970.

40. Pauley, T., "Reinforced Concrete Shear Walls," New Zealand Engineering, Oct. 1969.

41. Tso, W. K. and Biswas, J. K., "Seismic Analysis of Multi-Story Shear Wall Buildings," Civil Engineering and Engineering Mechanics Research Report, Faculty of Engineering, McMaster University, Canada, 1971.

42. Irwin, A. W., and Heidebrecht, A. C., "Dynamic Response of Coupled Shear Wall Buildings," ASCE National Structural Engineering Meeting, Baltimore, 1971.

43. Timoshenko, D., "Vibration Problems in Engineering," 3rd edition, D. Van Nostrand Company, Inc., 1961, page 334.